Department of Automation and Systems Technology

Model-Based Optimal Control of Multidimensional and Multi-Tonal Frequency Varying Disturbances

Juha Orivuori

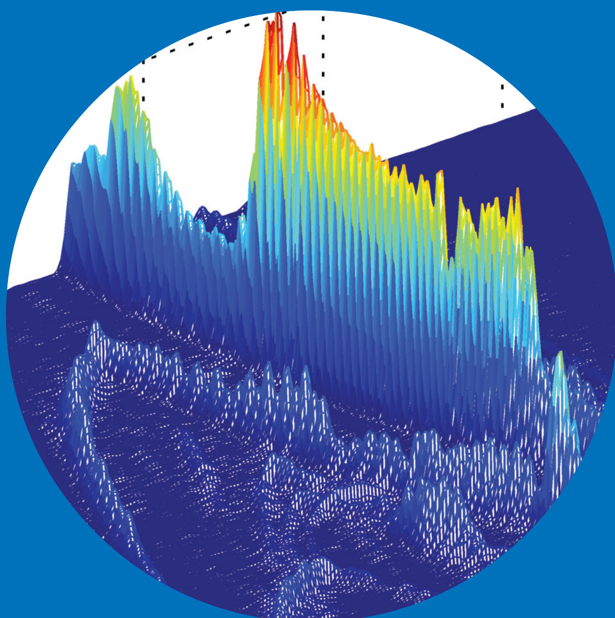

DOCTORAL
DISSERTATIONS

Aalto University publication series
DOCTORAL DISSERTATIONS 11/2013

Model-Based Optimal Control of Multidimensional and Multi-Tonal Frequency Varying Disturbances

Juha Orivuori

A doctoral dissertation completed for the degree of Doctor of Science (Technology) to be defended, with the permission of the Aalto University School of Electrical Engineering, at a public examination held at the lecture hall AS1 of the school on 25 January 2013 at 12.

Aalto University
School of Electrical Engineering
Department of Automation and Systems Technology

Supervising professor
Professor Kai Zenger

Thesis advisor
Professor Kai Zenger

Preliminary examiners
Professor Stephen Elliott, University of Southampton, UK
Professor Matti Vilkko, Tampere University of Technology, Finland

Opponents
Professor Erno Keskinen, Tampere University of Technology, Finland
Professor Matti Vilkko, Tampere University of Technology, Finland

Aalto University publication series
DOCTORAL DISSERTATIONS 11/2013

ISBN 978-952-60-4977-9 (printed)
ISBN 978-952-60-4978-6 (pdf)
ISSN-L 1799-4934
ISSN 1799-4934 (printed)
ISSN 1799-4942 (pdf)
http://urn.fi/URN:ISBN:978-952-60-4978-6

Unigrafia Oy
Helsinki 2013

Finland

NORDIC ECOLABEL
441 697
Printed matter

A! Aalto University

Abstract

Aalto University, P.O. Box 11000, FI-00076 Aalto www.aalto.fi

Author
Juha Orivuori

Name of the doctoral dissertation
Model-Based Optimal Control of Multidimensional and Multi-Tonal Frequency Varying Disturbances

Publisher School of Electrical Engineering

Unit Department of Automation and Systems Technology

Series Aalto University publication series DOCTORAL DISSERTATIONS 11/2013

Field of research Control Engineering

Manuscript submitted 27 September 2012 **Date of the defence** 25 January 2013

Permission to publish granted (date) 5 November 2012 **Language** English

☐ **Monograph** ☒ **Article dissertation (summary + original articles)**

Abstract

Vibration is a phenomenon related to every physical system that has the potential to cause severe problems that range from increased structural fatigue to potential operator health hazards. The traditional approach to solve the vibration related problems is to dissipate the vibration energy through the addition of passive damping elements consisting of springs, masses and dampers. Even though these methods have been widely applied in all branches of industry, they are becoming increasingly inadequate in meeting the industrial standards of today.

In the past decade the significant increase in the available computational power has given a rise to another approach to tackle the vibration related problems; namely the active control of vibrations, which is capable of meeting the tightened standards. In this approach, the vibrations are suppressed through the excitation of external energy in a suitable form into the system, resulting in the compensation of the vibrations. The use of this approach has enabled the mitigation of vibrations in very complex structures in a deterministic manner. The major benefit of the method is the change of the underlying design problem. Namely, the original structural design problem is converted into a standard control design problem, enabling the designer to use the very powerful tools of control theory.

In this thesis, a novel method for active vibration mitigation is presented. The proposed approach shares many similarities with the existing model-based methods while addressing many of the drawbacks and problems encountered with the current approaches. The proposed method is a generic nonlinear control law capable in the simultaneous suppression of multiple tonal disturbances in multiple dimensions. The control design procedure is simplified such that the number of free parameters is minimal and the impact of these parameters on the process performance is transparent. Such an approach enables the method to be applied by an industrial system specialist with possibly very little experience in control theory, unlike what is the case with the most of the existing methods. In addition, the essential tools for the performance and stability evaluation of the obtained control law are presented in detail with the focus being in the problems commonly encountered in the practical implementation.

This thesis consists of a summary and five publications with the focus being on the control design, performance analysis and test-bed implementation in several industrial processes. An extensive comparison of the proposed method against the existing linear control approaches is also included in this work.

Keywords active vibration control, continuous gain-scheduling, nonlinear optimal control, optimal control, performance evaluation, vibration isolation

ISBN (printed) 978-952-60-4977-9 **ISBN (pdf)** 978-952-60-4978-6

ISSN-L 1799-4934 **ISSN (printed)** 1799-4934 **ISSN (pdf)** 1799-4942

Location of publisher Espoo **Location of printing** Helsinki **Year** 2013

Pages 233 **urn** http://urn.fi/URN:ISBN:978-952-60-4978-6

A! **Aalto-yliopisto**

Aalto-yliopisto, PL 11000, 00076 Aalto www.aalto.fi

Tiivistelmä

Tekijä
Juha Orivuori

Väitöskirjan nimi
Taajuusmuuttuvien Häiriöiden Mallipohjainen Optimaalinen Vaimennus

Julkaisija Sähkötekniikan korkeakoulu

Yksikkö Automaatio- ja Systeemitekniikan laitos

Sarja Aalto University publication series DOCTORAL DISSERTATIONS 11/2013

Tutkimusala Systeemitekniikka

Käsikirjoituksen pvm 27.09.2012 **Väitöspäivä** 25.01.2013

Julkaisuluvan myöntämispäivä 05.11.2012 **Kieli** Englanti

☐ **Monografia** ☒ **Yhdistelmäväitöskirja (yhteenveto-osa + erillisartikkelit)**

Tiivistelmä

Värähtely on kaikille rakenteille tyypillinen ilmiö, jonka vaikutukset vaihtelevat rakenteiden lisääntyneestä väsymisestä ja kulumisesta mahdollisiin prosessin käyttäjän terveyshaittoihin. Perinteisesti värähtelyn haittavaikutuksia on pyritty vähentämään lisäämällä rakenteisiin jousista, vaimentimista ja massoista koostuvia vaimenninelementtejä, jotka sitovat värähtelyenergiaa. Vaikka näitä passiivisia vaimennusmenetelmiä on käytössä kaikkialla teollisuudessa, ne ovat yhä harvemmin riittäviä vastaamaan teollisuuden kasvaneisiin laatuvaatimuksiin.

Viime vuosikymmenen aikana tapahtunut huomattava tietojärjestelmien laskentatehon kasvu on mahdollistanut tehokkaampien vaihtoehtoisten menetelmien käytön värähtelyjen vaimennukseen. Näihin menetelmiin lukeutuu myös aktiivinen värähtelyn vaimennus. Tämä menetelmä perustuu ulkoisen energian syöttämiseen prosessiin siten, että värähtelyenergia minimoituu, mikä osaltaan mahdollistaa hyvin ennakoitavissa olevan toiminnan myös erittäin monimutkaisissa järjestelmissä. Menetelmän suurin etu perustuu tarkasteltavan ongelman muuntamiseen rakenteiden suunnittelusta nk. perinteiseksi säätöteknisesksi ongelmaksi, mikä mahdollistaa tehokkaiden säätöteoreettisten työkalujen täyden hyödyntämisen.

Tässä työssä esitellään uusi menetelmä värähtelyjen aktiiviseen vaimennukseen, jolla on useita samankaltaisuuksia jo olemassa olevien menetelmien kanssa, kuitenkin siten, että suurin osa näiden sisältämistä ongelmista ratkeaa. Esitetty menetelmä on prosessista riippumaton yleiskäyttöinen epälineaarinen säätölaki, joka kykenee vaimentamaan useita häiriön taajuuskomponentteja monissa eri suunnissa samanaikaisesti. Lopullinen säätösuunnittelu muodostuu yksinkertaiseksi, jolloin vapaiden suunnittelumuuttujien määrä on mahdollisimman pieni ja joiden vaikutus prosessin toimintaan on selkeä. Tämä yksinkertaistettu lähestymistapa mahdollistaa menetelmän käytön myös sellaisen prosessisuunnittelijan toimesta, jonka säätötekniikan tuntemus on vähäinen, toisin kuin olemassa olevia menetelmiä käytettäessä. Työssä esitetään myös aihepiirin kannalta oleellisimmat analyysimenetelmät stabiilisuuden ja toimintatehokkuuden arviointiin, painopisteen ollessa käytännön sovelluksessa.

Tämä työ koostuu tiivistelmästä sekä viidestä julkaisusta, joiden painopiste on säätösuunnittelussa, suorituskyvyn analysoinnissa sekä menetelmän soveltamisessa useassa erillisessä teollisuusprosessissa.

Avainsanat aktiivinen värähtelyn vaimennus, epälineaarinen optimisäätö, jatkuva vahvistustaulukointi, optimisäätö, suorituskyvyn arviointi, värähtelyn eristys

ISBN (painettu) 978-952-60-4977-9 **ISBN (pdf)** 978-952-60-4978-6

ISSN-L 1799-4934 **ISSN (painettu)** 1799-4934 **ISSN (pdf)** 1799-4942

Julkaisupaikka Espoo **Painopaikka** Helsinki **Vuosi** 2013

Sivumäärä 233 **urn** http://urn.fi/URN:ISBN:978-952-60-4978-6

Preface

This thesis summarises the work and research done during the six-year course I was working at the Department of Automation and Systems Technology at the Aalto University (the former Helsinki University of Techonology) as both undergraduate and post-graduate student under the work titles of research assistant, researcher, doctoral student and teaching assistant. The results presented in this work have originated from several research projects, which had similar underlying problems, yet completely different practical problems. This diversity of problems had a significant impact on the direction of the research and the quality of the results. It is rather trivial to solve some well-defined problem for a single application; however, the usability of such results for problems in general tends to be rather limited. Hence, the fact that the underlying problems remained the same while the applications changed, gave a clear direction in which the research should focus on. I consider myself privileged for being able to take part in the research in such a wide variety of practical processes, not only it gave the common thread of this work, but it also helped to verify that the results are actually generic.

During the course of work, I have been able to be in a rather close co-operation with several industrial companies. I was surprised how welcome one can feel, even as you are just some outsider coming to ‘tell how things should be made’. From my behalf, this co-operation was very fruitful; I was able to get the first-hand information and opinions from professionals who have been working with similar problems for years – a piece of knowledge that should never be underestimated. However, I also learned that there are some prevailing views in the industry that somewhat prevent the penetration of the today’s effective control solutions. Namely, if you want to control something, you should use PID-control; if you want to estimate something, you should use Kalman-filter. It is obvious that both of these methods are the ones that are being taught on the first basic courses on control engineering. They are - no doubt – the most widely applied approaches today and the major breakthroughs in the field of control engineering on their time, a time on which very few of the current more computationally demanding approaches could be used. However, these approaches are the best only when used in the proper circumstances, and this is the part that is usually overlooked. For the problems considered in this work, the PID-control for instance is a completely unsuitable approach, due to the wide frequency band on which the control has an impact on the process. Such controller, especially when implemented in more complex systems may have very undesirable consequences. Similarly, the Kalman-filter is very effective when parameterised correctly, and in fact this work also utilises a special case of such filters. However, with poor parameterisation, the results may well be of sub-standard. I am hopeful that in the future the views will start to change and the more advanced approaches become more widely utilised in all kinds of industry, instead of just being buried deep in the academic world and the process industry. There is a vast amount of resources to be saved or freed simply by introducing a control method or by changing the prevailing approach.

In this work, I have tried to do my best to put the results and the methods used in a form that is both clear and easy to use for anyone with some basic knowledge in control engineering. As in the end, I think that the control engineering is of no use, unless it can be applied in practice (of course the theoretical research validating the methodologies is of utmost importance, yet not the ultimate goal).

This thesis received financial support from Finnish Foundation of Technology Promotion, Neles Foundation, Walter Ahlström Foundation and Automation Foundation, whose generosity is gratefully acknowledged.

This thesis was pre-examined by the professors Stephen Elliot from the University of Southampton and Matti Vilkko from the Tampere University of Technology, who both are leading experts in their respective fields. I thank you for the good input that enhanced the quality of this work and verified that it can be considered meeting the requirements set for a doctoral dissertation.

I would like to thank the industrial professionals Dr. Timo Virtanen and Dr. Marko Jorkama with whom I had the great pleasure to work with and from whom I got a rather through introduction to a one of the fields where unwanted vibrations are a real problem.

Reflecting back, there are several people who played a major role (although most of them do not recognise it) that this work was done in the first place. First of all I wish to thank professor (now emeritus) Heikki Koivo, the former head of the department for hiring me to a summer trainee position in the laboratory. My application was rejected at first by the board choosing the trainees. The day after I received the rejection, I was contacted and told that I got the position after all. Later on I found out that Heikki had decided to hire me anyway regardless of the decision of the board. Should this not have happened, I would most likely have carried out my original plan of getting the master's degree and moved to the industry right away, implying that I wouldn't be writing this now. Besides that, Heikki has always been an easy person to approach, willing to give advice when needed and more importantly been a just supervisor and manager for the employees, something that should never be overlooked.

After being a while in the department I got the chance to make my master's thesis on the same subject as this work, under the guidance of Professor Kai Zenger, who also became the supervisor and instructor of this thesis. Kai didn't seem to be the easiest person to work with when I met him the first time, but after a while it became evident that he is one of the best people one can have as a superior. We have had hours and hours of discussions both on the issues concerning this work and on more general subjects. An interesting feature in these discussions was how they started, namely I remember typically being told: "Once again, you have no clue of what you are doing", something that one might consider rather discouraging. However, I have always had a bad habit of not believing everything I am told, unless it is proven true. As it happens, the whole content of this work is something, which started with those exact words when I first presented my ideas. Regardless, when looking back, I think I had the best possible instructor, as having such arguments is the key for getting new results.

When I first started to work with the active control of vibration, I had very little knowledge in the field, yet I decided to make my master's thesis on the topic. During this time, I had the great pleasure of working with a bunch of great people, namely Dr. Antti Laiho and Anssi Sinervo, on the active control of radial rotor vibrations in an electric machine. It turned out that the chance to work with such enthusiastic people also made me to reconsider whether I was going to pursue any further degrees after the master's, and evidently I decided to. Had I been working with people who showed no interest in the application, it would be rather unlikely that I would have either, which would indeed have been a pity.

During the course of the work, I was offered a chance to take a visiting researcher's position to the University of Sheffield, working under the guidance of Professor Steve Daley. At the time, I thought that why not, going somewhere to see how things are made would be nice. It turned out to be one of the best choices I have ever made. I was privileged to work under Steve's guidance with Dr. Ilias Zazas on the active vibration isolation in marine diesel engines. During this time, I did the most of the research covered in this work. Getting to work with people with such background in this given field is something that cannot be covered by reading books or

taking courses. Working abroad is always somewhat challenging, yet I felt welcome since the very first day I met Steve and Ilias, something that I still highly appreciate. I would have no doubts on working with these people again if a suitable occasion was to arise.

Finally, there are several people, that had no direct impact on this work, but their indirect impact is even greater. The atmosphere at a working place is something that is not usually given enough credit; however I think that this is one of the major aspects when considering the well-being and productivity of the employees. I have been fortunate of being able to work in a place with unique atmosphere, something I had never experienced before and I doubt I will experience again. Therefore there is a bunch of colleagues that deserve to be mentioned, after all, during the last six years, I spent one third of my time among you although many of you have become more of a friend than a colleague. First, I wish to thank Pauli Sipari and Jari-Pekka Ruonio for helping out with all the bureaucracy and computer related issues and just being there for an occasional chat. I would also like to thank Samuel Aulanko, Dr. Olli Haavisto, Dr. Vesa Hasu, Tapani Hyvämäki, Petri Hänninen, Dr. Jani Kaartinen, Ville Liimatainen, Alex Mattsson, Ali Peckan, Janne Pietilä, Iiris Routa, Dr. Veikko Sariola, Dr. Robert Tenno, Dr. Kalevi Tervo, Joonas Varso and Dr. Jean-Peter Ylén for numerous on and off topic discussions. I think that if you don't share your ideas and views or listen to the others' (even if you don't completely agree with them), you will lose your perspective, so thank you for helping prevailing mine.

Also, besides only working, I had the nice opportunity to participate in our weekly (or supposedly weekly) board gaming events that offered some counterbalance to the normal routines and made the working overall more pleasurable. So thank you, Annamaija, Antti, Iiris, Janne, Veikko and Ville for the good time. I would also like to thank Dr. Kalle Halmevaara, Dr. Antti Remes and the rest of our biannual 'old colleagues' dinner group', it is always nice to meet new people and work with them, but it is even more rewarding when you find yourself still being in contact even after people have changed their place of work.

Not so surprisingly, life is not only work, and in order to balance for the work one needs to have free-time for just to relax. I considered myself privileged to have several very good friends, who have helped me to set my mind somewhere else than work. During the years, I have noticed that friends and acquaintances come and go, but good friends stay, something that shouldn't be taken for granted. I am grateful for you just being there and I know that no names need to be mentioned, you know who you are, thank you.

Finally, I would like to thank my parents for being supportive and letting me to do my own decisions as I have seen the best while still giving rather firmly the direction where it would be good to go. You never had any doubts whether I would be able to complete this work, and even if I wouldn't have, I know it would not have made any difference – that is what being of the family is all about. Then, the last but not the least I want to dedicate this work to my late grandparents who all unfortunately passed away during the course of this work, you will not be forgotten.

Espoo, December 2012

Juha Orivuori

List of publications

[PUB I] Orivuori J, Zenger K, Sinervo A, Laiho A. (2012). Active control of rotor vibration in an electric machine by cascaded optimal and convergent control methods. *International Journal of Acoustics and Vibration*. 17(1), 14-22

[PUB II] Orivuori J, Zazas I, Daley S. (2010). Active control of a frequency varying tonal disturbance by a nonlinear optimal controller with frequency tracking. *Proceedings of IFAC WORKSHOPS – Periodic Control Systems PSYCO2010*

[PUB III] Orivuori J, Zenger K. (2011). Active control of vibration in a rolling process by nonlinear optimal controller. *Journal of System Design and Dynamics*. 5(5), 681-695

[PUB IV] Orivuori J, Zazas I, Daley S. (2012). Active control of frequency varying disturbances in a diesel engine. *Control engineering practice*. 20(11), 1206-1219

[PUB V] Orivuori J, Zenger K. (2012). Comparison and performance analysis of some active vibration control algorithms. *Journal of Vibration and Control*.
(Available online: http://dx.doi.org/10.1177/1077546312462441)

Contributions of the author

[PUB I] The author wrote the paper and developed the optimal and the cascaded LTI control laws under the guidance of Prof. Zenger. The test-bed implementation was realised by the author, Dr. Laiho and Mr. Sinervo. The convergent control law was designed for the system in co-operation with Dr. Laiho and Mr. Sinervo.

[PUB II] The author wrote most of the paper apart from the frequency estimation section. The nonlinear control law and the signal reconstruction scheme were developed by the author with constructive feedback from Prof. Daley. The test-bed implementation was done by the author and Dr. Zazas. The frequency estimator was designed by Prof. Daley and Dr. Zazas.

[PUB III] The paper was written and its contents were solely done by the author under the guidance of Prof. Zenger.

[PUB IV] The author wrote the paper under the guidance and instructions of Prof. Daley. The applied control scheme and the analysis tools were developed by the author. The test-bed implementation was done by the author and Dr. Zazas under the supervision of Prof. Daley.

[PUB V] The paper was written and its contents were solely done by the author under the guidance of Prof. Zenger.

Nomenclature

Symbols

a	real part
$\bar{a}$	rate of change of a frequency
$\mathbf{a}$	vector of operation points
$\mathbf{a}_{rn}$	vector of polynomial coefficients for gain-scheduling, estimator
A	disturbance amplitude
$\mathbf{A}$	system matrix, plant
$A(k)$	amplitude of the sinusoidal signal, in frequency estimation
$\hat{A}(k)$	estimated amplitude of the sinusoidal signal, in frequency estimation
$\mathbf{A}_{\mathrm{c}}$	system matrix, controller
$\mathbf{A}_{\mathrm{d}}$	system matrix, biased multi-tonal multi-dimensional disturbance
$\mathbf{A}_{\mathrm{di}}$	system matrix, one dimensional disturbance
$\mathbf{A}_{\mathrm{p}}$	system matrix, process
$\mathbf{A}_{\mathrm{s}}$	system matrix
$\mathbf{A}_{\mathrm{ud}}$	system matrix, unbiased multi-dimensional disturbance
b	imaginary part
$\mathbf{b}(t)$	disturbance bias
$\mathbf{b}_{mr}$	vector of polynomial coefficients for gain-scheduling, state-feedback
$\mathbf{B}$	input system matrix, plant
$\mathbf{B}_{\mathrm{c}}$	input system matrix, controller
$\mathbf{B}_{\mathrm{d}}$	input system matrix, biased multi-tonal multi-dimensional disturbance
$\mathbf{B}_{\mathrm{di}}$	input system matrix, one dimensional disturbance
$\mathbf{B}_{\mathrm{p}}$	input system matrix, process
$\mathbf{B}_{\mathrm{s}}$	input system matrix
$\mathbf{B}_{\mathrm{ud}}$	input system matrix, multi-dimensional disturbance
c	damping coefficient
$\mathbf{C}$	output system matrix, plant
$\mathbf{C}_{\mathrm{c}}$	output system matrix, controller
$\mathbf{C}_{\mathrm{p}}$	output system matrix, process
$\mathbf{C}_{\mathrm{s}}$	output system matrix

$\mathbf{C}_{\mathrm{z}}$	state weighting matrix, performance
d	decay magnitude
$d(k)$	measured disturbance signal, in frequency estimation
$\mathbf{d}(t)$	output disturbance
$\hat{\mathbf{d}}(k)$	reconstructed disturbance signal
$\mathbf{d}_{\mathrm{I}}(t)$	input disturbance
$\mathbf{d}_{\mathrm{u}}(t)$	unbiased multi-dimensional disturbance
$\mathbf{D}$	feed-through matrix, plant
$\mathbf{D}(\omega)$	unit vector, disturbance
$\mathbf{D}_{\mathrm{c}}$	feed-through matrix, controller
$\mathbf{D}_{\mathrm{p}}$	feed-through matrix, process
$\hat{\mathbf{e}}(t)$	output estimation error
$\mathbf{E}$	matrix of decay factors
f_0	initial frequency of the sinusoidal sweep signal
f_f	final frequency of the sinusoidal sweep signal
f_{high}	higher cut-off frequency in the Fourier filtering
f_{low}	lower cut-off frequency in the Fourier filtering
$f_{\mathrm{m}}(\omega_{\mathrm{hz}})$	scheduling function, estimator
$\mathbf{F}$	solution of the ARE, LQG-design
$F(s)$	Laplace transformed force
$F(t)$	force
$\mathbf{F}(t)$	force vector
$\tilde{\mathbf{F}}(t)$	modal force vector
$\mathbf{g}$	state scaling factors, plant
$\mathbf{g}_{\mathrm{b}}$	state scaling factors, bias
$\mathbf{g}_{\mathrm{d}}$	state scaling factors, disturbance
$g_{mr}(\omega_{\mathrm{hz}})$	scheduling function, state-feedback
$\mathbf{g}_{\mathrm{p}}$	state scaling factors, process
$\mathbf{G}$	gyroscopic matrix
$G(s)$	transfer function
$\mathbf{G}(s)$	process model
$\mathbf{G}_0(s)$	nominal process model
$\mathbf{G}_{\mathrm{c}}(s)$	controller model
$\mathbf{G}_{\mathrm{cont}}(s)$	transfer function matrix, controller
$\mathbf{G}_{\mathrm{cs}}(s)$	transfer function matrix, controlled states
$\mathbf{G}_{\mathrm{e}}(s)$	process model containing error
$\bar{\mathbf{G}}_{\mathrm{m}}(jq)$	process FRF, obtained directly from the data
$\mathbf{G}_{\mathrm{OL}}(s)$	open-loop transfer function matrix, ouput
$\bar{\mathbf{G}}_{\mathrm{OL}}(s)$	open-loop transfer function matrix, input
$\mathbf{G}_{\mathrm{p}}(s)$	process model
$\mathbf{G}_{\mathrm{p}}(z)$	process dynamics, true

$\hat{\mathbf{G}}_{\mathrm{p}}(z)$	process dynamics, modelled
$\mathbf{G}_{\mathrm{scale}}$	state scaling matrix
$\mathbf{G}_{\mathrm{tf}}(s)$	transfer function matrix, process
h	sample time
$\mathbf{H}$	Hamiltonian matrix
$\mathbf{H}_{\mathrm{s}}$	circulatory matrix
i	disturbance signal dimension
j	imaginary unit
J	cost function value, feedback design
J_{LQG}	cost function value, LQG-design
J_{obs}	cost function value, estimator
k	sample number
$\bar{k}$	spring stiffness
k_{high}	higher cut-off sample number in the Fourier filtering
k_{low}	lower cut-off sample number in the Fourier filtering
$\mathbf{k}_{\mathrm{rn}}$	vector of scheduling values, estimator
$\mathbf{K}$	estimator feedback matrix
$\mathbf{K}_{\mathrm{a}}$	matrix of scheduling coefficients, estimator
$\mathbf{K}_{f}$	Kalman gain
K_{G}	open-loop gain
$\mathbf{K}_{\mathrm{s}}$	stiffness matrix
$\mathbf{K}(s)$	controller model
$\mathbf{l}_{\mathrm{rn}}$	vector of scheduling values, state-feedback
$\mathbf{L}$	state feedback matrix
$\mathbf{L}_{\mathrm{s}}$	state feedback matrix
$\mathbf{L}_{\mathrm{b}}$	matrix of scheduling coefficients, state-feedback
m	number of plant inputs
$\bar{m}$	mass
$\mathbf{M}$	system matrix, observer
$\mathbf{M}(j\omega)$	inverse process dynamics
$\mathbf{M}_{\mathrm{c}}$	controllability matrix
$\mathbf{M}_{\mathrm{o}}$	observability matrix
$\mathbf{M}_{\mathrm{s}}$	mass matrix
n	number of plant outputs
$n(k)$	signal noise, in frequency estimation
$\mathbf{n}(t)$	measurement noise
$\mathbf{N}$	cross-term weighting matrix, feedback design
p	number of disturbance tones
$\mathbf{P}$	solution of the ARE, estimator
$\mathbf{P}_{\mathrm{c}}$	controllability Gramian
$\bar{\mathbf{P}}_{\mathrm{c}}$	transformed controllability Gramian

$\mathbf{P}_{\mathrm{o}}$	observability Gramian
$\bar{\mathbf{P}}_{\mathrm{o}}$	transformed observability Gramian
$\mathbf{q}(t)$	position vector
$\mathbf{Q}$	state weighting matrix, feedback design
$\mathbf{Q}_{\mathrm{obs}}$	state weighting matrix, estimator
$\mathbf{Q}_{\mathrm{z}}$	performance weighting matrix, performance variable
r	number of plant states
$\mathbf{r}(k)$	reference vector, in frequency estimation
$\mathbf{R}$	control weighting matrix, feedback design
$R(t)$	ratio of two sinusoidal signals
$\mathbf{R}_{\mathrm{obs}}$	control weighting matrix, estimator
$\mathbf{R}_{\mathrm{z}}$	performance weighting matrix, control effort
$\mathbf{S}$	solution of the ARE, feedback-design
$\mathbf{S}(s)$	sensitivity function
$\mathbf{S}(t)$	solution of the Riccati-equation
$S_{\mathrm{bias}}(\omega)$	singular value spectra, bias states
$S_{\mathrm{c}}(\omega)$	singular value spectra, controller states
$\mathbf{S}_{\mathrm{I}}(s)$	input sensitivity function
t_f	duration of the sinusoidal sweep
$\mathbf{T}$	similarity transformation matrix
$\mathbf{T}(s)$	complementary sensitivity function
$\mathbf{T}_{\mathrm{I}}(s)$	input complementary sensitivity function
$\mathbf{u}(t)$	control signal
$u_{\mathrm{d}}(t)$	sinusoidal sweep signal
$u_{\mathrm{ext}}(t)$	external control signal
$\mathbf{u}_{\mathrm{obs}}(t)$	artificial control signal
$\mathbf{u}_{\mathrm{p}}(t)$	process input
$\mathbf{u}_{\mathrm{s}}(t)$	process input
$\bar{U}_m(q)$	Fourier transformed input
$\mathbf{W}$	control performance weighting matrix
$\mathbf{W}_{\mathrm{d}}(\omega)$	disturbance scaling matrix
$\mathbf{v}_{\mathrm{I}}(t)$	white noise sequence, input
$\mathbf{v}_{\mathrm{o}}(t)$	white noise sequence, output
$\mathbf{V}_{\mathrm{I}}$	noise PSD, input
$\mathbf{V}_{\mathrm{o}}$	noise PSD, output
$x(n)$	unfiltered data
$x(t)$	position
$\mathbf{x}(t)$	state vector, plant
$\bar{\mathbf{x}}(t)$	relative state estimation error
$\hat{\mathbf{x}}(t)$	state estimate
$\tilde{\mathbf{x}}(t)$	state estimation error

$\mathbf{x}_{\mathrm{aug}}(t)$	state vector, bias
$\mathbf{x}_{\mathrm{c}}(t)$	state vector, controller
$\mathbf{x}_{\mathrm{d}}(t)$	state vector, biased multi-tonal multi-dimensional disturbance
$\mathbf{x}_{\mathrm{di}}(t)$	state vector, one dimensional disturbance
$x_{\mathrm{filt}}(k)$	filtered data
$\mathbf{x}_{\mathrm{p}}(t)$	state vector, process
$\mathbf{x}_{\mathrm{s}}(t)$	state vector
$\mathbf{x}_{\mathrm{sen}}(t)$	state vector, sensitivity functions
$\mathbf{x}_{\mathrm{ud}}(t)$	state vector, unbiased multi-dimensional disturbance
$X(k)$	Fourier transformed data
$X(s)$	Laplace transformed displacement
$\mathbf{y}(t)$	measured output
$\bar{\mathbf{Y}}_{m}(q)$	Fourier transformed outputs
$\hat{\mathbf{y}}_{\mathrm{p}}(k)$	estimated process output
$\mathbf{y}_{\mathrm{p}}(t)$	process output
$\mathbf{y}_{\mathrm{s}}(t)$	output vector
$\mathbf{z}(t)$	performance variable
$\hat{\mathbf{z}}(t)$	estimated performance variable
$\mathbf{z}_{\mathrm{m}}(t)$	state vector, modal coordinates
α	performance weighting coefficient, process states
α_{s}	proportional damping coefficient
β	performance weighting coefficient, disturbance states
β_{s}	proportional damping coefficient
γ	performance weighting coefficient, bias states
$\mathbf{\Delta}$	diagonalised system matrix
$\mathbf{\Delta}_{\mathrm{I}}(s)$	input model error
$\mathbf{\Delta}_{\mathrm{o}}(s)$	output model error
ε	control design damping parameter
$\boldsymbol{\eta}(t)$	modal displacement vector
$\boldsymbol{\theta}(k)$	parameter vector, frequency estimation
$\mathbf{\Theta}$	state-space diagonalisation matrix
λ	eigenvalue
$\boldsymbol{\lambda}(\omega)$	characteristic loci
$\mathbf{\Lambda}$	vector of actuator limits
$\mathbf{\Lambda}_{\mathrm{m}}$	modal damping matrix
ξ	damping ratio
$\mathbf{\Sigma}$	diagonalised Gramians
φ	phase of the sinusoidal signal
$\mathbf{\Phi}$	modal coordinate transformation matrix
$\mathbf{\Phi}(k)$	phase of the disturbance signal
$\hat{\mathbf{\Phi}}(k)$	estimated phase of the disturbance signal

ω	frequency
ω_{d}	disturbance frequency
$\hat{\omega}_{\mathrm{d}}(k)$	estimated disturbance frequency
$\omega_{\mathrm{e}}(k)$	deviation from the reference frequency
$\boldsymbol{\omega}_{\mathrm{hz}}$	vector of disturbance frequencies
ω_n	nominal natural frequency
ω_{ref}	reference frequency
$\boldsymbol{\Omega}$	matrix of disturbance frequencies
$\boldsymbol{\Omega}_{\mathrm{m}}$	modal frequency matrix

Operations

$\lvert\cdot\rvert$	absolute value, Euclidean norm
$\lVert\cdot\rVert_\infty$	Hinf-norm
$\otimes$	Kronecker product
$(\cdot)^H$	conjugate-transpose
$(\cdot)^T$	transpose
$(\cdot)^{-T}$	transposed inverse of a matrix
$E\{\cdot\}$	mathematical expectation
$F(\cdot)$	discrete Fourier transformation
s	Laplace operator
z	time-shift operator
$\lambda(\cdot)$	eigenvalues of a matrix
$\sigma(\cdot)$	singular values of a matrix
$\bar{\sigma}(\cdot)$	largest singular value of a matrix
$\underline{\sigma}(\cdot)$	smallest singular value of a matrix

Abbreviations

ARE	algebraic Riccati-equation
BIBO	bounded input, bounded output
CC	convergent control
DFT	discrete Fourier-transformation
DOF	degrees of freedom
DOFC	direct optimal feedback compensation
FEM	finite element model
FRF	frequency response function
FSCF	frequency shaped cost functionals
HHC	higher harmonic control
IDC	input disturbance cancellation
IHC	instantaneous harmonic control
IMC	internal model control
LHP	left half-plane
LMI	linear matrix inequality
LPV	linear parameter-varying
LQ	linear quadratic
LQG	linear quadratic Gaussian
LTI	linear time-invariant
LTV	linear time-varying
MIMO	multiple input, multiple output
ODE	ordinary differential equation
PR	pseudo-random
PSD	power spectral density
RLS	recursive least squares
SFSCF	simplified frequency shaped cost functionals
TMD	tuned mass damper
UMP	unbalanced magnetic pull

Contents

1. Introduction

This chapter briefly summarises the background and motivation of the work done in this thesis. The research topics are further discussed in the subsequent chapters. Also, the scope of this work and the contributions of the author are defined. Finally, a brief survey of the publications included and the structure of the thesis are given.

1.1 Background and motivation

Vibration, defined as "*a periodic motion of the particles of an elastic body or medium in alternately opposite directions from the position of equilibrium when that equilibrium has been disturbed (as when a stretched cord produces musical tones or molecules in the air transmit sounds to the ear)*" (Merriam-Webster, 1995), is usually an unwanted phenomenon present in any physical structure. The vibration as a concept is a sub-class of a phenomenon usually referred to as noise, with the major difference of being persistent and deterministic in nature compared with white noise disturbance, which is considered a stochastic phenomenon. As one would expect, vibrations are part of everyday life and they are mostly not problematic enough to be even noticeable. However, in certain situations this phenomenon can be very problematic, and some measures have to be taken to minimise its impact. From the historical point of view, the solution to the problem of vibration control is closely related to the design of the physical system (Icerman, 1969). Namely, the structures and systems are designed such that the vibrations are of no significance in the expected operation conditions. Many of these structures such as bridges, buildings, cars and ships are indeed present in everyday life. Another group of processes that can be found in all fields of the industry today are electric and combustion motors, propellers, rollers, shakers, pneumatic and hydraulic systems, basically any system which has reciprocating components or inertia. Ultimately, the problem field can be extended to signals and data, where the problems are traditionally solved by signal processing techniques, such as suitable pre- and post-filtering. Hence, it is apparent that the field of applications where the problems may occur is significantly vast.

The problems that vibration causes vary depending on application. In cars and other machinery operated from within by a human operator, the problems are typically directed to the operator with the impact varying from discomfort and nausea to severe medical conditions (Seidel, 1993). In structures, the causes are typically related to structural wear and tear, potentially resulting in a catastrophic structural failure (Ammann *et al.*, 1941). In process industry, the causes vary from increased costs due to increased process downtimes and maintenance that are a direct consequence of the wear and tear of the process components (Nandi *et al.*, 2005). Another cause is directly related to the end-product of the process, which may become defect or of a lower grade due to the inconsistency resulting from the vibrations along the process line (Virtanen, 2006). Additionally, the design specifications of a process may be governed by limitations targeted to minimise the potential vibration. As a whole, the minimisation of the impact of vibration in a system may yield significant cost savings and prevention of potential health hazards.

Due to the vast number of problems presented above and the vast number of potential applications where they may occur, the field of vibration mitigation has been a very active field of study for decades. The majority of the solutions are so-called passive approaches, simply due to the fact that the problems have been present for a long time, while adequate computational power has been available for a relatively short time. Probably the best known of these solutions is the car suspension (Sharp and Crolla, 1987). This simple element consisting of a spring and a viscous damper is used to effectively prevent the bumps in a road to cause any significant movement of the chassis. Other approaches can be found in tall buildings, where the addition of a specific element in the structure prevents the building from swaying (Kareem *et al.*, 1999). Finally, in bridges the addition of damper elements or specific design of the bridge span prevents the structure from vibrating under varying load or external excitation forces such as wind (Spencer and Nagarajaiah, 2003). The common goal for any of these passive approaches is to change the dynamics of the structure in a way that makes it insensitive to vibrations occurring at its presumed operational frequency band. The resulting modified system is guaranteed to be inherently stable, which is one of the major benefits of the approach in addition to the low costs.

Although the passive approaches may seem a perfect solution for the problem, they still suffer from several disadvantages, which are directly related both to the feasibility of the resulting structure and the obtainable performance. In the industry today, the requirements for the acceptable performance under external disturbance can be very demanding. In addition, the vibration may be excited externally with varying frequency, effectively rendering the passive approaches inadequate thereof. For this purpose, the problem of vibration mitigation has been re-evaluated and redefined as a control problem; hence enabling the use of the very powerful tools of control engineering. In active vibration mitigation, an additional force is generated through an actuator realising a control signal that effectively negates the vibration forces. This approach enables the mitigation of disturbances at any frequency in any system without the need for changing the structure of the system itself. These active approaches have been widely applied e.g. in automotive (Bohn *et al.*, 2004), aviation (Hall and Wereley, 1989; Bittanti *et al.*, 1996), marine (Daley *et al.*, 2004) and process (Knospe *et al.*, 1995) industries. Today, even the higher quality washing machines (Spelta *et al.*, 2008) are equipped with a system that compensates the force vibrations. The impact of such system is clearly distinguishable during the spin cycle as the machine actually stays in place instead of slowly crawling around the room. What is notable is the fact that previously these machines used passive vibration damping, with satisfactory, yet rather inadequate performance. Hence, the current trend to higher performance machinery is apparent even in the everyday household items.

The significant increase in the available computation power which took place in the last decade has made active vibration control both a feasible and a plausible approach. Today, the computational power is both inexpensive and very powerful. It is anticipated that this trend continues and in the near future even more complex control algorithms can be cost-effectively implemented in many applications, in which active vibration control currently may not be a feasible approach. Hence, it is obvious that the research devoted to active vibration mitigation is more actual than ever.

1.2 The scope and objectives of the thesis

The control methods applied in active vibration control today cover practically all of the traditional methodologies, ranging from the adaptive to the model based approaches, where the methodologies such as optimal and robust control have been exploited. Although these methods have provided good results, they suffer from several disadvantages, depending on the applied control approach, varying from very complex design procedures, a high number of free tuning variables, inability to perform well in non-square systems, poor robustness and stability in multi-tonal problems, inability to suppress frequency varying disturbances to high demand for computational power and data storage.

This thesis focuses on the compensation of frequency varying multi-tonal vibrations by the means of model based optimal and nonlinear control. Adaptive control methodologies, although very applicable, are excluded from the scope of this study. Also, the assumption of disturbances occurring at discrete frequencies excludes the problems related to general active sound and noise control (ANC) algorithms from this study.

The objective of this work is to introduce a novel generic nonlinear control algorithm for the compensation of multiple frequency varying tonal disturbances in a process with arbitrary input-output dimensions. The control approach should yield a good closed-loop robustness and performance while minimising the number of free design parameters. The proposed approach utilises the very powerful tools of optimal control theory and continuous gain-scheduling in finding the optimal solution to the given problem. The main focus of the work is in applied control theory; however the aspects related to the practical implementation are discussed whenever applicable, since control engineering is ultimately a field of science for practical applications.

1.3 Contributions of the author

The main contributions of this thesis, ordered by the importance, can be summarised as follows:

- A proposal is made for an optimal linear control law, capable of mitigating multiple static frequency tones in a linear system with arbitrary input-output dimensions. The major differences with regard to the existing control approaches are the low number of free design parameters, normalised performance in terms of the underlying process dynamics and the possibility to alter the robustness properties of the closed-loop system directly.
- A proposal for a nonlinear control law is made, capable of mitigating multiple disturbances with time varying frequencies in a system with arbitrary input-output dimensions in the presence of known nonlinearities. The nonlinear controller is realised as a continuously gain-scheduled set of linear controllers. There are major differences with regard to the existing methods. Namely, the gain-scheduling is realised by replacing the elements of the feedback matrices with continuous functions of the scheduled variables. A set of optimal linear controllers are used as the basis for the gain-scheduling, hence providing the same benefits for the performance and design as in the linear case. The design procedure is simpler than for example in robust control approaches.

- A proposal is made for the determination of weighting matrices in the optimal estimator design, applicable for problems related to active vibration control. The weighting matrices are defined such that the variations of the internal state variables of the process are scaled to approximate unity, hence allowing the application of the same design parameters for similar performance, regardless of the underlying process dynamics. In essence, the process models are normalised over a set of discrete predefined frequency points.
- An identification procedure applicable to models for active vibration control problems is designed. The enhancement is based on direct band-pass filtering of the signals in the frequency domain. Such filtered signals yield a natural and predictable model reduction, where the information over a desired frequency band is preserved. The identification routine itself is standard (Ljung, 1999).
- A definition of functions required for an extensive performance evaluation of a control law in active vibration control problems is presented. The given functions can be used to verify the performance, stability and robustness of the resulting closed-loop system. The functions themselves are standard and generally rather well-known, yet they are seldom applied in studies regarding vibration mitigation problems. The analysis concept is further extended to consider the absolute performance analysis obtained directly from the signals used for the modelling, instead of the model, which is always biased.
- An extensive survey and comparison of the most popular present linear control approaches for active vibration control is carried out. The performance of the controllers is evaluated in a common framework both in the frequency domain for steady state analysis and in the time-domain for transient time analysis. The results of the comparison are collected and evaluated, enabling the designer to choose a suitable control approach for a particular problem at hand.
- A procedure for control scheme feasibility evaluation is designed. The design of an active vibration control system typically includes the choice of proper actuators. The suitability of such actuators for a particular problem can be evaluated through the determination of the control scheme feasibility. The evaluation is based on the concept of perfect vibration mitigation. The procedure allows the designer to decide whether an acceptable level of mitigation is

obtainable and whether there is an excessive or an inadequate number of actuators.

- An internal model control (IMC)-like approach to the reconstruction of the output signal frequency content in a controlled process is designed. Such reconstruction is essential when the disturbance frequency is estimated from the controlled quantity. Without the reconstruction, the frequency information is lost.

1.4 Summary of the publications

This thesis is an article dissertation composed of five research articles of which four are journal articles and one is a conference article. The articles represent the research made on the subject in several case studies in several research projects. The methods applied for the vibration mitigation evolved during the course of the research; hence the applied control law is not exactly the same as presented in this thesis in every article. Yet, similar results are obtainable with the proposed approach, although with better performance. The articles are chosen such that they cover several different processes and control problems hence allowing the generality evaluation of the proposed approach. Also, an article comparing the most popular control approaches against the proposed approach is included. That allows the evaluation of the performance of the proposed approach with respect to the existing methods. There are also several articles by the author not included herein, since the results are more or less overlapping with those included; however the references to these works are contained in the publications. The publications are considered in detail in Chapters 5 and 6; however, a brief summary of their content is given in the sequel.

Publication I. The paper considers the problem related to the suppression of radial rotor vibrations in an electric machine. This is a problem very common for any process containing rotating shafts or rotors. The obtained results can be generalised for any such system. In this paper, the design procedure for a controller composed of a linear optimal controller cascaded with an instantaneous harmonic controller (IHC) is presented in detail. The results show that by introducing such control law into the process, the performance and stability of the system can be considerably increased.

Publication II. The paper describes a study related to the blocking of mount force transmissions in a steel bar mounted on a flexible surface. The tests were carried out in a laboratory test-bed environment. The disturbance excited in the system has unmeasurable time varying frequency; hence the nonlinear controller with an embedded frequency estimator is implemented. The performance and stability of the proposed approach are evaluated under two scenarios, in which the frequency of the disturbance is varying either linearly or subject to a discrete change. The results show that the nonlinear control approach is capable of providing a very high rate of mitigation while remaining robustly stable.

Publication III. The paper considers vibration mitigation in another family of processes, namely those including rolling of some kind. As an example of a such process, the problems related to a specific industrial scale rolling process are considered. Although these are rather similar to the processes considered in PUB. II, they still have some specific features not typically encountered in other systems. The control approach used to tackle the perceived force variations encountered in such processes is described in the paper. The required control forces are generated by hydraulic actuators, which are in general nonlinear and have characteristics not encountered in other actuators. The obtained results show that the control approach proposed in the thesis is capable of providing high vibration mitigation in the family of processes considered, despite the actuator input nonlinearity.

Publication IV. The paper considers vibration mitigation at the mounts of a machinery raft, essentially resulting in the blockage of the mount force transmissions. The particular process considered a marine diesel engine and a generator mounted on a raft. Such rafts can be found practically in any branch of industry and they all share similar vibration problems. From the point of view of the thesis, this article considers the worst case scenario in the field of application for the proposed control approach, hence being the final test for its applicability. The process contains high level background noise, several deterministic vibrations that are not to be controlled, and several tonal disturbances with unmeasurable time varying frequencies that are to be mitigated by the use of several actuators with strong cross-couplings. In essence, the system is a full multiple-input, multiple-output (MIMO) system with high demand for controller robustness. The results show that the proposed control approach was capable of providing close to the best obtainable rate of mitigation, while remaining robust to the noise and modelling errors.

Publication V. In this paper a survey of some of the most popular linear vibration mitigation approaches is conducted. The performance of the existing controllers is cross-validated versus themselves and versus the approach proposed in the thesis. The evaluation is carried out both in the frequency domain for steady state performance and in the time-domain for transient time performance. The main results of the analyses are collected in tables allowing a system designer to choose a proper approach for a particular problem at hand.

1.5 The structure of the thesis

This thesis is structured as follows. In Chapter 2, the concept of vibration control and the underlying problems are discussed in detail. The problem formulation and aspects related to the identification and system modelling for the purposes of active vibration control are discussed in Chapter 3. In Chapter 4, some issues related to the estimation of the disturbance frequency are discussed along with the detailed description of the design of both linear and nonlinear control law. The concepts related to performance, feasibility and robustness analysis of the closed-loop system are presented in Chapter 5. In Chapter 6, the performance and applicability of the proposed control approach are evaluated by several case studies. The concluding remarks and discussion are given in Chapter 7.

2. Vibration control

Vibration control is a concept of many meanings and interpretations, depending on the field of study of the engineer working with the problem. For control engineers, the problem is clearly related to the actual control of vibrations by some external means. For engineers from different disciplines the term control may have a completely different meaning. In this chapter the elementary concepts related to vibration are given, as well as a classification of the different control approaches into distinct groups.

2.1 Fundamentals of vibrations

Vibration is a common phenomenon in any physical structure. In the context here, vibration is defined as a periodic (i.e. sinusoidal) signal (for example force) acting at a distinct discrete frequency. In the context of sinusoidal disturbance, the vibration may act at several distinct frequencies simultaneously and in multiple dimensions; yet it is always considered a deterministic signal thus making a clear distinction to random noise and stochastic processes.

Vibration occurring in a process can be divided into two categories, namely free and forced vibration (Inman, 2006). The former class represents systems, whose response is not resulting from some external force input. In essence, the response is a result from some initial perturbation from the equilibrium state of the system. In these cases, the perceived vibrations are dominated by the characteristics of the system, namely by its natural frequencies. A common example of such a system is a car driving into a bump in the road that causes an oscillation of the car frame that mitigates relatively fast. Although the concept of free vibration explicitly excludes any external inputs, within this thesis the impulse responses of the systems are regarded as free vibration. The latter class represents systems that are subject to some persistent force excitation. The excitation energy can be spread over the whole frequency band, or be concentrated on one or several narrow frequency bands, forcing the system to oscillate at those frequencies regardless whether it is the natural frequency or not. A common example of such system is a revolving rotor with some mass imbalance generating a sinusoidal external force at the revolution frequency. The focus of this thesis is in the latter class of persistent sinusoidal disturbances. The problems related to the control of freely oscillating processes are in a sense similar, yet rather trivial to tackle with the existing methods (Fuller *et al.*, 1996).

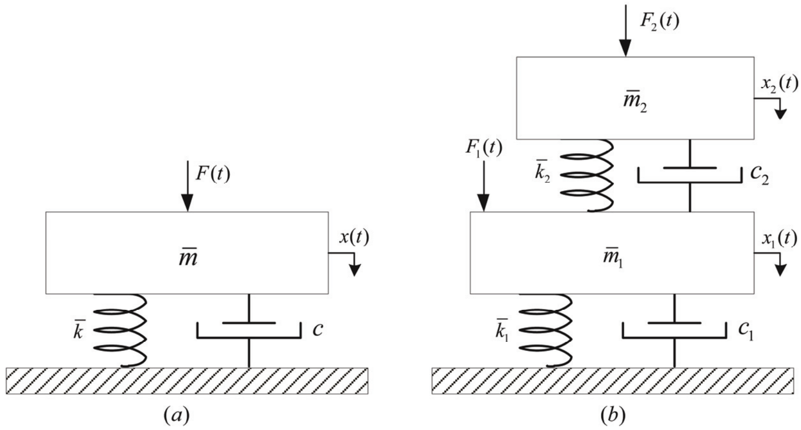

Figure 2.1 (a) 1DOF-spring-mass-damper system. (b) 2DOF-spring-mass-damper system.

In order to gain understanding of the underlying problems, the concept of natural frequency needs to be established. Consider a trivial example of a simple one-degree of freedom (1DOF) mass-spring-damper system illustrated in Figure. 2.1a.

It is straightforward to derive the governing ordinary differential equation (ODE) as:

$$\bar{m}\ddot{x}(t) + c\dot{x}(t) + \bar{k}x(t) = F(t)\,, \tag{2.1}$$

which can be written in the transfer function form as:

$$G(s) = \frac{X(s)}{F(s)} = \frac{\frac{1}{\bar{m}}}{s^2 + \frac{c}{\bar{m}}s + \frac{\bar{k}}{\bar{m}}}\,. \tag{2.2}$$

By comparing Eq. (2.2) with the general transfer function for a second order system (found in any basic control engineering textbook e.g. (Dorf and Bishop, 2008)), given as:

$$G(s) = \frac{K_G\omega_n^2}{s^2 + 2\xi\omega_n s + \omega_n^2}\,, \tag{2.3}$$

where ω_n is the nominal natural frequency and ξ is the damping coefficient of the system. It is now straightforward to derive the connection between the system parameters and the natural frequency and the damping coefficient as:

$$\omega_n = \sqrt{\frac{\bar{k}}{\bar{m}}}$$
$$\xi = \frac{c}{2\sqrt{\bar{k}\bar{m}}} . \qquad (2.4)$$
$$K_G = \frac{1}{\bar{k}}$$

It is obvious that the natural frequency is determined by the mass of the system and the stiffness of the spring. The height and sharpness of the resonance peak are determined by the ratio between the damper coefficient and the combined characteristics of the spring and the mass.

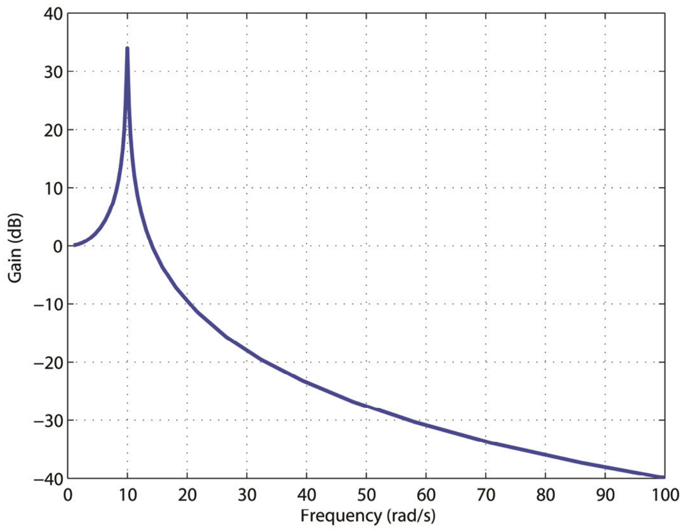

Figure 2.2 Frequency response function of the 1DOF- spring-mass-damper-system.

An illustrative frequency response function (FRF) is given in Figure 2.2, with the values of the coefficients set as: $\bar{m} = 1000\text{kg}$, $\bar{k} = 100000\frac{\text{kg}}{\text{s}^2}$ and $c = 200\frac{\text{kg}}{\text{s}}$, implying: $\omega_n = 10\frac{\text{rad}}{\text{s}}$ and $\xi = 0.01$.

The implication of the natural frequency is now evident. It is the frequency where the input signal is subject to substantial amplification when compared with the adjacent frequencies. Naturally, a higher order system may have multiple natural frequencies, in fact as many as there are pole pairs with imaginary components. However, the natural frequency does not always imply a distinct amplification peak (in the case of over-damped poles), which is essentially the goal in some of the passive control methods. Often, for proper systems the maximal amplification usually takes place at the first frequency peak and then decreases as a function of frequency for the latter peaks. Hence, the vibration control problems are often, yet not nearly always, related to the first mode (first natural frequency) of the system.

A 1DOF-system is usually inadequate for describing the phenomenon taking place in real processes. Fortunately, the model is readily extended to nDOF-systems. For this purpose the dynamics of a 2DOF-system, illustrated in Figure 2.1b, are derived as:

$$\begin{cases} \bar{m}_1\ddot{x}_1(t)+\left(c_1+c_2\right)\dot{x}_1(t)-c_2\dot{x}_2(t)+\left(\bar{k}_1+\bar{k}_2\right)x_1(t)-\bar{k}_2x_2(t)=F_1(t) \\ \bar{m}_2\ddot{x}_2(t)-c_2\dot{x}_1(t)+c_2\dot{x}_2(t)-\bar{k}_2x_1(t)+\bar{k}_2x_2(t)=F_2(t) \end{cases}. \tag{2.5}$$

By defining $\mathbf{q(t)}=\left[x_1(t) \quad x_2(t)\right]^T$, Eq. (2.5) can be written as:

$$\underbrace{\begin{bmatrix} \bar{m}_1 & 0 \\ 0 & \bar{m}_2 \end{bmatrix}}_{\mathbf{M}_s}\ddot{\mathbf{q}}(\mathbf{t})+\underbrace{\begin{bmatrix} c_1+c_2 & -c_2 \\ -c_2 & c_2 \end{bmatrix}}_{\mathbf{C}}\dot{\mathbf{q}}(\mathbf{t})+\underbrace{\begin{bmatrix} \bar{k}_1+\bar{k}_2 & -\bar{k}_2 \\ -\bar{k}_2 & \bar{k}_2 \end{bmatrix}}_{\mathbf{K}_s}\mathbf{q}(\mathbf{t})=\underbrace{\begin{bmatrix} F_1(t) \\ F_2(t) \end{bmatrix}}_{\mathbf{F}(t)}, \tag{2.6}$$

where $\mathbf{M}_s$ is called the mass matrix, $\mathbf{C}$ is called the viscous damping matrix and $\mathbf{K}_s$ is called the stiffness matrix (Inman, 2006). It is notable that due to the symmetry of these matrices, their corresponding eigenvalues are positive real, implying that the system is guaranteed to be bounded input, bounded output (BIBO) stable.

In the literature, the possible gyroscopic and circulatory phenomena in a system are typically included in the dynamics, yielding the general representation for nDOF systems (Inman, 2006):

$$\mathbf{M}_s\ddot{\mathbf{q}}(t)+\left(\mathbf{C}+\mathbf{G}\right)\dot{\mathbf{q}}(t)+\left(\mathbf{K}_s+\mathbf{H}_s\right)\mathbf{q}(t)=\mathbf{F}(t). \tag{2.7}$$

It should be noted that due to the inclusion of the skew symmetric matrices $\mathbf{H}_s$ and $\mathbf{G}$, the guaranteed stability of the system is lost.

The ODE representation of the system dynamics is not very usable for the control engineering purposes. Hence, a general state-space representation of nDOF systems is derived as:

$$\begin{cases} \dot{\mathbf{x}}_s(t)=\mathbf{A}_s\mathbf{x}_s(t)+\mathbf{B}_s\mathbf{u}_s(t) \\ \qquad =\left[\begin{array}{c|c} \mathbf{0} & \mathbf{I} \\ \hline -\mathbf{M}_s^{-1}\left(\mathbf{K}_s+\mathbf{H}_s\right) & -\mathbf{M}_s^{-1}\left(\mathbf{C}+\mathbf{G}\right) \end{array}\right]\mathbf{x}_s(t)+\left[\begin{array}{c} \mathbf{0} \\ \hline \mathbf{M}_s^{-1} \end{array}\right]\mathbf{u}_s(t), \\ \mathbf{y}_s(t)=\mathbf{C}_s\mathbf{x}_s(t)=\left[\mathbf{I} \mid \mathbf{0}\right]\mathbf{x}_s(t) \end{cases} \tag{2.8}$$

with $\mathbf{x}_s(t)=\left[\mathbf{q}^T(t) \mid \dot{\mathbf{q}}^T(t)\right]^T$, $\mathbf{u}_s(t)=\mathbf{F}(t)$ and $\mathbf{y}_s(t)=\mathbf{x}_s(t)$.

Now, the natural frequencies of the system can be determined from the eigenvalues of the system matrix $\mathbf{A}_s$ as the Euclidian norm of the poles with imaginary components.

The benefit of the general representation for nDOF becomes apparent by considering the properties of mechanical systems. In practice, any mechanical structure or element can be split into infinitesimal pieces whose dynamics can be expressed by a 1DOF spring-mass-damper system. These subsystems are interconnected, forming an nDOF distributed parameter model representing the dynamics of the structure. Essentially, this modelling approach is the celebrated finite element modelling approach (FEM) (Inman, 2006). For practical purposes, the lumped parameter models are preferred, yet any generalised control approach derived for the system in Eq.(2.8), is applicable to any linear time-invariant (LTI) system, regardless of the physical dimensions.

In practice, the process dynamics are usually unknown and exact modelling based on the theoretical physical properties is impossible. In these cases, the dynamics of the system are described by black-box models describing the input – output relation. The internal process states of these models no longer have any physical interpretation. However, as the input-output relation still satisfies the true process dynamics, the interpretation of the natural frequencies of the system is exactly the same as it is for the models derived with the true system parameters. Therefore, the vibration mitigation methods described in the following sub-sections are directly applicable to any LTI-process (including non-mechanical systems).

2.1.1 Modal coordinates

For certain types of problems, it is beneficial to represent the dynamics of the mechanical system in modal form. In the modal coordinate basis, the system is parameterised according to its natural frequencies. In this relation, the original stiffness, damping and mass characteristics of the lumped system are divided over the different modes (natural frequencies), yielding modal mass, modal stiffness and modal damping coefficients that describe the behaviour of a single mode (Fuller *et al.*, 1996). Under the assumptions, $\mathbf{H}_s = \mathbf{0}$, $\mathbf{G} = \mathbf{0}$ and $\mathbf{D} = \alpha_s \mathbf{K}_s + \beta_s \mathbf{M}_s, \exists \alpha_s, \beta_s \in \mathbb{R}$ (proportional damping), the different modes of the system can be decoupled (Fuller *et al.*, 1996). Decoupling simplifies the control design significantly, which is one of the main reasons for the modal representation in the first place. Unfortunately, the assumptions are not, in general, valid in practice. However, if the assumptions are valid, the change to modal coordinate basis is straightforward. First, consider a linear transformation:

$$\mathbf{x}_s(t) = \mathbf{M}_s^{-\frac{1}{2}} \mathbf{\Phi} \boldsymbol{\eta}(t) . \tag{2.9}$$

By substituting Eq. (2.9) into the general representation of mechanical systems Eq. (2.7) (with the assumptions holding), we have:

$$\mathbf{M}_s \mathbf{M}_s^{-\frac{1}{2}} \mathbf{\Phi} \ddot{\boldsymbol{\eta}}(t) + \mathbf{D} \mathbf{M}_s^{-\frac{1}{2}} \mathbf{\Phi} \dot{\boldsymbol{\eta}}(t) + \mathbf{K}_s \mathbf{M}_s^{-\frac{1}{2}} \mathbf{\Phi} \boldsymbol{\eta}(t) = \mathbf{F}(t) . \tag{2.10}$$

Premultiplication of Eq. (2.10) by $\mathbf{\Phi}^T \mathbf{M}_s^{-\frac{1}{2}}$, yields the mass normalised modal representation of the system, given as:

$$\mathbf{\Phi}^T\mathbf{\Phi}\ddot{\mathbf{\eta}}(t)+\mathbf{\Phi}^T\mathbf{M}_s^{-\frac{1}{2}}\mathbf{D}\mathbf{M}_s^{-\frac{1}{2}}\mathbf{\Phi}\dot{\mathbf{\eta}}(t)+\mathbf{\Phi}^T\mathbf{M}_s^{-\frac{1}{2}}\mathbf{K}\mathbf{M}_s^{-\frac{1}{2}}\mathbf{\Phi}\mathbf{\eta}(t)=\mathbf{\Phi}^T\mathbf{M}_s^{-\frac{1}{2}}\mathbf{F}(t)\,. \quad (2.11)$$

The matrix $\mathbf{\Phi}$ is chosen as the eigenbasis of the matrix $\mathbf{M}_s^{-\frac{1}{2}}\mathbf{K}\mathbf{M}_s^{-\frac{1}{2}}$ and due to the symmetry of the matrix, this basis is orthonormal (Lay, 2006). Now, it follows that $\mathbf{\Phi}^T\mathbf{\Phi}=\mathbf{I}$, hence the Eq. (2.11) can be rewritten as:

$$\ddot{\mathbf{\eta}}(t)+\mathbf{\Lambda}_m\dot{\mathbf{\eta}}(t)+\mathbf{\Omega}_m\mathbf{\eta}(t)=\tilde{\mathbf{F}}(t)\,, \quad (2.12)$$

where $\tilde{\mathbf{F}}(t)$ is the modal force vector, $\mathbf{\eta}(t)$ is the modal displacement vector, $\mathbf{\Lambda}_m$ is the modal damping matrix and $\mathbf{\Omega}_m$ is a matrix of squared modal frequencies.

If the given assumptions are valid, the matrices in Eq. (2.12) are diagonal and given as:

$$\mathbf{\Omega}_m=\begin{bmatrix}\omega_1^2 & & 0\\ & \ddots & \\ 0 & & \omega_m^2\end{bmatrix},\quad \mathbf{\Lambda}_m=\begin{bmatrix}2\xi_1\omega_1 & & 0\\ & \ddots & \\ 0 & & 2\xi_m\omega_m\end{bmatrix} \quad (2.13)$$

where ω_i and ξ_i are the frequency and the damping coefficient of the *i*:th mode, respectively.

The benefit of the modal representation is now evident. Each mode of the system can be controlled individually without affecting the other modes. This is, naturally, possible with the original system also, yet the determination of a decoupling input signal for such systems is significantly harder. The drawback of the method is the rather tight assumption of proportional damping. If this assumption does not hold, the $\mathbf{\Lambda}_m$ is not diagonal, implying that the modes are coupled.

Another modal representation for the system is readily obtained by performing a similarity transformation on the state-space representation of the system Eq. (2.8). By choosing the transformation as:

$$\mathbf{x}_s(t)=\mathbf{\Theta}\mathbf{z}_m(t)\,, \quad (2.14)$$

where $\mathbf{\Theta}$ is invertible and satisfies the equality:

$$\mathbf{A}_s=\mathbf{\Theta}^{-1}\mathbf{\Delta}\mathbf{\Theta}\,, \quad (2.15)$$

where $\mathbf{A}_s$ is the system matrix of the system and $\mathbf{\Delta}$ is some diagonal matrix.

The above similarity transformation can be performed to any process with a diagonalisable system matrix $\mathbf{A}_s$, which is a significantly milder assumption than the assumptions used in the direct transformation of the system into the modal coordinates in Eq. (2.9). The modal representation of the system can now be given as:

$$\begin{cases} \dot{\mathbf{z}}_{\mathrm{m}}(t) = \mathbf{\Delta}\mathbf{z}_{\mathrm{m}}(t) + \mathbf{\Theta}^{-1}\mathbf{B}_{\mathrm{s}}\mathbf{u}_{\mathrm{s}}(t) \\ \mathbf{y}_{\mathrm{s}}(t) = \mathbf{C}_{\mathrm{s}}\mathbf{\Theta}\mathbf{z}_{\mathrm{m}}(t) \end{cases}, \tag{2.16}$$

where $\mathbf{\Delta}$ is a diagonal matrix with the poles of the system at its diagonal.

It should be noted that the physical modal coordinates $\boldsymbol{\eta}(t)$ do not directly coincide with the state-space modal coordinates $\mathbf{z}_{\mathrm{m}}(t)$. However, there is a direct connection between the elements of $\mathbf{\Delta}$ and the modal damping and frequency, given as:

$$\begin{cases} \omega_m = \sqrt{\lambda_i \lambda_i^*} \\ \xi_m = -\dfrac{\lambda_i + \lambda_i^*}{2\sqrt{\lambda_i \lambda_i^*}} \end{cases}, \tag{2.17}$$

where λ_i is the first pole of the *i*:th complex valued pole pair of the matrix $\mathbf{\Delta}$.

2.2 Passive vibration damping

Passive vibration mitigation methods are by far the most common and popular solutions for vibratory problems and can be found practically anywhere ranging from washing machines, cars, computer hard drives into high precision laboratory instruments and civil buildings (Rivin, 2003) . The working principle of passive methods is to absorb the kinetic (vibration) energy from the system without bringing any external energy into the system. In practice, this implies that some portion of the kinetic energy is converted into some other form, for example heat, that eventually leaves the system. Another appealing implication is the guaranteed process stability when passive dampers are used.

A typical and a well-known example for passive vibration damping is the vibration isolation taking place in the car suspension. Here, the resonance frequency of the car chassis is altered by tuning the damping and spring-stiffness coefficients such that when the tyres hit a bump in the road, the resulting overall oscillation is significantly decreased. This type of damping is based purely on the characteristics of the dampers and the springs. An illustrative example on the impact of different damper parameters on the height and the sharpness of the natural frequency peak is given in Figure 2.3.

Another commonly used passive vibration damper is called the tuned mass damper (TMD) (Preumont and Kazuto, 2008). In this approach, an additional mass is attached to the system with a spring (possibly in parallel with a damper). The working principle of the method is to choose the ratio between the additional mass and the spring such that when attached to the system the mass vibrates in the anti-phase of the original mass element. These types of dampers are commonly found in sky-scrapers, bridges and similar slim and long span buildings, which are prone to wind and earthquake excited vibrations (Teramura and Yoshida, 1996; Lin *et al.*, 2000).

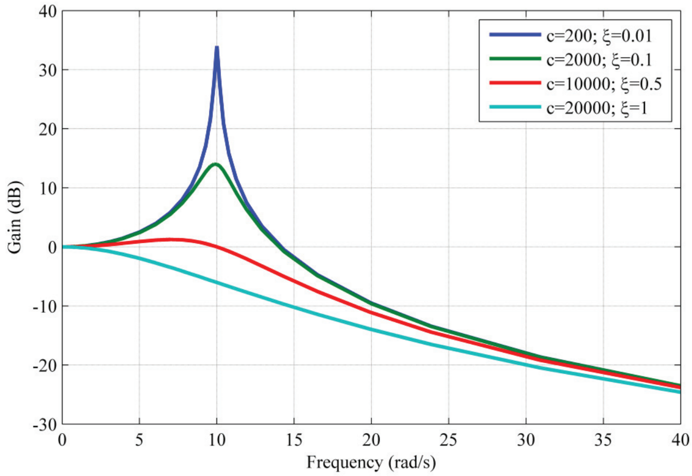

Figure 2.3 Frequency response of the 1DOF system with $\bar{k} = 100000\frac{kg}{s^2}$, $\bar{m} = 1000kg$ and different damping coefficients *c*.

For an example, consider the 1DOF-system given in Eq. (2.2). A TMD is designed for the system in order to cancel out the natural frequency peak. The parameters for the simple TMD are obtained from the equation (Preumont and Kazuto, 2008):

$$\omega_d = \sqrt{\frac{\bar{k}_d}{\bar{m}_d}}, \tag{2.18}$$

where ω_d is the frequency at which the additional damping is required, $\bar{k}_d$ is the stiffness of the spring attaching the additional mass to the system and $\bar{m}_d$ is the additional mass.

It is practical to choose the additional mass to be significantly smaller than the mass of the structure subject to vibration and obtain the desired damping frequency by adjusting the stiffness (a.k.a. spring constant) of the additional spring. In the example case, the disturbance frequency is $\omega_d = 10\text{rad/s}$ and the additional mass is chosen small, say $\bar{m}_d = 10\text{kg}$. According to the Eq. (2.18) the required spring stiffness is $\bar{k}_d = 1000\text{kg/s}^2$. As the additional mass is attached to the process, the dynamics of the resulting system are those of a 2DOF-system, illustrated in Figure. 2.1b. The resulting FRFs for the displacement of both mass elements are given in Figure 2.4.

The impact of the TMD is clearly visible in the FRFs as the frequency peak related to the original mass is split in two, resulting in two new potential problems. Also, the original vibration problem is now moved into the secondary mass. For nDOF-systems, the design procedure becomes quite more complicated as the parameters have to be adjusted based on the modal frequencies and the corresponding modal masses. It is also more likely that some unwanted phenomenon will occur in the other parts of the system than that considered in the original problem.

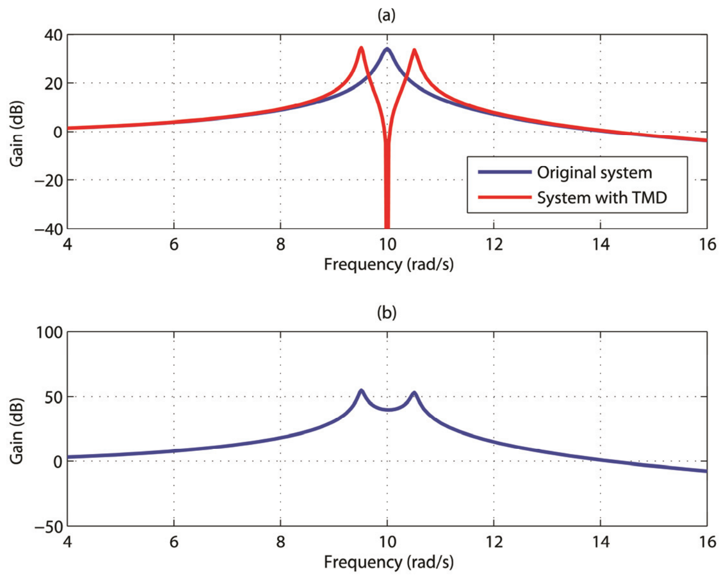

Figure 2.4 Impact of the tuned-mass-damper in a 1DOF-system. (a) The frequency response of the original mass element (with and without damper), (b) the frequency response of the mass element of the damper.

The rather surprising result in the preceding example is actually the fundamental property of linear systems, following directly from the Bode's integral theorem for stable systems (Skogestad and Postlethwaite, 2005), given as:

$$\int_0^\infty \ln\left|\mathbf{S}(j\omega)\right| d\omega = \mathbf{0}\,, \tag{2.19}$$

where $\mathbf{S}(j\omega)$ is the sensitivity function, describing the closed-loop sensitivity to the output disturbances. The phenomenon described by Eq. (2.19) is called the waterbed-effect, simply stating that the area under the FRF over infinite frequency range must be constant. From the vibration mitigation point of view, the implication of the waterbed-effect is rather discouraging, stating that if the amplitude of the frequency response is decreased at some frequencies, the same amount is added to other frequencies – regardless of what linear control approach is applied.

Under the light of the two preceding examples, the benefits and the drawbacks of the passive methods are readily defined as:

- Benefits:
    - Guaranteed process stability
    - Ease of design (for low order systems)
    - Rather inexpensive in terms both the materials and the design costs
- Drawbacks:
    - Limited performance at low frequencies
    - Very hard to design (for high order systems)
    - Intolerance to changes in the process dynamics (the system has to be redesigned)
    - Significant amplitude increase in the frequencies adjacent to the disturbance (for TMDs)

Overall, the passive methods should be preferred whenever they provide adequate vibration mitigation. For more complex systems, the semi-active and active methods should be considered.

2.3 Semi-active vibration control

The semi-active vibration mitigation methods are very similar to the passive ones, sharing most of the benefits and drawbacks. Like in the passive methods, the vibration energy is absorbed from the system without introducing any external control energy. However, there are some fundamental differences. The semi-active vibration control scheme is such that the parameters characterising the process, such as the spring stiffness, mass or the damping coefficient can be adjusted online. This enables the designer to change the dynamics of the system according to varying process operation conditions. Yet, by definition, no external energy is brought into the system, distinguishing it from the active vibration control. Hence, the process stability is guaranteed. A good collection of several semi-active control methodologies in different processes with different control schemes can be found in (Liu *et al.*, 2005; Zhou *et al.*, 2006). The semi-active vibration absorbers are divided into variable rate dampers and variable stiffness dampers that can be used in various situations (Symans and Constantinou, 1999; Jalili, 2002). The former group consists of such actuators as electro- and magneto-rheological dampers and adaptive fluid dampers. The latter group consists of piezo-electric actuators, hydraulic valves and springs with mechanically variable stiffness.

From the control engineering point of view, the semi-active vibration control schemes are actually linear time varying (LTV) processes as the system dynamics vary in time with respect to the adaptation signal (Rugh, 1993). The control principle is rather trivial, namely, if the process gain is high at the disturbance frequency, the process dynamics are changed to minimise the gain at that frequency.

As an example, consider a 1DOF-system with adjustable spring stiffness, given in the state-space form as:

$$\begin{cases} \dot{\mathbf{x}}_s(t,\bar{k}) = \mathbf{A}_s(\bar{k})\mathbf{x}_s(t,\bar{k}) + \mathbf{B}_s\mathbf{u}_s(t) \\ \mathbf{y}_s(t,\bar{k}) = \mathbf{C}_s\mathbf{x}_s(t,\bar{k}) \end{cases}, \tag{2.20}$$

where $\bar{k}$ is the variable spring stiffness.

The frequency characteristics of the system can now be given as a function of the spring stiffness as shown in Figure 2.5. Although, the "optimal" spring stiffness for any frequency is evident from the figure, the control law that realises it in every scenario is not. This is one of the biggest drawbacks of the semi-active control methods; the control law has to be tailored for the process, making the control design tedious.

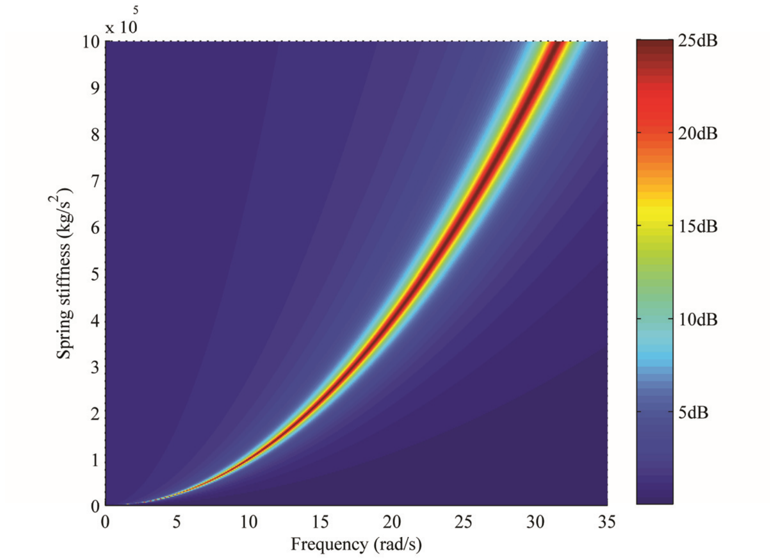

Figure 2.5 Frequency characteristics of a 1DOF-system as a function of the spring constant and correspondingly normalised damping factor.

2.4 Active vibration control

Active control is the most effective of the three methods for vibration mitigation. Unlike in passive methods, the working principle is to excite external energy into the system through some actuation in order to compensate the vibrations. In essence, an anti-phase sinusoidal force similar to the disturbance force is generated, resulting in a zero perceived net force. The major benefit of the method is the availability of all traditional control engineering tools and methods. This enables the designer to view the vibration problem as a common control problem with all the performance and robustness analysis tools available. Because of the external control forces, the control law can be designed in a similar manner for any process that can be expressed by an LTI-model. This eliminates one of the major drawbacks of the passive methods, where the whole physical process has to be redesigned whenever a part of it is changed. Another advantage of the method is the possibility to spread the additional gains in the FRF, which are due to gain minimisation at a frequency, over a wide frequency band thus minimising the impact of the waterbed effect. In its simplest form, the active vibration mitigation in a process can be obtained just as a few lines of standard C-code without any additional actuators or sensors, making it very cost effect thereof. Naturally, with some major benefits there come a few major drawbacks. By far the biggest drawback is the loss of guaranteed closed-loop stability that is characteristic for the passive and semi-active systems. Even though stability can be guaranteed to some extent by robust control design, the application of the method to critical systems, where instability would have disastrous consequences, is simply not possible. Another drawback is the required active control of the process. This implies the presence of some external energy source powering the actuators and some available computational power. Fortunately, the computation power is now days rather inexpensive and widely available. The control design for active systems is usually more demanding and tedious than for the simple passive systems, and therefore the design costs are in general rather high.

For active methods there is yet another way of dividing the vibratory control concept by classifying the problem to be either vibration cancellation or isolation. In the former class the source of the vibration itself is removed (or compensated), which is the more desirable option. However, in practice the forces required to direct compensation may be infeasibly high, or no actuation can be produced to the point of origin of the vibration. In the latter class, the transmission of the vibrations from a part of a structure to another is reduced. In this approach, the process itself is allowed to vibrate freely and only the transmission forces at the point of isolation are of interest. This is the more practical scenario, as the control satisfying the requirements can be produced without the need to actually address the source of the problem. The active methods can be readily used to tackle either one of the control problems, while for the passive methods the control goal is in the vibration isolation.

The focus of this thesis is in model based control designs for narrowband vibration mitigation. Hence, the examples of active control methods are picked from that field, even though there are a wide variety of effective methods that apply different control strategies. Also, the studied control problems are related to those of forced vibrations as the problem is somewhat more complex and the resulting control laws are applicable for free vibration problems as well. Typical applications, where active control is required, are processes in which the vibration occur at low frequencies, the desired suppression ratio is very high or the disturbance frequency or the process is time varying. There are plenty of publications on the successful applications of the active vibration control methods in various systems under both broad- and narrowband vibrations. These processes include structures (Sommerfeldt and Tichy, 1988; Chang and Yang, 1995; Moshrefi-Torbati *et al.*, 2006; Song *et al.*, 2006), helicopters (Hall and Wereley, 1989; Bittanti *et al.*, 1996), automotive engines (Bohn et al, 2004; Olsson, 2006), marine applications (Daley *et al.*, 2004), magnetic bearings and rotor systems (Knospe *et al.*, 1995; Fan and Lee, 1997; Knospe *et al.*, 1997a; Zhou and Shi, 2001; Knospe, 2007; Tammi, 2007; Chen and Zhu, 2008).

As an illustrative example of the free vibration control problems, consider the 1DOF of freedom system in Figure 2.1a, subject to some impulse disturbances (for example bumps in a road). The control goal is to minimise the frequency peaks at a desired frequency band. For simplicity, assume the process states to be measurable. Now, the trivial solution for the problem is to define a feedback gain $\mathbf{L}_s$ such that it moves the poles of the closed-loop system, corresponding to a particular vibration mode, into another location in the left half plane (LHP); where the poles are either real or as well damped as possible. The preceding control problem can be given in the closed loop form as:

$$\begin{cases} \dot{\mathbf{x}}_s(t) = \left(\mathbf{A}_s - \mathbf{B}_s\mathbf{L}_s\right)\mathbf{x}_s(t) + \mathbf{B}_s u_{ext}(t) \\ y_s(t) = \mathbf{C}_s\mathbf{x}_s(t) \end{cases}, \quad (2.21)$$

where $u_{ext}(t)$ is the external force input to the system described by Eq. 2.8 and $y_s(t)$ is the process output.

The control goal is now to choose the feedback such that the closed-loop eigenvalues corresponding to the vibration mode to be damped are of the form:

$$\lambda_m\left(\mathbf{L}_s\right) = a \pm jb\,, \quad (2.22)$$

where subscript *m* denotes the pole pair corresponding to the mode, *j* is the imaginary unit and $a \in \mathbb{R}$ and $b \in \mathbb{R}$ are the real and imaginary parts of the complex pole. For example, the following design rule can be derived for the pole locations

$$\sup_{\mathbf{L}_s}\{\xi\} = \sup_{\mathbf{L}_s}\left\{\left|\frac{a}{\sqrt{a^2+b^2}}\right|\right\}, a < 0\,, \quad (2.23)$$

in order to satisfy the design criteria for the pole placement. In essence, this simply states that the closed-loop poles should be placed on the negative real axis.

The impact on the closed-loop dynamics is apparent in Figure 2.6, where the open-loop poles are moved into a double pole at -10, thus flattening out the oscillation mode. However, there are some limitations on the usability of the given approach as the pole-positioning techniques usually result in excessive control actions, making the system less robust to model errors. Also, the poles of a high dimensional system may be moveable only along certain, unknown, trajectories, therefore making the problem significantly more complex. Then again, the control law is time-invariant, rather simple and readily solvable by the existing traditional control methods.

Remark 2.1. The problem can actually be solved as a H_∞-minimisation problem found in any robust control handbook (Zhou and Doyle, 1998), with the benefit of the possibility to restrict the control effort in the design.

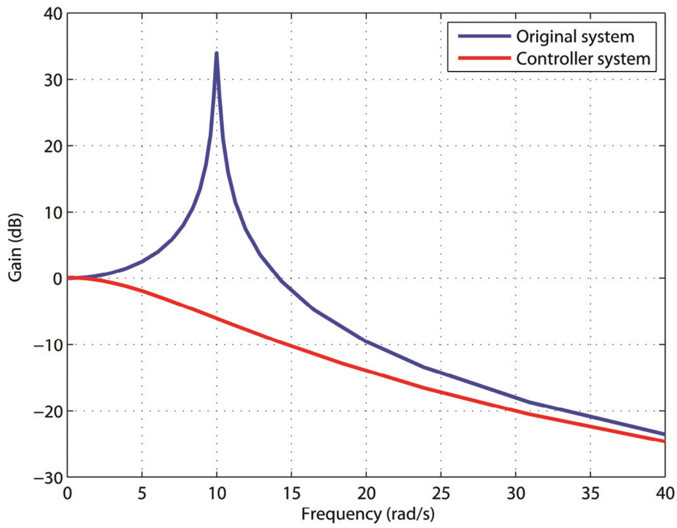

Figure 2.6 The impact of modal control in a 1DOF-system.

Another example illustrates the control problem related to forced vibrations in the 1DOF system shown in Figure 2.1a. Assume that the process is subject to some persistent input force disturbances at the same frequency as is the natural frequency of the system. The problem is tackled by an optimal control law that is the same as the one described in detail in Chapter 4. The resulting closed-loop system is shown in Figure 2.7.

According to the results, the control law minimises the vibrations at the given frequency, while spreading the impact of the waterbed-effect over a wide frequency band, producing substantially better results than those with the tuned mass damper given in Figure 2.4. Unlike to the modal control, the frequency peak related to the natural frequency is not removed; the damping takes place only at a very narrow frequency band. Hence, it is obvious that the modal control method is more suitable for broad band disturbance attenuation, while the tonal disturbance controller is suitable for mitigating distinct disturbance tones.

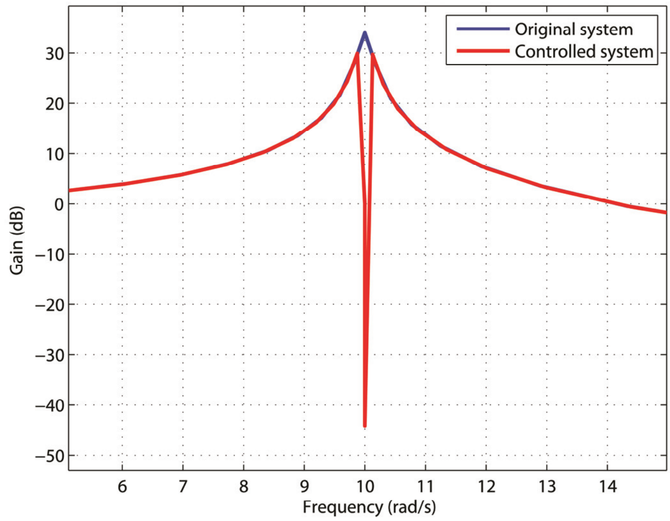

Figure 2.7 The impact of tonal disturbance controller for input disturbances in a 1DOF-system.

Again, under the given examples, the benefits and drawbacks of the active vibration mitigation methods can be collected as:

- Benefits:
  - Enables the use of the powerful control design techniques
  - Very high damping capability
  - Can be adjusted for varying process operation conditions
  - In some cases, no additional process components are required
- Drawbacks:
  - Inherently guaranteed system stability is lost
  - Design costs are typically higher than those of the passive methods
  - An external energy source is required for the actuation
  - Requires actively changing control signal and adequate computational power
  - A sudden loss of power of the control system may have disastrous consequences

As a conclusion, the designer should prefer passive control methods whenever they provide adequate and acceptable mitigation results. For high performance control and control in complex processes, the active control methods are preferable.

3. Problem formulation

In this chapter, the general control scheme for vibration control is introduced. In the following subsections, a model describing all phenomena of interest from the vibration control point of view is derived. The model is in general form and can be fitted to any vibration control problem that has the same base structure. In the last section, some aspects related to the identification of a model for vibration control purposes are discussed.

3.1 General problem definition

From the control engineering point of view, the problem of vibration mitigation can be interpreted as a problem of minimising some input or output disturbances in a process by applying (for example) feedback control. The main assumption distinguishing this specific control scheme from the other control problems is related to the nature of the disturbance. Namely, the disturbance is assumed to be deterministic and persistent, in essence, sinusoidal signals acting at one or several distinct discrete frequencies in one or several dimensions. The general control scheme representing the stated problem is shown in Figure 3.1.

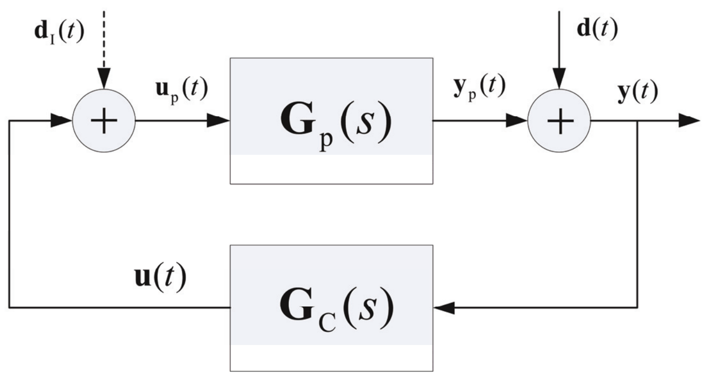

Figure 3.1. Layout of the general control scheme, where $\mathbf{G}_\mathrm{p}(s)$ and $\mathbf{G}_\mathrm{C}(s)$ are models representing the process and controller dynamics, respectively. $\mathbf{y}(t)$, $\mathbf{y}_\mathrm{p}(t)$, $\mathbf{u}_\mathrm{p}(t)$ and $\mathbf{u}(t)$ are the measured process output, realised process output, realised process input and control signals, respectively. $\mathbf{d}(t)$ and $\mathbf{d}_\mathrm{I}(t)$ are the sinusoidal output and input disturbances.

At the first glance, the control problem seems rather trivial as the ultimate goal is to mitigate one or several disturbances acting at distinct frequencies, in essence sinusoidal signals. This goal is readily met by exciting external sinusoidal signals into the system with the opposite phase and with the same amplitude.

Unfortunately, the problem becomes more complicated when the actuator dynamics and additional signals resulting from the normal process operation are introduced. Now, the external sinusoidal signals need to be realised such that only after passing through the actuator they cancel the disturbances. This realisation typically requires information on the actuator dynamics, namely a model. Also, some information on the disturbance signals is required, essentially their relative phase and amplitude. Because of the additional signals and measurement noise, the disturbance characteristics cannot be determined directly. Hence, the process measurements need to be filtered or an estimator has to be used. Additionally, due to the possible restrictions arising from the normal process operation, the process output cannot be controlled directly by for example a PID-controller as it would have an impact on the dynamics on a wide frequency band, while it may be strictly specified that only the sinusoidal disturbances are to be mitigated. Hence, the control scheme becomes such that the disturbances with known frequencies and unknown characteristics have to be determined, and a control effort has to be realised such that it has no impact on the adjacent frequencies and the process must remain stable in all possible scenarios.

An additional limitation on the applicable control strategies comes from the fact that it is practically impossible to distinguish the impact of the actuator from that of the disturbance when the process output signal is measured. This limitation prevents the use of many direct adaptive controllers as the process dynamics cannot be determined at the disturbance frequency. Finally, the disturbance frequency may vary over time, and in MIMO-processes it is plausible that a perfect mitigation is not realisable at all due to the internal cross-connections.

Ultimately, the seemingly trivial problem has become highly complex, requiring a very sophisticated control approach to fulfil all the requirements in a general process setup. Fortunately, there are methods that provide the desired control goal, one of which is discussed in greater detail in Chapter 4.

Another type of vibration control problem can be derived if the disturbance is assumed to be located at the process input. This corresponds to a case, where an unwanted process noise has corrupted some external control signal. A typical example of this is the additive disturbance in the realised control signal due to induced mains currents. This may cause very unwanted phenomena in the process response. The traditional solution is to replace the sensitive hardware with better-insulated hardware, which may be very expensive. This possibly expensive investment can be avoided by implementing another controller in the loop, which mitigates this input disturbance. Due to the assumption that the process is being controlled in such a way that it fulfils some well-defined performance criteria, it is required that the additional control-loop does not alter the input-output dynamics of the underlying process. In essence, the control effort is concentrated strictly on the disturbance frequency. This control problem is readily solved by using the same control law designed for the output disturbance but with a different performance weighting. This procedure is also described in detail in Chapter 4.

3.2 Modelling

A mathematical expression of the preceding control scheme is derived for the control design purposes. This expression describes both the process and the disturbance characteristics. The subsystems shown in Figure 3.1 and the corresponding overall model are derived in the following sub-sections.

3.2.1 Process model

The process model describes the dynamics between the applied control signals and the resulting response signals. The behaviour of the model is independent of the physical quantities and properties of the input and output signals. Hence, the same model structure is readily applicable to any process regardless whether the control signal is voltage, force or pressure etc. The process response can also be of an arbitrary quantity, for example acceleration, displacement, force or voltage etc. The limitations to the process model used here and the subsequent control design are the requirements for linearity and time invariance. Although these assumptions may seem rather restricting, the design is still applicable to many practical processes in which these assumptions do not exactly hold. This is because the process is quite often driven in the vicinity of a certain linear operation point and the time variance is so slow that it can be considered negligible.

Although the model is referred to as the process model, the dynamics that it describes are actually those arising from the interaction of the actuator and process characteristics. Hence, it should not be confused with the true process model, which is usually related to some other input-output behaviour. The general arbitrary dimensional state-space model representation of the process is given as

$$\begin{cases} \dot{\mathbf{x}}_\mathrm{p}(t) = \mathbf{A}_\mathrm{p}\mathbf{x}_\mathrm{p}(t) + \mathbf{B}_\mathrm{p}\mathbf{u}_\mathrm{p}(t) \\ \mathbf{y}_\mathrm{p}(t) = \mathbf{C}_\mathrm{p}\mathbf{x}_\mathrm{p}(t) + \mathbf{D}_\mathrm{p}\mathbf{u}_\mathrm{p}(t) \end{cases}, \tag{3.1}$$

where $\mathbf{A}_\mathrm{p} \in \mathbb{R}^{k\times k}$, $\mathbf{B}_\mathrm{p} \in \mathbb{R}^{k\times m}$, $\mathbf{C}_\mathrm{p} \in \mathbb{R}^{n\times k}$ and $\mathbf{D}_\mathrm{p} \in \mathbb{R}^{n\times m}$, where k, m and n denote the number of process states, inputs and outputs, respectively.

$\mathbf{u}_\mathrm{p}(t) \in \mathbb{R}^m$ is a vector of input signals exciting the process, $\mathbf{y}_\mathrm{p}(t) \in \mathbb{R}^n$ is a vector of process outputs and $\mathbf{x}_\mathrm{p}(t) \in \mathbb{R}^k$ is a vector of internal process states.

3.2.2 Disturbance model

A sinusoidal disturbance acting on a single frequency can be expressed as

$$d(t) = A\sin(\omega_d t), \tag{3.2}$$

where A and ω_d are the amplitude and the frequency of the disturbance in radians per second, respectively.

By differentiating the Eq. (3.2) twice and defining the state variables as $\dot{x}_1(t) = x_2(t)$ and $\dot{x}_2(t) = -\omega_\mathrm{d}^2 x_1(t)$, a state-space representation describing a sinusoidal signal driven by its initial values is obtained as

$$\begin{cases} \dot{\mathbf{x}}_{\mathrm{d}ip}(t) = \mathbf{A}_{\mathrm{d}ip}\mathbf{x}_{\mathrm{d}ip}(t) = \begin{bmatrix} 0 & 1 \\ -\omega_{\mathrm{d}ip}^2 & -\varepsilon \end{bmatrix}\mathbf{x}_{\mathrm{d}ip}(t) \\ d_{ip}(t) = \mathbf{C}_{\mathrm{d}ip}\mathbf{x}_{\mathrm{d}ip}(t) = \begin{bmatrix} 1 & 0 \end{bmatrix}\mathbf{x}_{\mathrm{d}ip}(t) \end{cases}, \tag{3.3}$$

with the initial values given as $\mathbf{x}_{\mathrm{d}ip}(0) = \begin{bmatrix} 0 & A_{ip}\omega_{\mathrm{d}ip} \end{bmatrix}^T$. The subscripts i and p denote the signal dimension and disturbance tone, respectively. The parameter ε is a design variable used for control design purposes, which is set zero unless stated otherwise.

A representation for a multi-tonal single dimensional disturbance, namely

$$d_i(t) = \sum_p A_p \sin(\omega_{ip} t), \tag{3.4}$$

is readily obtained as a composition of single tone disturbances, given as

$$\begin{cases} \dot{\mathbf{x}}_{\mathrm{d}i}(t) = \mathbf{A}_{\mathrm{d}i}\mathbf{x}_{\mathrm{d}i}(t) = \left[\begin{array}{c|c|c|c} \mathbf{A}_{\mathrm{d}i1} & \mathbf{0} & \cdots & \mathbf{0} \\ \hline \mathbf{0} & \mathbf{A}_{\mathrm{d}i2} & & \vdots \\ \hline \vdots & & \ddots & \mathbf{0} \\ \hline \mathbf{0} & \cdots & \mathbf{0} & \mathbf{A}_{\mathrm{d}ip} \end{array}\right]\mathbf{x}_{\mathrm{d}i}(t) \\ d_i(t) = \mathbf{C}_{\mathrm{d}i}\mathbf{x}_{\mathrm{d}i}(t) = \left[\begin{array}{c|c|c|c} \mathbf{C}_{\mathrm{d}i1} & \mathbf{C}_{\mathrm{d}i2} & \cdots & \mathbf{C}_{\mathrm{d}ip} \end{array}\right]\mathbf{x}_{\mathrm{d}i}(t) \end{cases}, \tag{3.5}$$

where $\mathbf{A}_{\mathrm{d}i} \in \mathbb{R}^{2p\times 2p}$, $\mathbf{C}_{\mathrm{d}i} \in \mathbb{R}^{2p}$ and $\mathbf{x}_{\mathrm{d}i} \in \mathbb{R}^{2p}$ with the initial values given as $\mathbf{x}_{\mathrm{d}i}(0) = \left[\begin{array}{c|c|c|c} \mathbf{x}_{\mathrm{d}i1}(0)^T & \mathbf{x}_{\mathrm{d}i2}(0)^T & \cdots & \mathbf{x}_{\mathrm{d}ip}(0)^T \end{array}\right]^T$.

Similarly, a multi-tonal multi-dimensional sinusoidal disturbance is obtained as a trivial composition of multi-tonal disturbances, given as

$$\begin{cases} \dot{\mathbf{x}}_{\text{ud}}(t) = \mathbf{A}_{\text{ud}}\mathbf{x}_{\text{ud}}(t) = \left[\begin{array}{c|c|c|c} \mathbf{A}_{\text{d}1} & \mathbf{0} & \cdots & \mathbf{0} \\ \hline \mathbf{0} & \mathbf{A}_{\text{d}2} & & \vdots \\ \hline \vdots & & \ddots & \mathbf{0} \\ \hline \mathbf{0} & \cdots & \mathbf{0} & \mathbf{A}_{\text{d}i} \end{array}\right]\mathbf{x}_{\text{ud}}(t) \\ \mathbf{d}_{\text{u}}(t) = \mathbf{C}_{\text{ud}}\mathbf{x}_{\text{ud}}(t) = \left[\begin{array}{c|c|c|c} \mathbf{C}_{\text{d}1} & \mathbf{0} & \cdots & \mathbf{0} \\ \hline \mathbf{0} & \mathbf{C}_{\text{d}2} & & \vdots \\ \hline \vdots & & \ddots & \mathbf{0} \\ \hline \mathbf{0} & \cdots & \mathbf{0} & \mathbf{C}_{\text{d}i} \end{array}\right]\mathbf{x}_{\text{ud}}(t) \end{cases}, \tag{3.6}$$

where $\mathbf{A}_{\text{ud}} \in \mathbb{R}^{2pi \times 2pi}$, $\mathbf{C}_{\text{ud}} \in \mathbb{R}^{i \times 2pi}$, $\mathbf{d}_{\text{u}}(t) \in \mathbb{R}^{i}$ and $\mathbf{x}_{\text{ud}} \in \mathbb{R}^{2pi}$ with the initial values given as: $\mathbf{x}_{\text{ud}}(0) = \left[\mathbf{x}_{\text{d}1}(0)^T \mid \mathbf{x}_{\text{d}2}(0)^T \mid \cdots \mid \mathbf{x}_{\text{d}i}(0)^T\right]^T$.

Eq. (3.6) is a representation of the dynamics of a general multi-tonal multi-dimensional sinusoidal disturbance. However, from the practical implementation point of view, it has a severe disadvantage. The disturbance is assumed to be of zero mean with no noise present, a scenario that is rather unlikely to ever exist in practice. Hence, the disturbance model is revised such that it takes the possibility of non-zero mean biased sinusoidal disturbance signals into account. Such disturbance is formulated as

$$\mathbf{d}(t) = \mathbf{d}_{\text{u}}(t) + \mathbf{b}(t), \tag{3.7}$$

where $\mathbf{b}(t)$ is an arbitrary function of time representing the deviation from zero at a time instant. For the case of static off-set this function simplifies into a static vector with the off-set for each dimension as its elements. This off-set can be included in the disturbance model derived in Eq. (3.6) by introducing augmented states $\mathbf{x}_{\text{aug}}(t) \in \mathbb{R}^{i}$ given as

$$\mathbf{x}_{\text{aug}}(t) = \mathbf{b}. \tag{3.8}$$

For control design purposes the augmented states are further modified by including a very slow exponential decay term, transforming Eq. (3.8) into

$$\mathbf{x}_{\text{aug}}(t) = e^{-\mathbf{E}t}\mathbf{b}, \tag{3.9}$$

where $\mathbf{E} = \text{diag}\{[\varepsilon_1 \ \cdots \ \varepsilon_i]\}$ is a matrix of the decay factors for each separate disturbance dimension.

As the decay factor is defined by the designer, it can be chosen without the loss of generality the same as the design parameter ε related to the Eq. (3.3) ; hence $\mathbf{E} = \varepsilon\mathbf{I}$. The final form of the augmented state is obtained by taking the time derivative of Eq. (3.9), resulting in

$$\dot{\mathbf{x}}_{\text{aug}}(t) = -\mathbf{E}\mathbf{x}_{\text{aug}}(t). \tag{3.10}$$

Remark 3.1. In the case of time varying deviation from zero, the exact augmented state would be of the form

$$\dot{\mathbf{x}}_{\text{aug}}(t) = \left(\text{diag}\{\mathbf{b}(t)\}^{-1}\dot{\mathbf{b}}(\mathbf{t}) - \mathbf{E}\right)\mathbf{x}_{\text{aug}}(t). \tag{3.11}$$

However, as the rate of change of the offset and the process noise is generally unknown, it is neglected from the deterministic disturbance model and considered as noise. This purposefully overlooked bias in the dynamics can be justified when state-estimation is being used, as the estimator updates the states in a way that minimises the estimation error - although it would be slightly more effective if all known dynamics were included in the model.

By augmenting the unbiased disturbance model in Eq. (3.6) with the bias-states given in Eq. (3.11), the final multi-tonal multi-dimensional biased sinusoidal disturbance signal is given as

$$\begin{cases} \dot{\mathbf{x}}_{\mathrm{d}}(t) = \mathbf{A}_{\mathrm{d}}\mathbf{x}_{\mathrm{d}}(t) = \left[\begin{array}{c|c} \mathbf{A}_{\mathrm{ud}} & \mathbf{0} \\ \hline \mathbf{0} & \mathbf{E} \end{array}\right]\mathbf{x}_{\mathrm{d}}(t) \\ \mathbf{d}(t) = \mathbf{C}_{\mathrm{d}}\mathbf{x}_{\mathrm{d}}(t) = \left[\begin{array}{c|c} \mathbf{C}_{\mathrm{ud}} & \mathbf{E} \end{array}\right]\mathbf{x}_{\mathrm{d}}(t) \end{cases}, \tag{3.12}$$

where $\mathbf{A}_{\mathrm{d}} \in \mathbb{R}^{(2p+1)i\times(2p+1)i}$, $\mathbf{C}_{\mathrm{d}} \in \mathbb{R}^{i\times(2p+1)i}$, $\mathbf{d}(t)\in \mathbb{R}^{i}$ and $\mathbf{x}_{\mathrm{d}} \in \mathbb{R}^{(2p+1)i}$ with the initial values given as $\mathbf{x}_{\mathrm{d}}(0) = \left[\begin{array}{c|c} \mathbf{x}_{\mathrm{ud}}(0)^T & \mathbf{b}^T \end{array}\right]^T$.

3.2.3 Plant model

A model describing the interaction between the actuator and the sinusoidal disturbances is required for control design purposes. Such model is readily obtained by combining the partial models derived in the preceding subsections; the resulting model is referred to as the plant from here on.

In the most common scenario, corresponding to the process induced vibrations, the perceived output signals are a summation of the actuator outputs and the sinusoidal disturbances. The model for such case is given as

$$\begin{cases} \dot{\mathbf{x}}(t) = \mathbf{A}\mathbf{x}(t) + \mathbf{B}\mathbf{u}_{\mathrm{p}}(t) = \left[\begin{array}{c|c} \mathbf{A}_{\mathrm{p}} & \mathbf{0} \\ \hline \mathbf{0} & \mathbf{A}_{\mathrm{d}} \end{array}\right]\left[\begin{array}{c} \mathbf{x}_{\mathrm{p}}(t) \\ \hline \mathbf{x}_{\mathrm{d}}(t) \end{array}\right] + \left[\begin{array}{c} \mathbf{B}_{\mathrm{p}} \\ \hline \mathbf{0} \end{array}\right]\mathbf{u}_{\mathrm{p}}(t) \\ \mathbf{y}(t) = \mathbf{C}\mathbf{x}(t) + \mathbf{D}\mathbf{u}_{\mathrm{p}}(t) = \left[\begin{array}{c|c} \mathbf{C}_{\mathrm{p}} & \mathbf{C}_{\mathrm{d}} \end{array}\right]\left[\begin{array}{c} \mathbf{x}_{\mathrm{p}}(t) \\ \hline \mathbf{x}_{\mathrm{d}}(t) \end{array}\right] + \mathbf{D}_{\mathrm{p}}\mathbf{u}_{\mathrm{p}}(t) \end{cases}, \tag{3.13}$$

where $\mathbf{A} \in \mathbb{R}^{r\times r}$, $\mathbf{B} \in \mathbb{R}^{r\times m}$, $\mathbf{C} \in \mathbb{R}^{n\times r}$ and $\mathbf{D} \in \mathbb{R}^{n\times m}$. The vectors $\mathbf{u}_{\mathrm{p}}(t)$ and $\mathbf{y}(t) \in \mathbb{R}^{n}$ denote the plant inputs and measured plant outputs, respectively, where the state-space dimension is defined as $r = k + (2p+1)n$.

In a special scenario corresponding to additive sinusoidal disturbances in external control signals, the realised actuator input signal is a summation of these disturbances and desired actuator input signals (control signals). Hence, the perceived output signals are the realised actuator input signals filtered through the actuator dynamics. The model describing this special case is given as

$$\begin{cases} \dot{\mathbf{x}}(t) = \mathbf{A}\mathbf{x}(t) + \mathbf{B}\mathbf{u}_{\mathrm{p}}(t) = \left[\begin{array}{c|c} \mathbf{A}_{\mathrm{p}} & \mathbf{B}_{\mathrm{p}}\mathbf{C}_{\mathrm{d}} \\ \hline \mathbf{0} & \mathbf{A}_{\mathrm{d}} \end{array}\right] \left[\begin{array}{c} \mathbf{x}_{\mathrm{p}}(t) \\ \hline \mathbf{x}_{\mathrm{d}}(t) \end{array}\right] + \left[\begin{array}{c} \mathbf{B}_{\mathrm{p}} \\ \hline \mathbf{0} \end{array}\right] \mathbf{u}_{\mathrm{p}}(t) \\ \mathbf{y}(t) = \mathbf{C}\mathbf{x}(t) + \mathbf{D}\mathbf{u}_{\mathrm{p}}(t) = \left[\begin{array}{c|c} \mathbf{C}_{\mathrm{p}} & \mathbf{D}_{\mathrm{p}}\mathbf{C}_{\mathrm{d}} \end{array}\right] \left[\begin{array}{c} \mathbf{x}_{\mathrm{p}}(t) \\ \hline \mathbf{x}_{\mathrm{d}}(t) \end{array}\right] + \mathbf{D}_{\mathrm{p}}\mathbf{u}_{\mathrm{p}}(t) \end{cases}, \quad (3.14)$$

where $\mathbf{u}_{\mathrm{p}}(t)$ and $\mathbf{y}(t)$ are vectors of plant inputs and measured plant outputs, respectively, where state-space dimension is defined as $r = k + (2p+1)m$.

The choice for a proper model is essential and depends on the problem at hand. This is further discussed in Chapter 4. Also, it should be noted that for non-square plants the dimension of the disturbance model varies depending whether it located at the process input or output. In a case where the difference between the number of the process inputs and outputs is high; a change in the disturbance location may lead to significant model reduction.

3.3 Identification of the process model

A mathematical expression of the process dynamics, a model, is required for the control design. The best approach would be to derive such ideal model starting from the principles of basic physics. In addition to describing the process dynamics over the whole frequency space, this ideal model would also describe all the possible nonlinearities of the process. Unfortunately, in practice most of the industrial processes are too complex to be modelled analytically, thus preventing the use of such models. Another approach to the modelling is based on the finite element analysis, which is a very good tool for the analysis of the process dynamics through simulations. However, these models are too complex to be used for the design purposes although they serve well as a test-bed environment for the control performance evaluation prior to the actual implementation in the true process. Hence, the feasible modelling approach is to derive the process model through data-based model fitting, which is essentially a 'black-box'-approach (Johansson, 1993).

3.3.1 Data-based modelling

The data-based modelling of LTI dynamical models has been a rigorously studied field with some well-known general results; hence their operation principle is just briefly introduced here. These methods can be utilised directly for the problem at hand after some pre-processing described in the following subsection.

The first of the two methods readily applicable to the identification of LTI MIMO-systems is based on subspace identification (Van Overschee and De Moor, 1996; Katayama, 2005). This is a batch-type identification approach based on linear regression. Roughly generalising, the required steps are given as follows. First, the time-series of the input and output data are assigned into vectors. This data is used to define a redundant state-space which is then projected into a subspace (spanned by the latent vectors). The state-space is then reduced through utilisation of principal component analysis (PCA) for example. The reduced state vectors can be interpreted as virtual inputs, which are then used to define a mapping to the measured outputs. The major advantages of this method are the natural suitability for MIMO-systems and the inherently defined model order. However, rather long data sets are required for the modelling and the data must be of high quality. In essence, no missing data points are tolerated and the data must be Gaussian and linear.

The second method is an iterative gradient based approach to state-space model identification (Ljung, 1999). The parameter update law is determined such that it minimises a cost function, which is usually chosen as a quantity describing the squared prediction error between the measured and the estimated process outputs. The approach is rather straightforward and can be roughly generalised as follows. The process is first initialised by assigning the matrices in a state-space representation with some initial values. The representation is typically chosen to be in a canonical form in order to minimise the number of free parameters. The first iteration step is to determine the response of the model candidate to an input signal measured from the true process. The second step is to define the squared-error between measured and predicted process responses. The third step is to determine the error gradient (in the direction of the steepest descent) with respect to the free model parameters. Finally, the parameters are updated according to the gradient and an iteration cycle is completed. The iteration is carried on until a certain error threshold or a minimum is reached. The advantages of this approach are the relative intolerance to measurement noise and nonlinearities although they cannot be included in the deterministic linear model being sought. The drawbacks are the rather high computational load, requirement for predefined model order and the possibility of convergence in local minima.

In practice, the latter of the above methods gives better model fits. This is due to the fact that the processes are never linear and the Gaussianity of the data cannot be guaranteed, and especially with shorter data sets the second method is preferred.

3.3.2 Data acquisition and pre-processing

Probably the most important phase in modelling is data acquisition. A poor choice for the test setup may cause the whole identification procedure to fail. A successful data acquisition relies on some *a priori* information of the system being identified. If no such information is available, the process becomes iterative. The information is gathered first for example by oversampling the process data and then evaluating its frequency spectrum, after which the actual data acquisition or resampling can be carried out. Another crucial part in the acquisition of discrete sampled data is to prevent aliasing, which is essentially a summation of high frequency components on the lower frequency data. The impact of the aliasing is minimised by including an analogue low-pass filter with the cut-off frequency set at the end of the frequency band of interest in the model, say ω. The minimal applicable sampling frequency that prevents aliasing is then explicitly defined as $\omega_h > 2\omega$, which is known as the Nyquist frequency (Kamen, 1990). As a rule of thumb the sampling rate should be chosen to be, whenever possible, three to five times over this (Ljung, 1999). Besides the aliasing, there are further aspects to be considered when determining the sampling rate. First, it should be chosen high enough to capture all the phenomena of interest; namely the process dynamics to be modelled. Secondly, it should be as low as possible to preserve the low frequency dynamics; otherwise the numerical identification methods may interpret the process as a simple integrator, should the variation of the signal between two consecutive samples be close or below the available numerical resolution. It is apparent that the choice for the sampling rate is a trade-off between accuracy and the obtainable frequency band for the model. Fortunately, a satisfactory sampling rate can be found in the most situations. If this is not the case, separate low and high frequency band models are identified and then combined with a suitable method.

The next phase is to choose an appropriate test signal. The most common approach is to use a pseudo-random (PR) signal that emulates white noise, exciting the whole frequency band of the process thereof. This is a very applicable and preferable approach to processes with low internal damping, such as metal structures. However, if the internal damping of the process is high, the pseudo-random signal does not provide sufficient excitation energy at a frequency at a time instant to overcome the impact of the damping. Hence, the process dynamics at these frequencies are not sufficiently excited and virtually no variation is perceived in the process response. One type of processes belonging to this group is hydraulic actuators, where the hydraulic seal washers with high static friction absorb the low energy excitations. In these processes, the preferred test signal is a sinusoidal sweep over the frequency band of interest. Here the whole excitation energy is concentrated on a single frequency at a time instant. A general sinusoidal signal with varying frequency can be given as:

$$u_d(t) = A\sin\left(2\pi F(t)\right), \tag{3.15}$$

where A is the signal amplitude and

$$F(t)=\int_0^t f(\tau)d\tau \tag{3.16}$$

is the integral of the function $f(t)$ describing the frequency variation.

A function describing linear frequency variation is of the form:

$$f(t)=f_0+\bar{a}t\,, \tag{3.17}$$

where f_0 is the initial frequency in Hertz and $\bar{a}$ is the rate of change of the frequency.

Trivially, the integral is now given as:

$$F(t)=f_0t+\frac{1}{2}\bar{a}t^2\,, \tag{3.18}$$

from which the rate of change can be solved for some desired final frequency at a known final time as:

$$\bar{a}=\frac{f_f-f_0}{t_f}\,, \tag{3.19}$$

where f_f is the final frequency of the sweep in Hertz and t_f is the sweep length is seconds.

By substituting the Eqs. (3.19) and (3.18) into Eq. (3.15) a sinusoidal signal with linear frequency variation is given as:

$$u_\mathrm{d}(t)=A\sin\left(2\pi\left(f_0t+\frac{f_f-f_0}{2t_f}t^2\right)\right), \tag{3.20}$$

where $u_\mathrm{d}(t)$ is the sinusoidal sweep signal.

If the frequency band to be identified is wide or there are very low frequency components, a sinusoidal sweep signal with exponential frequency variation is more preferable. A function describing exponential frequency variation is given as:

$$f(t)=f_0\bar{a}^t\,, \tag{3.21}$$

from which through the straightforward process of integration and solving for some final time, a sinusoidal signal with exponential frequency variation is obtained as:

$$\begin{cases} u_d(t)=A\sin\left(2\pi\left(t_f\dfrac{\bar{f}(t)-1}{\ln\left(f_f\right)-\ln\left(f_0\right)}\right)\right) \\ \bar{f}(t)=f_0e^{\frac{\ln\left(f_f\right)-\ln\left(f_0\right)}{t_f}t} \end{cases}, \tag{3.22}$$

where $u_\mathrm{d}(t)$ is the sinusoidal sweep signal, A is the signal amplitude, f_0 and f_f are the initial and final frequencies of the sweep in Hertz; and t_f is the sweep length in seconds.

If the identified process is a MIMO-system, the model can be formed in two ways. The first approach is to feed a test signal into one input at a time and measure the resulting responses. A model for each subsystem is then derived separately and combined into a single model. Finally, the minimal realisation for the aggregated model is sought. It should be noted that this approach is valid only for processes where the superposition principle applies, in essence linear processes. Another approach is to excite all input channels simultaneously. If PR-signals are used, they are initialised with different seed numbers. If sinusoidal sweeps are used, they are set to have different starting times. This distinguishes the impact of each input on the outputs; otherwise the problem is improper as the inputs would be linearly dependent. Again, it should be stressed that if the process is nonlinear, no information on the nonlinearity is obtained with the presented test signals.

Prior to the model fitting, the data acquired from the process is preprocessed in order to remove the measurement noise, which is always present, and data trends. Due to its special nature, active vibration control also brings another preprocessing step which is not feasible in general control schemes. This step is the truncation of the model to the frequency band where the vibrations are likely to occur, allowing the use of models with lower order than those that would be required for the complete description of the process dynamics. It should be noted that if such truncated models are used, the robust stability of the closed-loop process at the frequencies omitted from the model has to be verified. All preceding preprocessing steps can be satisfied simultaneously by introducing an ideal pass-band filtering in the frequency domain. The filtering is realised by first introducing a modified discrete Fourier transformation (DFT), where the components outside the chosen frequency pass-band are set zero

$$X(k)=\begin{cases} 0 & ,k \le k_{\text{low}}+1 \\ F(k) & ,k_{\text{low}}+1<k<k_{\text{high}}+1 \\ 0 & ,k_{\text{high}}+1 \le k \le N-k_{\text{high}}+1 \\ F(k) & N-k_{\text{high}}+1<k<N-k_{\text{low}}+1 \\ 0 & N-k_{\text{low}}+1 \le k \end{cases}, \tag{3.23}$$

where k is the sample number, N is the length of the data vector, k_{low} and k_{high} are the lower and higher cut-off samples defined as

$$\begin{cases} k_{\text{low}} = f_{\text{low}}(N-1)h \\ k_{\text{high}} = f_{\text{high}}(N-1)h \end{cases}, \tag{3.24}$$

where h is the sampling rate and f_{low} and f_{high} f_{high} are the lower and higher cut-off frequencies in Hertz, respectively. The function $F(k)$ is the DFT defined as (Kamen, 1990)

$$F(k) = \sum_{n=0}^{N-1} x(n) e^{-j\frac{2\pi nk}{N}} \quad , \tag{3.25}$$

where $x(n)$ is the signal being filtered.

The preprocessed signal is then obtained by performing an inverse DFT on the filtered frequency domain signal. The inverse transformation is given as

$$x_{\text{filt}}(k) = \frac{1}{N} \sum_{n=0}^{N-1} X(n) e^{j\frac{2\pi nk}{N}}, k = 0,1,\cdots,N-1 \,. \tag{3.26}$$

The impact of the preprocessing is illustrated in Figure 3.2 where both the original and filtered signals for a single channel are given. The impact of the preprocessing on the model truncation is illustrated in Figure 3.3, where the frequency range of interest was determined as 55-75Hz. The impact of the filtering is clearly distinguishable when the predicted process dynamics of the low order models are compared against the measured process dynamics. A second order model obtained for the filtered data provides sufficient estimation accuracy, while the fourth order model obtained for the original data fails completely in the estimation. In the given example, at least a sixth order model is required for the original data to provide satisfactory accuracy; and in this case it is just a sheer coincidence that the identification procedure converges to the local minimum, which corresponds to the second frequency peak.

Next, a suitable model order is determined. In practice this is again an iterative process, where an initial guess is made and a model of the given order is fitted for the data. Then, another model with perturbed model order is fitted for the data. The fit of the models is then compared and the one with the better fit is chosen as the model candidate. This procedure is carried on until the best model order fit is obtained. It should be borne in mind that for scarce data sets an excessively high order model may easily result in over parameterisation, a scenario where the model no longer represents the true dynamics of the process. An initial guess for the model order can be based on the analysis of the ratio of the frequency amplitude spectra of the input and output signals, essentially the measured process gain and phase shift. In this spectrum, each frequency peak represents a pole pair giving an approximation of the overall number of process poles and the order of the process thereof.

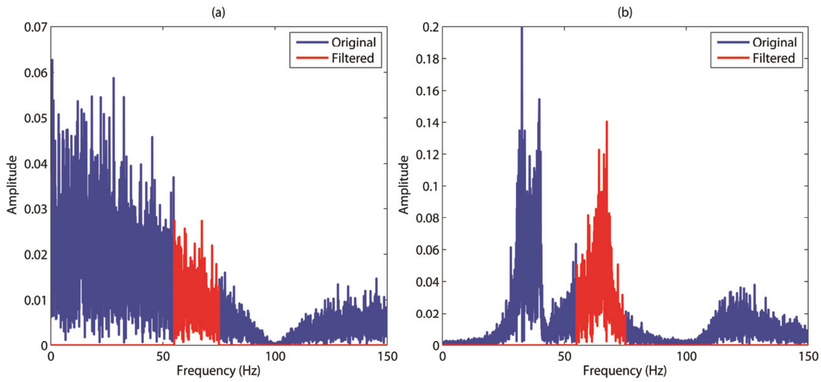

Figure 3.2. The impact of the signal filtering. (a) The amplitude spectrum of the input signal. (b) The amplitude spectrum of the output signal.

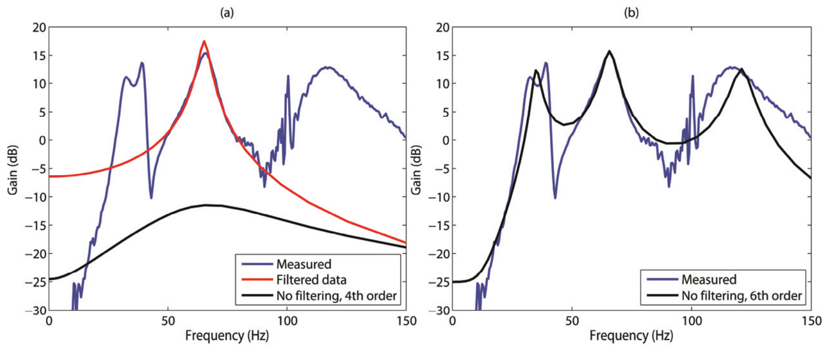

Figure 3.3. Comparison of the model estimates against the measured process dynamics. (a) The second and fourth order models obtained for the filtered and original input-output data. (b) The sixth order model obtained for the original input-output data.

The final part of the identification process is the model validation. Although being very important, this phase seems to be overlooked rather often in studies that include some modelling, especially in the field of neural-networks. Prior to the validation, the model fitted against the identification data is simply a mapping that minimises the estimation error, in essence a high order regression curve. For modelling purposes it is of utmost importance that the obtained model describes the underlying dynamics of the phenomenon under study. This can be verified by evaluating the fit of the estimated and the measured process outputs obtained for a data set that is independent of the modelling data. If the model still provides an adequate fit within the range of 70%-80% for noisy processes, it can be considered to describe the dynamics of the true system with adequate accuracy.

3.3.3 Balanced model realisation

Typically, the state-space models obtained through data based identification are in an observer canonical form. This choice minimises the number of free parameters, simplifying the identification procedure thereof. Although, this model structure is very usable for identification, it is not necessarily the best option for the control design. This is especially true with methods applying state-feedback and state-estimators. For these purposes, the models having certain properties regarding the controllability and observability are more desirable; namely, such models that are as observable as they are controllable. This enhances the control design and the numerical properties of the resulting feedback and estimator gain matrices. The types of models that fulfil the requirements are obtained through the balanced model realisation, which has been a widely studied field in the 1980s with several significant works (Moore, 1981; Laub *et al.*, 1987). The main points of the balancing procedure adopted from these works and (Zhou and Doyle, 1998; Skogestad and Postlethwaite, 2005) are presented next. For simplicity, the identified model is assumed to be a linear time invariant minimal order system, which is completely controllable and observable; although in the original references this is not required.

Consider a general state-space representation:

$$\begin{cases} \dot{\mathbf{x}}(t) = \mathbf{A}\mathbf{x}(t) + \mathbf{B}\mathbf{u}(t) \\ \mathbf{y}(t) = \mathbf{C}\mathbf{x}(t) + \mathbf{D}\mathbf{u}(t) \end{cases}, \tag{3.27}$$

with the controllability $\mathbf{P}_\mathrm{C} \in \mathbb{R}^{k\times k}$ and observability $\mathbf{P}_\mathrm{O} \in \mathbb{R}^{k\times k}$ Gramians given as:

$$\begin{aligned} \mathbf{P}_\mathrm{C} &= \mathbf{M}_\mathrm{C}\mathbf{M}_\mathrm{C}^T = \int_0^\infty e^{\mathbf{A}t}\mathbf{B}\mathbf{B}^T e^{\mathbf{A}^T t} dt \\ \mathbf{P}_\mathrm{O} &= \mathbf{M}_\mathrm{O}^T\mathbf{M}_\mathrm{O} = \int_0^\infty e^{\mathbf{A}^T t}\mathbf{C}^T\mathbf{C} e^{\mathbf{A}t} dt \end{aligned}, \tag{3.28}$$

where $\mathbf{M}_\mathrm{C} \in \mathbb{R}^{k\times m}$ and $\mathbf{M}_\mathrm{O} \in \mathbb{R}^{n\times k}$ are the extended controllability and observability matrices.

The most convenient way to obtain the Gramians is to note that they satisfy a pair of Lyapunov equations given as:

$$\begin{cases} \mathbf{A}\mathbf{P}_\mathrm{C} + \mathbf{P}_\mathrm{C}\mathbf{A}^T + \mathbf{B}\mathbf{B}^T = \mathbf{0} \\ \mathbf{A}^T\mathbf{P}_\mathrm{O} + \mathbf{P}_\mathrm{O}\mathbf{A} + \mathbf{C}^T\mathbf{C} = \mathbf{0} \end{cases}. \tag{3.29}$$

Now, the balanced realisation of the system is defined as: "a *balanced realization* is an asymptotically stable minimal realization in which the controllability and observability Gramians are equal and diagonal." (Skogestad and Postlethwaite, 2005). Hence, the problem can be formulated as a problem of finding a suitable state-transformation that diagonalises the product of the two Gramians. A general system subject to some state-transformation $\mathbf{z}(t) = \mathbf{T}\mathbf{x}(t)$, where $\mathbf{T}$ is an invertible matrix, is given as:

$$\begin{cases} \dot{\mathbf{z}}(t) = \mathbf{TAT}^{-1}\mathbf{z}(t) + \mathbf{TBu}(t) \\ \mathbf{y}(t) = \mathbf{CT}^{-1}\mathbf{z}(t) + \mathbf{Du}(t) \end{cases}, \tag{3.30}$$

with corresponding Gramians given as:

$$\begin{cases} \mathbf{TAT}^{-1}\overline{\mathbf{P}}_{\mathrm{C}} + \overline{\mathbf{P}}_{\mathrm{C}}\mathbf{T}^{-T}\mathbf{A}^{T}\mathbf{T}^{T} + \mathbf{TBB}^{T}\mathbf{T}^{T} = \mathbf{0} \\ \mathbf{T}^{-T}\mathbf{A}^{T}\mathbf{T}^{T}\overline{\mathbf{P}}_{\mathrm{O}} + \overline{\mathbf{P}}_{\mathrm{O}}\mathbf{TAT}^{-1} + \mathbf{T}^{-T}\mathbf{C}^{T}\mathbf{CT}^{-1} = \mathbf{0} \end{cases}, \tag{3.31}$$

where $\overline{\mathbf{P}}_{\mathrm{C}}$ and $\overline{\mathbf{P}}_{\mathrm{O}}$ are the transformed controllability and observability Gramians, respectively; and $(\cdot)^{-T}$ denotes the transpose of the inverted matrix.

Next, with the obvious pre- and post-multiplying the Eq. (3.25) can be rewritten as:

$$\begin{cases} \mathbf{AT}^{-1}\overline{\mathbf{P}}_{\mathrm{C}}\mathbf{T}^{-T} + \mathbf{T}^{-1}\overline{\mathbf{P}}_{\mathrm{C}}\mathbf{T}^{-T}\mathbf{A}^{T} + \mathbf{BB}^{T} = \mathbf{0} \\ \mathbf{A}^{T}\mathbf{T}^{T}\overline{\mathbf{P}}_{\mathrm{O}}\mathbf{T} + \mathbf{T}^{T}\overline{\mathbf{P}}_{\mathrm{O}}\mathbf{TA} + \mathbf{C}^{T}\mathbf{C} = \mathbf{0} \end{cases}, \tag{3.32}$$

from which it follows:

$$\begin{cases} \overline{\mathbf{P}}_{\mathrm{C}} = \mathbf{TP}_{\mathrm{C}}\mathbf{T}^{T} \\ \overline{\mathbf{P}}_{\mathrm{O}} = \mathbf{T}^{-T}\mathbf{P}_{\mathrm{O}}\mathbf{T}^{-1} \end{cases}. \tag{3.33}$$

By studying the product of the transformed Gramians, given as:

$$\overline{\mathbf{P}}_{\mathrm{C}}\overline{\mathbf{P}}_{\mathrm{O}} = \mathbf{TP}_{\mathrm{C}}\mathbf{T}^{T}\mathbf{T}^{-T}\mathbf{P}_{\mathrm{O}}\mathbf{T}^{-1} = \mathbf{TP}_{\mathrm{C}}\mathbf{P}_{\mathrm{O}}\mathbf{T}^{-1}, \tag{3.34}$$

it becomes evident that the eigenvalues of the product of the Gramians are invariant to state-transformations. Hence, a suitable transformation matrix is obtained such that it diagonalises the product of the Gramians in the original system, in essence:

$$\mathbf{TP}_{\mathrm{C}}\mathbf{P}_{\mathrm{O}}\mathbf{T}^{-1} = \overline{\mathbf{P}}_{\mathrm{C}}\overline{\mathbf{P}}_{\mathrm{O}} = \mathbf{\Sigma}^{2}, \tag{3.35}$$

implying $\overline{\mathbf{P}}_{\mathrm{C}} = \overline{\mathbf{P}}_{\mathrm{O}} = \mathbf{\Sigma}$, fulfilling the given problem statement thereof.

The elements of the diagonal matrix $\mathbf{\Sigma}^{2}$ are called the Hankel singular values of the system. The elements are usually arranged in the decreasing order and they define the amount of the input-output dynamics each of the transformed system states describes. This information can be further used in model reduction, where the states corresponding to the lowest Hankel singular values are omitted first from the reduced order model. In the given problem, the model is already of desirable order and no further reduction is required.

4. Control design

In this chapter, the synthesis of a generic nonlinear control law for vibration mitigation is presented. The design procedure starts with the design of a linear controller capable of mitigating an arbitrary number of tonal disturbances with known static frequencies. The design of such control algorithm is presented in detail in the following subsection. Although the linear control law is designed to be generic and robust to modelling errors, it has a significant drawback limiting its applicability, namely, the disturbances act on a preknown static frequency. Such assumption is seldom viable in practice; hence the control law is redesigned such that it is effective in the presence of frequency varying disturbances. The linear controller, as presented herein, is readily extended to a nonlinear optimal controller through the introduction of gain-scheduling and time-varying system parameters. The design of a nonlinear controller is presented in detail in Section 4.2. The nonlinear controller requires information on the disturbance frequency, which may not be readily available; hence the disturbance frequency needs to be extracted from the existing process measurements. Some aspects related to the frequency estimation in the systems of the given type are discussed in Section 4.3.

4.1 Linear control law

The mitigation of one or several sinusoidal disturbances with static frequency has been a rigorously studied problem. The studies have resulted in several potential and very applicable solutions ranging from notch filters (Gupta, 1980; Herzog *et al.*, 1996) and recursive least squares (RLS)-algorithms (Daley *et al.*, 2008; Daley and Zazas, 2011) to higher harmonic control (HHC) (Lovera *et al.*, 2003) and state-feedback based approaches (Sievers and von Flotow, 1988; Bittanti *et al.*, 1996; Bohn *et al.*, 2004). The approach proposed and considered herein is based on optimal state-feedback. The major drawbacks of such approach are the requirements for a process model and state-measurements. On the other hand, the use of the state-feedback enables the use of the very powerful and effective control design tools such as the linear quadratic (LQ) optimal control theory. The realised controller produces a control law that minimises a quadratic cost function with respect to the state variation and the applied control effort.

The major benefit of the LQ-controller is the guaranteed stability and minimum phase behaviour of the closed-loop system (Anderson and Moore, 1989); the non-minimum phase processes do not pose any additional problems thereof.

The proposed control approach bears many similarities with the existing LQ-based control laws. However, by addressing some of the problems encountered with these methods, the proposed approach has some significant advantages over them. Namely, the number of free design parameters is decreased; the closed-loop robustness properties can be manipulated in a natural way with a single parameter; the underlying process models are normalised, yielding similar control performance to the most of the systems through the use of the same design parameterisation, apart from the control weighting. Finally, the problems encountered in some designs related to non-square processes are avoided. Although the approach considered herein does not yield the best performance in every scenario, when compared against the existing methods, it yields the best overall performance, as discussed further in Chapter 5.

The design of an LQ-controller consists of two parts. First, an optimal state-feedback weighting matrix is determined and then, due to the fact that the internal process states are seldom measurable, an optimal state-estimator is derived. Finally, the feedback gain matrix is combined with the estimator dynamics, yielding the sought controller. The feedback and the estimator have no interconnections in their design; hence they can be designed independently. The design procedures of these individual parts and their composition into a single controller are described in detail in the sequel.

4.1.1 State-feedback design

The optimal state-feedback is such that it minimises a predefined cost function with respect to some performance variable $\mathbf{z}(t) \in \mathbb{R}^n$ and the applied control signal $\mathbf{u}(t)$. In order to guarantee the global optimality of the solution, the cost function is required to be convex. Hence, a suitable cost function is defined as the integral of the sum of the weighted squared signals, given as (with no penalty set for the final state):

$$J = \int_0^t \left(\mathbf{z}^T(\tau)\mathbf{Q}_z\mathbf{z}(\tau) + \mathbf{u}^T(\tau)\mathbf{R}_z\mathbf{u}(\tau) \right) d\tau \, , \tag{4.1}$$

where $\mathbf{0} \leq \mathbf{Q}_z \in \mathbb{R}^{n \times n}$ and $\mathbf{0} < \mathbf{R}_z \in \mathbb{R}^{m \times m}$ are symmetric diagonal weighting matrices for the performance variable and the control signal, respectively.

The performance variable can be chosen arbitrarily, depending on the problem at hand. In the problem of vibration mitigation, it is desirable that only the perceived sinusoidal disturbances at the output of the plant model in Eq. (3.13) are minimised. Hence, the control law should have no impact on the outlying frequencies; in essence, the bias term is not to be controlled. It is notable that if the disturbance dynamics were not included in the plant model, a more complex servo problem of following a reference signal specified by the perceived disturbance would be obtained instead of a simple regulator problem. With this choice of the minimised quantity and under the assumption of no input disturbances, that is $\mathbf{u}_{\mathrm{p}}(t)=\mathbf{u}(t)$, the performance variable is given as:

$$\mathbf{z}(t)=\left[\mathbf{C}_{\mathrm{p}} \;\middle|\; \left[\mathbf{C}_{\mathrm{ud}} \;\middle|\; \mathbf{0}\right]\right]\mathbf{x}(t)+\mathbf{D}\mathbf{u}(t)=\mathbf{C}_{z}\mathbf{x}(t)+\mathbf{D}\mathbf{u}(t)\,, \tag{4.2}$$

where $\mathbf{C}_{\mathrm{z}} \in \mathbb{R}^{n\times r}$ is the performance state weighing matrix and $\mathbf{x}(t)$ is as in the Eq. (3.13).

Now, the cost function in Eq. (4.1) can be rewritten as:

$$J=\int_{0}^{t}\left(\mathbf{x}^{T}(\tau)\mathbf{Q}\mathbf{x}(\tau)+2\mathbf{x}^{T}(\tau)\mathbf{N}\mathbf{u}(\tau)+\mathbf{u}^{T}(\tau)\mathbf{R}\mathbf{u}(\tau)\right)d\tau\,, \tag{4.3}$$

where $\mathbf{Q}=\mathbf{C}_{\mathrm{z}}^{T}\mathbf{Q}_{\mathrm{z}}\mathbf{C}_{\mathrm{z}}$, $\mathbf{N}=\mathbf{C}_{\mathrm{z}}^{T}\mathbf{Q}_{\mathrm{z}}\mathbf{D}$ and $\mathbf{R}=\mathbf{R}_{\mathrm{z}}+\mathbf{D}^{T}\mathbf{Q}_{\mathrm{z}}\mathbf{D}$.

The cost function in Eq. (4.3) is of the standard form, for which the minimum is readily found for example by applying the calculus of variations (Kirk, 2004). The optimal control effort minimising the cost function is now given as (the notion of optimality omitted in the sequel):

$$\mathbf{u}(t)=-\mathbf{L}(t)\mathbf{x}(t)=-\mathbf{R}^{-1}\left(\mathbf{B}^{T}\mathbf{S}(t)+\mathbf{N}^{T}\right)\mathbf{x}(t)\,, \tag{4.4}$$

where $\mathbf{L}(t)\in\mathbb{R}^{m\times r}$ and $\mathbf{S}(t)\in\mathbb{R}^{r\times r}$ is the positive symmetric solution of the Riccati-equation (Skogestad and Postlethwaite, 2005):

$$-\dot{\mathbf{S}}(t)=\mathbf{A}^{T}\mathbf{S}(t)+\mathbf{S}(t)\mathbf{A}-\left(\mathbf{S}(t)\mathbf{B}+\mathbf{N}\right)\mathbf{R}^{-1}\left(\mathbf{B}^{T}\mathbf{S}(t)+\mathbf{N}^{T}\right)+\mathbf{Q}\,, \tag{4.5}$$

satisfying the boundary conditions $\mathbf{S}(t_{f})=\mathbf{0}$. A unique solution is found if all unstable system modes are controllable.

Due to the time dependency, the obtained optimal control law is not feasible for practical problems. This problem can be avoided by letting the optimisation horizon tend to infinity, in essence $t\rightarrow\infty$. Now the time invariant solution is obtained from the algebraic Riccati-equation (ARE):

$$\mathbf{A}^{T}\mathbf{S}+\mathbf{S}\mathbf{A}-\left(\mathbf{S}\mathbf{B}+\mathbf{N}\right)\mathbf{R}^{-1}\left(\mathbf{B}^{T}\mathbf{S}+\mathbf{N}^{T}\right)+\mathbf{Q}=\mathbf{0}\,, \tag{4.6}$$

for which the solution is readily obtained through numerical means (Arnold and Laub, 1984).

The drawbacks of the numerical solution are the stricter requirements for the system properties and design parameters. It is required that the system is strictly stable, in essence it has no poles on the imaginary axis and $\mathbf{Q}_{\mathrm{z}}>\mathbf{0}$. These additional restrictions come directly from the computation method utilising the Hamiltonian matrix:

$$\mathbf{H}=\left[\begin{array}{c|c}\mathbf{A}-\mathbf{B}\mathbf{R}^{-1}\mathbf{N}^T & -\mathbf{B}\mathbf{R}^{-1}\mathbf{B}^T \\ \hline \mathbf{N}\mathbf{R}^{-1}\mathbf{N}^T-\mathbf{Q} & -\mathbf{A}^T+\mathbf{N}\mathbf{R}^{-1}\mathbf{B}^T\end{array}\right],\mathbf{H}\in\mathbb{R}^{2r\times 2r}, \tag{4.7}$$

whose eigenvalues are symmetric with respect to the imaginary axis. The solution requires collecting the eigenvalues and their respective eigenvectors in the negative half-plane. Hence, in order to be separable, the Hamiltonian may not have any poles on the imaginary axis, implying that the original system has none either and that the weighting matrix is positive definite.

It is apparent that the plant model derived in Chapter 3 does not fulfil the above requirements as the poles related to the dynamics of the sinusoidal disturbances are located on the imaginary axis. This problem can be avoided by setting the design parameter ε a small value, typically chosen of the magnitude $\varepsilon \simeq 10^{-8}$.

The optimal control effort is now given as a static gain feedback:

$$\mathbf{u}(t)=-\mathbf{R}^{-1}\left(\mathbf{B}^T\mathbf{S}+\mathbf{N}^T\right)\mathbf{x}(t)=-\mathbf{L}\mathbf{x}(t)\,. \tag{4.8}$$

Remark 4.1. Theoretically speaking, the obtained control law is no longer optimal but suboptimal. This follows from the introduction of the design parameter ε and the use of an infinite optimisation horizon. However, from the practical point of view, the impact on the optimality is negligible. This claim becomes rather evident when the assumption of an unbiased process model, used in the design, is considered. In essence, the control action is optimal if and only if the assumption of a perfect model holds, which is assumption that is never satisfied in practice. Hence, the true optimality can never be obtained in practice.

The impact of the inclusion of the design parameter, a small damping coefficient for the sinusoidal disturbance, is readily evaluated by studying the ratio between the slowly decaying signal resulting thereof and the original signal with static amplitude. Consider a pair of such signals:

$$\begin{cases} y_1(t)=A\sin(\omega t) \\ y_2(t)=\dfrac{A\omega}{\sqrt{\omega^2-0.25\varepsilon^2}}e^{-0.5\varepsilon t}\sin\left(\left(\sqrt{\omega^2-0.25\varepsilon^2}\right)t\right)\end{cases}, \tag{4.9}$$

where $y_2(t)$ the signal representation of the disturbance in Eq. (3.3), which for $\varepsilon << 1$ can be approximated by:

$$\begin{cases} y_1(t)=A\sin(\omega t) \\ y_2(t)=Ae^{-0.5\varepsilon t}\sin\left(\omega t\right)\end{cases}. \tag{4.10}$$

Now, the ratio describing the difference in the signal amplitudes over time is given as:

$$R(t)=\frac{y_2(t)}{y_1(t)}=e^{-0.5\varepsilon t}\,. \tag{4.11}$$

Next, the time it takes for the signal amplitude to decay by magnitude d is considered. That gives insight to the rate of decay with respect to the time constants of the process dynamics. The decay time is readily obtained from Eq. (4.11) as:

$$\begin{aligned} d &= 1 - R(t) = 1 - e^{-0.5\varepsilon t} \\ \Rightarrow t &= -\frac{2\ln(1-d)}{\varepsilon} \end{aligned} \quad . \tag{4.12}$$

Now, by assuming that 1% decay is considered significant and the design variable is set as $\varepsilon = 10^{-8}$, the resulting decay time is of the magnitude $t \approx 2*10^{6}$. Such rate of decay is clearly insignificant for problems, where the dynamics of interest occur at the frequency band above 1Hz. Hence, the inclusion of the decay term cannot be considered having any significant impact on the optimal solution. However, a more important issue is the potential signal amplitude convergence to zero, in scenarios, where the control is on for extended time periods. Fortunately, this is not an issue either as the state-observer incorporated in the control law compensates the signal decay due to the addition of the design variable ε.

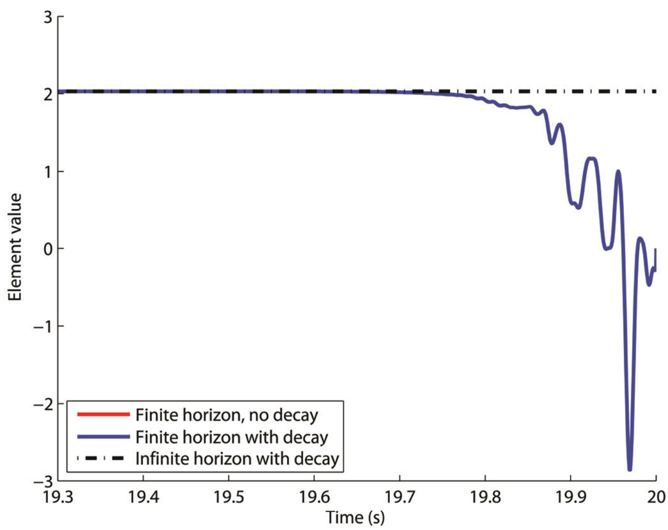

Figure 4.1. The value of a gain element with different optimisation horizons and decay factors.

The second possible issue is related to the use of an infinite optimisation horizon. This however does not have any significant impact either unless the process is to be run for very short periods of time. It is a well-known fact that the solutions of the Riccati-equation with finite and infinite time horizons coincide over the most of the time interval. The major deviations in the values occur at the end of the optimisation interval. To verify this, a gain element of the **L**-matrix is drawn in Fig. 4.1 in three different scenarios; namely for a finite optimisation horizon without the decay term and the finite and infinite optimisation horizons with the decay term. The obtained results agree with the interpretation made above; hence the proposed control law yields performance that can be considered optimal in practical solutions, even as such notion is not theoretically valid.

4.1.1.1 State-feedback design for input disturbance mitigation

The preceding derivation of the feedback control law is suitable for the mitigation of tonal output disturbances. However, as mentioned in Chapter 3, there is another control scenario, where the control goal is to suppress tonal input disturbances. The control design for such problems is exactly the same as in the preceding derivation apart from the applied plant model and the performance variable. The necessary changes to those quantities are derived next. The major differences of the designs are the sensitivities to the input and output disturbances and to the tolerable input and output modelling errors in certain non-square processes. In square systems, the performances are approximately the same.

In the mitigation of input disturbances, the plant model given in Eq. (3.14) is used for the control and estimator designs. The control goal is to produce a signal that compensates the sinusoidal component(s) of the disturbance signal at the process input; hence the performance variable is defined as:

$$\mathbf{z}(t)=\mathbf{d}_{\mathrm{I}}(t)+\mathbf{u}(t)=\left[\mathbf{0}\;\vdots\;\mathbf{C}_{\mathrm{ud}}\;\vdots\;\mathbf{0}\right]\mathbf{x}(t)+\mathbf{u}(t)=\mathbf{C}_{z}\mathbf{x}(t)+\mathbf{u}(t)\,, \tag{4.13}$$

where $\mathbf{z}(t)\in\mathbb{R}^{m}$ and $\mathbf{C}_{z}\in\mathbb{R}^{m\times r}$.

The corresponding cost function is given as:

$$J=\int_{0}^{t}\left(\mathbf{x}^{T}(\tau)\mathbf{Q}\mathbf{x}(\tau)+2\mathbf{x}^{T}(\tau)\mathbf{N}\mathbf{u}(\tau)+\mathbf{u}^{T}(\tau)\mathbf{R}\mathbf{u}(\tau)\right)d\tau\,, \tag{4.14}$$

with $\mathbf{Q}=\mathbf{C}_{z}^{T}\mathbf{Q}_{z}\mathbf{C}_{z}$, $\mathbf{N}=\mathbf{C}_{z}^{T}\mathbf{Q}_{z}$ and $\mathbf{R}=\mathbf{Q}_{z}+\mathbf{R}_{z}$, where $\mathbf{Q}_{z}\in\mathbb{R}^{m\times m}$.

4.1.2 State-estimator design

The internal process states are seldom measurable; an issue which poses a severe problem for the controllers based on state-feedback. Fortunately, the behaviour of the internal process states can be estimated by studying the input-output relations of the system with a known structure. In essence, the state-space is reconstructed based on these relations. In order for the state reconstruction to be possible, the input-output relation must contain the information of the process states. Roughly generalising, the input must correlate with the internal process states and the states must correlate with the process output. A system with these properties for every state is called observable. In the absence of external disturbances, the state-trajectories of an observable system can be determined exactly based on the input-output history of the system. There are several ways of estimating the internal process states, of which the well-known deterministic state-observer can be shown to yield an unbiased estimate over time.

The dynamics of a deterministic state-estimator are given as (Dorf and Bishop, 2011):

$$\begin{aligned}\dot{\hat{\mathbf{x}}}(t) &= \mathbf{A}\hat{\mathbf{x}}(t) + \mathbf{B}\mathbf{u}(t) + \mathbf{K}\hat{\mathbf{e}}(t) \\ &= \left(\mathbf{A} - \mathbf{KC}\right)\hat{\mathbf{x}}(t) + \mathbf{B}\mathbf{u}(t) + \mathbf{K}\mathbf{y}(t)\end{aligned}, \tag{4.15}$$

where $\hat{\mathbf{x}}(t) \in \mathbb{R}^r$ is a vector of the state estimates, $\mathbf{K} \in \mathbb{R}^{r\times n}$ is the estimator gain matrix and $\hat{\mathbf{e}}(t) = \mathbf{y}(t) - \mathbf{C}\hat{\mathbf{x}}(t)$ is the perceived estimation error in the process output as a function of the estimated states.

The output error is an insufficient quantity for evaluating the performance of a state estimator because the problem is to minimise the estimation error of the states. The state estimation error is readily obtained by subtracting the estimated states from the true (unknown) process states, yielding:

$$\dot{\tilde{\mathbf{x}}}(t) = \dot{\mathbf{x}}(t) - \dot{\hat{\mathbf{x}}}(t) = \mathbf{A}\tilde{\mathbf{x}}(t) - \mathbf{KC}\tilde{\mathbf{x}}(t) = \left(\mathbf{A} - \mathbf{KC}\right)\tilde{\mathbf{x}}(t), \tag{4.16}$$

where $\tilde{\mathbf{x}}(t) \in \mathbb{R}^r$ is a vector of the state estimation errors.

Now, the problem definition becomes evident; *find the estimator feedback gain matrix* $\mathbf{K}$ *that minimises the state estimation error and guarantees its convergence to zero*. In essence, find a feedback that places the poles of the matrix $\mathbf{M} = \left(\mathbf{A} - \mathbf{KC}\right)$ on the left half-plane in some optimal way.

By noting that the eigenvalues of the matrix $\mathbf{M}$ do not change under transposition and by introducing a new auxiliary state-vector describing the relative state-estimation error, the Eq. (4.16) can be rewritten as:

$$\dot{\overline{\mathbf{x}}}(t) = \mathbf{M}^T\overline{\mathbf{x}}(t) = \mathbf{A}^T\overline{\mathbf{x}}(t) - \mathbf{C}^T\mathbf{K}^T\overline{\mathbf{x}}(t) = \mathbf{A}^T\overline{\mathbf{x}}(t) + \mathbf{C}^T\mathbf{u}_{\text{obs}}(t), \tag{4.17}$$

where $\overline{\mathbf{x}}(t) \in \mathbb{R}^r$ is an auxiliary state-vector and $\mathbf{u}_{\text{obs}}(t) = -\mathbf{K}^T\overline{\mathbf{x}}(t), \mathbf{u}_{\text{obs}}(t) \in \mathbb{R}^n$ is an artificial control signal determining the convergence speed of the estimates.

It should be emphasised that the relative estimation-error is not related to the original estimation-error, yet the dynamics of the closed-loop system determined by its poles are exactly the same. The estimation problem can now be restated as a minimisation problem of a quadratic cost function of the relative estimation error:

$$J_{\text{obs}} = \int_0^t \left(\overline{\mathbf{x}}(\tau)^T\mathbf{Q}_{\text{obs}}\overline{\mathbf{x}}(\tau) + \mathbf{u}_{\text{obs}}^T(\tau)\mathbf{R}_{\text{obs}}\mathbf{u}_{\text{obs}}(\tau)\right)d\tau, \tag{4.18}$$

where $\mathbf{0} < \mathbf{Q}_{\text{obs}} \in \mathbb{R}^{r\times r}$ and $\mathbf{0} < \mathbf{R}_{\text{obs}} \in \mathbb{R}^{n\times n}$ are symmetric weighting matrices determining the converge properties of the estimate.

The optimal solution for the minimisation problem in Eq. (4.18) is readily found by exploiting the duality properties of the state-space system, namely, the observability of the pair $(\mathbf{A},\mathbf{C})$ is dual to the controllability of the pair $(\mathbf{A}^T,\mathbf{C}^T)$ (Rugh, 1996). It has been shown that the optimal estimator problem is dual to the optimal control problem with the substitution $t \to -t$ and $s \to -s$ (Anderson and Moore, 1989). Here, the optimisation horizon starts from some time in the past, possibly negative infinity, and stops at the current time instant, which can be chosen as zero without the loss of generality. The optimal state-estimation gain is now obtained as:

$$\mathbf{K} = \mathbf{P}\mathbf{C}^T\mathbf{R}_{\text{obs}}^{-1}, \tag{4.19}$$

where $\mathbf{P} \in \mathbb{R}^{r \times r}$ is the positive symmetric solution of the ARE:

$$\mathbf{A}\mathbf{P} + \mathbf{P}\mathbf{A}^T - \mathbf{P}\mathbf{C}^T\mathbf{R}_{\text{obs}}^{-1}\mathbf{C}\mathbf{P} + \mathbf{Q}_{\text{obs}} = \mathbf{0}\,. \tag{4.20}$$

Remark 4.2. If the process is subject to measurement noise, the deterministic estimator becomes biased. For these cases, the estimator should be chosen such that it minimises the impact of the noise in the mathematical expectation of the estimation error. Traditionally the Kalman-filter (Bar-Shalom and Xiao-Rong, 2001) is used for this purpose, which can be shown to be the optimal estimator for such cases. In the applications of the active vibration control, the process measurements are potentially subject to very high noise levels. Despite this *a priori* information, a deterministic state-observer is used in the design. This choice is justified as the structure of the plant model includes internal filtering, the bias state, which reduces the impact of the noise on the remaining process and disturbance states thereof. It will be shown subsequently that the proposed design ultimately coincides with the celebrated linear quadratic Gaussian (LQG) control scheme, with explicitly defined noise covariance properties.

4.1.2.1 Determination of the state weighting matrix

In the optimal control problem, the state weighting matrix was inherently defined as $\mathbf{Q} = \mathbf{C}_z^T\mathbf{Q}_z\mathbf{C}_z$, a weighting that guarantees that the found solution is the global minimiser in terms of the performance variable. Unfortunately, there is no such parameterisation for the optimal estimation problem and the optimum obtained as the solution yields only the optimal performance in terms of the weighting matrices. In essence, the optimal cost is a function of the weighting parameters. Hence, a poor choice for the state weighting matrix may yield very bad estimation performance even though it minimises the cost function. Although there are some rules of thumb for choosing the weights (Anderson and Moore, 1989), there still is no obvious way to choose them such that the optimal performance can be guaranteed in every possible scenario. In the special problem of active vibration control, the existing rules of thumb do not yield very good performance. In order to obtain consistent performance, a certain type of weighting is proposed for the problems belonging to the class considered herein. The weighting matrix is now split into two parts, namely:

$$\mathbf{Q}_{\text{obs}} = \mathbf{W}\mathbf{G}_{\text{scale}}\,, \tag{4.21}$$

where $\mathbf{G}_{\text{scale}} \in \mathbb{R}^{r\times r}$ is a matrix scaling the squared state variation into unity, in essence allowing the use of the same design parameters to obtain similar performance regardless of true system dynamics. $\mathbf{W} \in \mathbb{R}^{r\times r}$ is a weighting matrix used to determine the control performance and robustness, given as:

$$\mathbf{W} = \operatorname{diag}\left\{\left[\alpha\mathbf{I}_{\text{p}} \;\middle|\; \beta\mathbf{I}_{\text{d}} \;\middle|\; \gamma\mathbf{I}_{\text{b}}\right]\right\}, \tag{4.22}$$

where subscripts p, d and b denote identity matrices of appropriate dimensions related to the process, disturbance and bias states, respectively. The scalars α, β and γ are the tuning parameters determining the convergence and robustness properties of the controller. The impact of these parameters is described in detail in Subsection 4.1.4.

The scaling matrix is defined such that it scales the weighting of the plant states according to their highest possible variation. The derivation of these scaling coefficients is a straightforward procedure. The variation of the process states is obtained by replacing the output matrix $\mathbf{C}_{\text{p}}$ in Eq. (3.1) with an identity matrix and converting the resulting model into a transfer-function matrix $\mathbf{G}_{\text{tf}}(s)$. This matrix represents the decomposition of the dynamics from the process inputs into each state, given as:

$$\mathbf{G}_{\text{tf}}(s) = \begin{bmatrix} G_{11}(s) & \cdots & G_{1m}(s) \\ \vdots & \ddots & \vdots \\ G_{n1}(s) & \cdots & G_{nm}(s) \end{bmatrix} = \begin{bmatrix} \mathbf{G}_1(s) \\ \vdots \\ \mathbf{G}_n(s) \end{bmatrix}, \tag{4.23}$$

where the transfer-functions $G_{nm}(s)$ describe the dynamics of each separate channel.

The highest possible variation of each process state is now found as the H_∞-norm of the related row vectors, defining the vector of the process state scaling coefficients as:

$$\mathbf{g}_{\text{p}} = \begin{bmatrix} g_1 & \cdots & g_n \end{bmatrix}^T = \begin{bmatrix} \|\mathbf{G}_1(s)\|_\infty & \cdots & \|\mathbf{G}_n(s)\|_\infty \end{bmatrix}^T. \tag{4.24}$$

The scaling now guarantees the boundedness of the state variation from above by unity. However, this type of scaling can be very conservative, yielding a poor scaling for the studied problem where the input signals are dominated by the realised control signals that are acting on some a priori known frequencies. The scaling can be enhanced by taking this piece of information into account and considering only the variation occurring at these known frequencies. The upper-bound for the state variation at a frequency is then given as:

$$\begin{aligned} g_n &= |x_n(j\omega)| \\ &= |G_{n1}(j\omega)||u_1(j\omega)| + |G_{n2}(j\omega)||u_2(j\omega)| + \cdots + |G_{nm}(j\omega)||u_m(j\omega)| \end{aligned} . \quad (4.25)$$

Without the loss of generality, the control inputs can be assumed to be of a relative unit variance, yielding $|u_1(j\omega)| = |u_2(j\omega)| = \cdots = |u_m(j\omega)| = 1$. The Eq. (4.25) can then be rewritten as:

$$g_n = |x_n(j\omega)| = |G_{n1}(j\omega)| + |G_{n2}(j\omega)| + \cdots + |G_{nm}(j\omega)| = \sum_{k=1}^{m} |G_{nk}(j\omega)| . \quad (4.26)$$

The Eq. (4.26) defines the upper bound for the maximal state variation subject to sinusoidal excitation acting on a single frequency. It is notable that the upper bound may still be rather conservative due to unknown phase and amplitude properties of the excitation signal. However, the bounds are significantly tighter than those obtained as the H_∞-norm. Finally, by taking the possibility of multiple tonal disturbances and the resulting multiple tonal excitations into account, the scaling is extended to:

$$\begin{aligned} g_n &= |x_n(j\omega)| = \sum_{k=1}^{m} |G_{nk}(j\omega_1)| + \sum_{k=1}^{m} |G_{nk}(j\omega_2)| + \cdots + \sum_{k=1}^{m} |G_{nk}(j\omega_i)| \\ &= \sum_{r=1}^{i} \sum_{k=1}^{m} |G_{nk}(j\omega_r)| \end{aligned} . \quad (4.27)$$

The scaling vector for the process states can then be rewritten as:

$$\mathbf{g}_\mathrm{p} = [g_1 \ \cdots \ g_n]^T = \left[\sum_{r=1}^{i} \sum_{k=1}^{m} |G_{1k}(j\omega_r)| \ \cdots \ \sum_{r=1}^{i} \sum_{k=1}^{m} |G_{nk}(j\omega_r)| \right]^T . \quad (4.28)$$

The second part of the scaling vector is related to the disturbance and the bias states. The variation of the disturbance states is unambiguously defined by the disturbance frequency. Under the assumption of unit amplitude, the related scaling vector for a disturbance formulated as in Eq. (3.12) is given as:

$$\begin{aligned} \left[\mathbf{g}_\mathrm{d}^T \mid \mathbf{g}_\mathrm{b}^T \right]^T = & \left[\left[[1 \ \ \omega_{d11} \ \cdots \ 1 \ \ \omega_{d1p}] \mid \cdots \right. \right. \\ & \left. \left. \mid [1 \ \ \omega_{di1} \ \cdots \ 1 \ \ \omega_{dip}] \right] \mid [\varepsilon \ \cdots \ \varepsilon] \right] \end{aligned} . \quad (4.29)$$

By combining the results in Eqs. (4.28) and (4.29), the scaling vector describing the variation of the plant states is given as:

$$\mathbf{g} = \left[\mathbf{g}_\mathrm{p}^T \mid \mathbf{g}_\mathrm{d}^T \mid \mathbf{g}_\mathrm{b}^T \right]^T . \quad (4.30)$$

Finally, the scaling matrix $\mathbf{G}_\mathrm{scale}$ bounding the squared state-vector in the cost function to approximate unit variance is given as the element wise squared inverse of the scaling factors $\mathbf{g}$ as:

$$\mathbf{G}_{\text{scale}} = \left(\operatorname{diag}\{\mathbf{g}\}\right)^{-2}. \tag{4.31}$$

4.1.3 Interpretation in the LQG-framework

The estimator design presented in Section 4.1.2 is optimal in the absence of measurement noise. Naturally, this is not a viable assumption in practice. There are controllers that have been shown to yield the optimal performance in the presence of noise with known characteristics. These are called LQG-controllers whose design can be found in many textbooks (Kwakernaak and Sivan, 1972; Anderson and Moore, 1989; Skogestad and Postlethwaite, 2005). The model structure used in the LQG-design is given as:

$$\begin{cases} \dot{\mathbf{x}}(t) = \mathbf{A}\mathbf{x}(t) + \mathbf{B}\mathbf{u}(t) + \mathbf{v}_{\text{I}}(t) \\ \mathbf{y}(t) = \mathbf{C}\mathbf{x}(t) + \mathbf{D}\mathbf{u}(t) + \mathbf{v}_{\text{o}}(t) \end{cases}, \tag{4.32}$$

where $\mathbf{v}_{\text{I}}(t) \in \mathbb{R}^r$ and $\mathbf{v}_{\text{o}}(t) \in \mathbb{R}^n$ are uncorrelated zero mean white noise sequences for input (process) and output (measurement) noises with the power spectral density (PSD) matrices $\mathbf{V}_{\text{I}} \in \mathbb{R}^{r\times r}$ and $\mathbf{V}_{\text{o}} \in \mathbb{R}^{n\times n}$, respectively.

The control problem is to find a control effort minimising the mathematical expectation of the related cost function, given as:

$$J_{\text{LQG}} = E\left\{ \int_0^{\infty} \left(\hat{\mathbf{z}}(\tau)^T \mathbf{Q}_z \hat{\mathbf{z}}(\tau) + \mathbf{u}(\tau)^T \mathbf{R}_z \mathbf{u}(\tau) \right) d\tau \right\}, \tag{4.33}$$

where $\hat{\mathbf{z}}(t)$ is the estimated value of the performance variable.

The design procedure is divided into two parts, namely the feedback and the observer design. The feedback design is exactly the same as in Section 4.1.1. However, the estimator is designed such that it provides a minimally biased state estimate under disturbances with known PSD characteristics. Such estimator is the best known as the static Kalman filter (Bar-Shalom and Xiao-Rong, 2001), which provides the optimal estimator weighting matrix, given as:

$$\mathbf{K}_f = \mathbf{F}\mathbf{C}^T\mathbf{V}_{\text{o}}^{-1}, \tag{4.34}$$

where $\mathbf{K}_f \in \mathbb{R}^{r\times n}$ is the Kalman gain and $\mathbf{F} \in \mathbb{R}^{r\times r}$ is the solution of the ARE:

$$\mathbf{A}\mathbf{F} + \mathbf{F}\mathbf{A}^T - \mathbf{F}\mathbf{C}^T\mathbf{V}_{\text{o}}^{-1}\mathbf{C}\mathbf{F} + \mathbf{V}_{\text{I}} = \mathbf{0}. \tag{4.35}$$

By comparing the Eqs.(4.34) and (4.35) with the Eqs. (4.19) and (4.20), the similarity of the two design methods becomes apparent. In essence, the optimal state-estimator presented in Section 4.1.2 can be interpreted as a Kalman filter with noise covariance matrices defined in a special way, more natural for the problem under study. The input covariance matrix $\mathbf{V}_{\text{I}}$ is essentially the same as the state-weighting matrix $\mathbf{Q}_{\text{obs}}$ and the output covariance matrix $\mathbf{V}_{\mathrm{o}}$ coincides with the matrix $\mathbf{R}_{\mathrm{obs}}$ used to define the estimator convergence speed.

4.1.4 Controller composition

Finally, the optimal control effort in Eq. (4.8) is combined with the observer dynamics in Eq. (4.15) yielding a state-space representation for a control law providing the required control effort in terms of the measured process output. The controller is hence given as:

$$\begin{cases} \dot{\mathbf{x}}_{\mathrm{c}}(t) = \mathbf{A}_{\mathrm{c}}\mathbf{x}_{\mathrm{c}}(t) + \mathbf{B}_{\mathrm{c}}\mathbf{y}(t) \\ \mathbf{u}(t) = \mathbf{C}_{\mathrm{c}}\mathbf{x}_{\mathrm{c}}(t) \end{cases}, \tag{4.36}$$

where $\mathbf{x}_{\mathrm{c}}(t) \in \mathbb{R}^{r}$ is the controller state-vector, with the controller system matrices defined as $\mathbf{A}_{\mathrm{c}} = \mathbf{A} - \mathbf{KC} - \mathbf{BL}$, $\mathbf{B}_{\mathrm{c}} = \mathbf{K}$ and $\mathbf{C}_{\mathrm{c}} = -\mathbf{L}$.

For the practical implementation purposes, the controller can be discretised with any method and sampling rate suitable for the problem.

Remark 4.3. For the notational convenience, the preceding derivation of the controller is in continuous time. In practice it is more feasible to design the controller in the discrete time as the process model is already a discrete representation due to the identification procedure. The discrete time control design is exactly the same as in continuous time with the exception of the AREs in Eqs. (4.6) and (4.20) are replaced by their respective discrete counter-parts (Arnold and Laub, 1984) given as:

$$\mathbf{A}^{T}\mathbf{SA} - \mathbf{S} - \left(\mathbf{A}^{T}\mathbf{SB} + \mathbf{N}\right)\left(\mathbf{B}^{T}\mathbf{SB} + \mathbf{R}\right)^{-1}\left(\mathbf{B}^{T}\mathbf{SA} + \mathbf{N}^{T}\right) + \mathbf{Q} = \mathbf{0} \tag{4.37}$$

and

$$\mathbf{APA}^{T} - \mathbf{P} - \mathbf{APC}^{T}\left(\mathbf{CPC}^{T} + \mathbf{R}_{\mathrm{obs}}\right)^{-1}\mathbf{CPA}^{T} + \mathbf{Q}_{\mathrm{obs}} = \mathbf{0}, \tag{4.38}$$

respectively, with the related feedback matrices defined as:

$$\mathbf{L} = \left(\mathbf{B}^{T}\mathbf{SB} + \mathbf{R}\right)^{-1}\left(\mathbf{B}^{T}\mathbf{SA} + \mathbf{N}^{T}\right) \tag{4.39}$$

and

$$\mathbf{K} = \mathbf{APC}^{T}\left(\mathbf{CPC}^{T} + \mathbf{R}\right)^{-T} \tag{4.40}$$

respectively.

4.1.5 Impact of the tuning parameters

The overall performance of an LQ-controller depends on two independent factors. The steady-state performance is governed by the state-feedback design and the related weighting matrices $\mathbf{Q}_{\mathrm{z}}$ and $\mathbf{R}_{\mathrm{z}}$, which define the amount of weighting set to the separate plant inputs and outputs. The impact of these matrices defines the amount of applied control effort versus the output deviation from zero. In essence, the higher the relative input weighting, the higher the steady-state output signal amplitude. The relative ratios of the elements of these matrices are used in MIMO-systems to define the amount of the desired control effort between the actuators and the tolerable output amplitudes between the measured channels. Typically, these elements are chosen uniform unless there is some *a priori* information such as the different effectiveness of the actuators or outputs that are considered be more crucial considering the overall performance of the whole system.

Intuitively speaking, the input weighting should be set close to zero in order to obtain as good output suppression as possible. However, in practice the amount of the available control energy is limited and the weighting should be set high enough to prevent control saturation thereof. It is notable that the impact of the state-feedback is immediate; hence the output variation and the convergence speed are determined solely by the process dynamics. Under the assumption of a perfect model, the design guarantees a stable closed-loop system regardless of the weighting parameters. However, in practice the models are always inaccurate and the state estimators are used, biasing the controlled states. Hence, the amount of the applied control energy should be further restricted to preserve the closed-loop stability in the presence of these unidealities. Unfortunately for the traditional LQ design, as presented here, there is no feasible way of determining the realised control effort other than through a procedure of trial and error. In some other methods such as the ones utilising linear matrix inequalities (LMIs), the control limitations can be inherently included in the design, yet it still relies on a model of the process.

The dynamical convergence and the stability of an LQ-controller are governed by the estimator properties. This is a natural result as the state information used in the feedback is obtained as the state-estimates from the input-output relation of the process. A poor state-estimate yields biased control performance and potentially causes closed-loop instability. The convergence rate of the estimates on the other hand determines the convergence speed of the overall system; therefore it is crucial that the state-estimates have rather fast asymptotic convergence and that they are insensitive to the process and the measurement noises. These properties are adjusted by the choices made for the estimator weighting matrices $\mathbf{Q}_{\text{obs}}$ and $\mathbf{R}_{\text{obs}}$, where the relative weighting of the states and artificial control signals determine the overall performance. The weighting matrix $\mathbf{R}_{\text{obs}}$ has a significant impact on the convergence speed of the estimate and some impact on the sensitivity to the measurement noise. In the given design, the robustness properties are governed by the weighting of the bias states; hence $\mathbf{R}_{\text{obs}}$ should be chosen small in amplitude in order to provide faster convergence speed as the potential measurement noise does not have as big an impact on the robustness.

The estimation error weighting matrix $\mathbf{Q}_{obs}$ is crucial for the estimator performance. As noted in Section 4.1.3, the diagonal elements of the matrix are related to the autocovariance of the state-estimation errors. The higher the relative amplitude, the more the state-error is penalised in the optimisation. Because of the inclusion of the scaling matrix, all states can be assumed to have similar variance and hence the states should be penalised equally to obtain similar estimation error for each state. This, however, is not practical due to the modelling errors and the process noise present in the system. In the design, this noise and uncertainties are described by the bias states. As these states do not have any impact on the control action, the closed-loop robustness to these phenomena is increased thereof. The weighting matrix $\mathbf{W}$ is used to adjust the estimation performance and the amount of signal energy set on the bias states.

The estimator performance is directly determined by the relative ratio of the parameters α, β and γ, related to the process, disturbance and bias states, respectively. The impact of these parameters can be roughly summarised as follows. The larger the parameter α, the less robust the process is to the modelling errors, while the convergence of the initial estimation error is faster. The larger the parameter β, the faster the convergence speed and the ratio of the obtained damping is, while the closed-loop system becomes more sensitive to modelling errors. Finally, the larger the parameter γ, the more of the signal energy is directed to the bias states, which in turn, results in an increase in the closed-loop robust stability margins as these states are not used in the control feedback. However, the high value of γ results in a slower convergence speed; hence introducing a trade-off between the performance and the stability. In general, the parameters α and β are set first, providing satisfactory performance for a given problem. The parameter γ is then used to determine the final closed-loop robust stability margins and the convergence speed.

As mentioned previously, one of the main benefits of the proposed control law is the possibility of adjusting the closed-loop robustness properties with a single parameter. This is a direct consequence of the fact that the bias-states are not used in the realised control effort at all; otherwise the measurement noise and modelling errors would have a direct impact on the control action. In essence, the energy of the estimator input signal (process measurements) is spread over the estimator outputs (state-estimates) in some predefined fashion. The more of this energy is diverted to the bias states, the less of the process output energy is used in the control. However, by defining the disturbance and process weighting parameters suitably, the signal energy at the disturbance frequencies is not diverted to the bias states, but to the disturbance states, hence enabling the use of that information in the control feedback. This phenomenon and the impact of the different parameterisations can be studied by expressing the controller dynamics in Eq. (4.36) as a transfer-function matrix with the states defined as the outputs, in essence $\mathbf{C}_c = \mathbf{I}$, yielding:

$$\mathbf{G}_{\text{cont}}(s) = \begin{bmatrix} \mathbf{G}_{\text{cs}}(s) \\ \hline \mathbf{G}_{\text{bias}}(s) \end{bmatrix}, \tag{4.41}$$

where $\mathbf{G}_{\text{cs}}(s)$ contains the transfer functions related to the plant states that are used in the control, essentially being the states that are given a non-zero weighting in the performance variable in Eq. (4.2). The matrix $\mathbf{G}_{\text{bias}}(s)$ contains the transfer functions related to the plant bias states, which have no impact on the control effort and are thus give zero weighting in Eq. (4.2).

Next, the distribution of the signal energy between the states can be studied by comparing the largest singular values related to $\mathbf{G}_{\text{cs}}(s)$ and $\mathbf{G}_{\text{bias}}(s)$ over the whole positive frequency domain, essentially:

$$S_c(\omega) = \bar{\sigma}\left(\mathbf{G}_{\text{cs}}(j\omega)\right) = \left\|\mathbf{G}_{\text{cs}}(j\omega)\right\|_\infty, \forall \omega \in \mathbb{R}^+ \tag{4.42}$$

and

$$S_{\text{bias}}(\omega) = \bar{\sigma}\left(\mathbf{G}_{\text{bias}}(j\omega)\right) = \left\|\mathbf{G}_{\text{bias}}(j\omega)\right\|_\infty, \forall \omega \in \mathbb{R}^+, \tag{4.43}$$

where $S_c(\omega)$ and $S_{\text{bias}}(\omega)$ denote the spectra of the singular values for control and bias states, respectively.

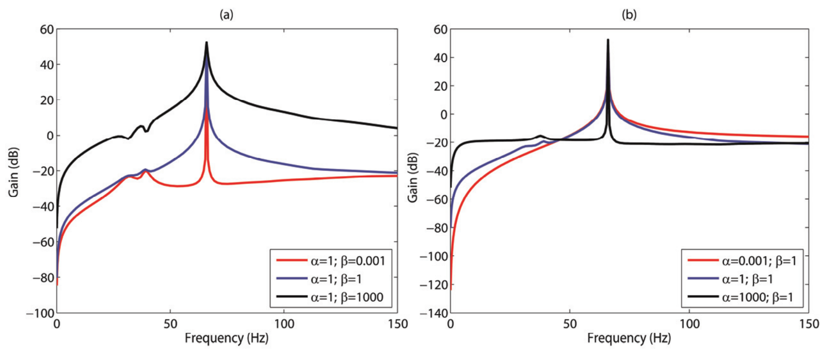

Figure 4.2. The singular values of the controller state outputs with the bias state excluded. (a) Under the variation of the β-parameter. (b) Under the variation of the α-parameter.

The impact of the relative ratio of the parameters α and β is illustrated in Fig. 4.2 with a constant bias weighting parameter. The impact of the γ parameter on the distribution of the signal energy to the bias states is illustrated in Fig. 4.3 with fixed α and β parameters. According to the figure, the connection of γ parameter to the closed-loop stability is now evident. While the measured process output passes through the controller, a certain amount of the resulting control 'energy' is diverted to the bias states, as seen in Fig. 4.3, the amount of the diverted energy is governed by the bias weighting parameter γ. In essence, as the bias states are excluded from the control action, the energy diverted to those states is also excluded from the realised control action; therefore making it more conservative and ultimately, more robust.

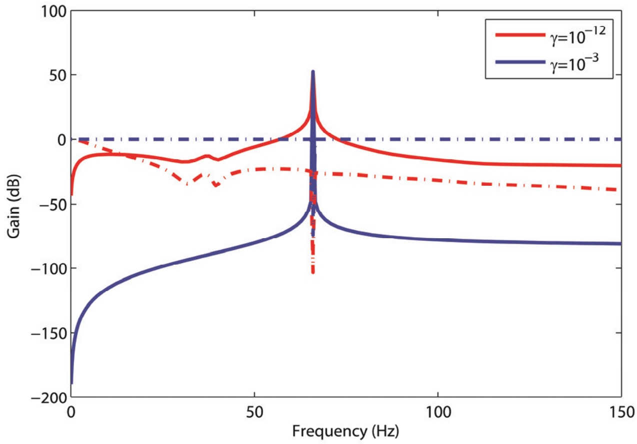

Figure 4.3. The singular values of the controller state outputs as a function of frequency with the bias state excluded (solid) and the output related to the bias states (dash-dotted).

4.2 Nonlinear control law

The linear control law presented in Section 4.1 is very effective for the mitigation of static tonal disturbances. Although there are several processes operating at static frequencies such as electric motors in a process with constant throughput, the more common scenario requiring vibration suppression occurs in processes with frequency varying tonal disturbances. These processes include electric and combustion motors used in process run-ups and downs, rolling processes where the frequency varies according to a constant line speed and several other processes where the operating speed varies based on an external speed reference, typically resulting from the higher level process optimisation. Because of the structure of the linear controller, it is completely ineffective in mitigation of disturbances outside its design frequency. This is a severe limitation in terms of the practical applications, where the disturbance frequency is seldom available *a priori* even if it was acting on a constant frequency. One example of those is the processes with varying types of end products, where the process parameters, in terms of the speed, may be altered between every batch. In such scenario, the operator would have to redesign the controller between each batch, which is both completely unfeasible and unacceptable approach.

In order to satisfy the refined problem statement, the applied control law must be able to adapt to the changes in the disturbance frequency. Unfortunately, given the model structure used for the plant, the system becomes linear parameter varying (LPV) and the related control law is a nonlinear function of the disturbance frequencies thereof. There are several very usable approaches to tackle the problem, varying from adaptive gain-scheduled control schemes (Kinney and de Callafon, 2006; Kinney and de Callafon, 2007; Tammi *et al.*, 2007) to robust control formulations, where the disturbance frequency is considered an unknown process parameter (Knospe *et al.*, 1997b; Bittanti and Cuzzola, 2002; Du *et al.*, 2003; Köroğlu and Scherer, 2011a; Köroğlu and Scherer, 2011b; Ballesteros and Bohn, 2011). These approaches have been shown to provide satisfactory results in SISO-systems where the point of excitation of the disturbance is assumed at the process input. Although these methods are extendable to the MIMO-systems, they suffer from several disadvantages in such problems. The performance of the robust control approach is dependent on the weighting transfer functions of the quantities, whose H_∞-norm is to be minimised. This is a rather trivial and straight-forward task in SISO-systems, yet it is not such in the MIMO-cases as the weighting transfer functions become matrices. In order to obtain a good performance, the elements of the matrix have to be specified such that its related singular values are acceptable over the whole frequency domain. Hence, the problem becomes highly complex as the number of the inputs and outputs of the studied process increases. Also, the robust control approach involves solving multiple LMIs, which is an easy task for an expert in control theory, but not necessarily for a system specialist running an industrial process. The IMC- approach, on the other hand, assumes the disturbance to be located at the process input. Such assumption may result in a very poor control performance in non-square plants with more inputs than outputs, as is the case with some of the present linear controllers addressed in Section 4.1.

In order to overcome some of the problems in the designs mentioned above, an extension to the linear control law derived in the previous section is proposed. In the resulting nonlinear optimal controller, the scalar elements of the feedback matrices $\mathbf{L}$ and $\mathbf{K}$ are replaced by the arbitrary functions of the frequency and the operation points. Such functions are obtained through the continuous gain-scheduling of a set of linear controllers designed for a single frequency and operation point. The resulting controller provides very high vibration damping over its whole frequency design range for a process subject to an arbitrary number of frequency varying tonal disturbances. The control design is presented in detail in the subsequent section.

4.2.1 Extension into a nonlinear control law

The approach taken in the extension of the linear controller into its nonlinear counterpart is based on the notion that every single linear controller is the optimal solution at its respective design frequency and process operation point. It naturally follows that the problem of several different operation points and disturbance frequencies can be tackled by designing a linear controller for every possible combination of the varying parameters. In essence, this requires an infinite set of linear controllers, from which the suitable controller is chosen depending on the process state. Naturally, such an approach is infeasible even if the set is sparse due to the space (or memory) requirements and the problems related to the controller switching. However, this is the typical approach chosen for the gain-scheduled controllers. In order to evade some of the problems related to the gain-scheduling based on a discrete set of controllers, a continuous approach is utilised. By studying the values of the elements in the gain matrices of the controllers designed for several distinct frequencies, it becomes apparent that the values of these elements coincide when the frequency deviation becomes infinitely small, implying for a single element:

$$k(\omega) = \lim_{x \to \omega_-} k(x) = \lim_{x \to \omega_+} k(x), \omega \in \mathbb{R}^+, \tag{4.44}$$

where ω_- and ω_+ denote the approach to the frequency ω from below and above, respectively.

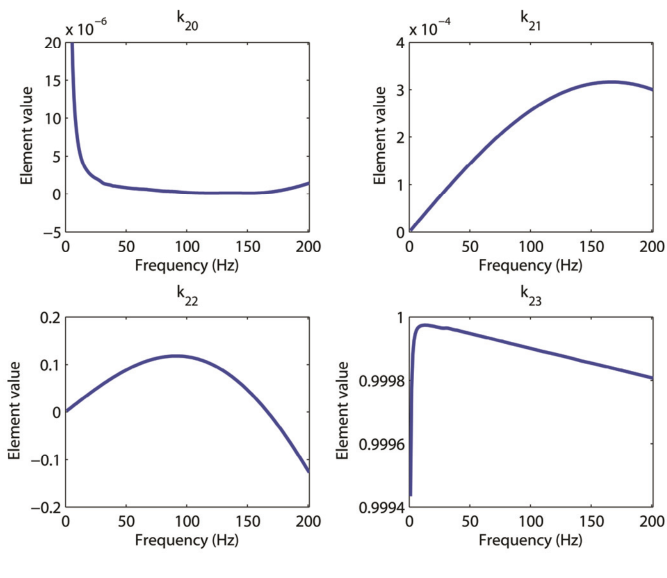

Figure 4.4. Some projections of a decision hypersurface describing the variation of the gain elements as a function of the frequency.

In essence, Eq. (4.44) states that the variation of the gain elements is smooth and their trajectories are differentiable. The projections of a decision hypersurface into the gain surfaces describing the variation of some of the gain elements in a certain system are illustrated in Fig. 4.4.

Remark 4.4. Scaling of the process model presented in the preceding section guarantees the smoothness of the gain element trajectories. This is a direct result of the fact that the same weighting matrices are used in the control design for every frequency. If these weighting matrices are required to vary in order to obtain satisfactory control performance, which is the case if the scaling is omitted, the smoothness cannot be guaranteed. In essence, the continuous gain-scheduling approach to the nonlinear controller composition is possible due to the applied scaling in the design of the linear controllers.

Because of the smoothness of the trajectories in Fig. 4.4, the variation of a gain element can be described with a suitable continuous function of the frequency and the operation points, hence eliminating the need for a database of predefined controllers. By using such formulation, the controller dynamics in Eq. (4.36) can be rewritten as:

$$\begin{cases} \dot{\mathbf{x}}_c(t,\boldsymbol{\omega}_{hz},\mathbf{a}) = \mathbf{A}_c(\boldsymbol{\omega}_{hz},\mathbf{a})\mathbf{x}_c(t,\boldsymbol{\omega}_{hz},\mathbf{a}) + \mathbf{B}_c(\boldsymbol{\omega}_{hz},\mathbf{a})\mathbf{y}(t) \\ \mathbf{u}(t,\boldsymbol{\omega}_{hz},\mathbf{a}) = \mathbf{C}_c(\boldsymbol{\omega}_{hz},\mathbf{a})\mathbf{x}_c(t,\boldsymbol{\omega}_{hz},\mathbf{a}) \end{cases}, \tag{4.45}$$

where $\boldsymbol{\omega}_{hz} \in \mathbb{R}^p$ is a vector defining current disturbance frequencies and $\mathbf{a} \in \mathbb{R}^a$ is a vector defining the current operation points of a nonlinear process. The system matrices with the elements defined as the arbitrary functions of the arguments $\boldsymbol{\omega}_{hz}$ and $\mathbf{a}$, in essence $f(\boldsymbol{\omega}_{hz},\mathbf{a}): \mathbb{R}^{p+a} \to \mathbb{R}^1$, are given as:

$$\begin{aligned} \mathbf{A}_c(\boldsymbol{\omega}_{hz},\mathbf{a}) &= \mathbf{A}(\boldsymbol{\omega}_{hz},\mathbf{a}) - \mathbf{K}(\boldsymbol{\omega}_{hz},\mathbf{a})\mathbf{C}(\mathbf{a}) - \mathbf{B}(\mathbf{a})\mathbf{L}(\boldsymbol{\omega}_{hz},\mathbf{a}) \\ \mathbf{B}_c(\boldsymbol{\omega}_{hz},\mathbf{a}) &= \mathbf{K}(\boldsymbol{\omega}_{hz},\mathbf{a}) \\ \mathbf{C}_c(\boldsymbol{\omega}_{hz},\mathbf{a}) &= -\mathbf{L}(\boldsymbol{\omega}_{hz},\mathbf{a}) \end{aligned}. \tag{4.46}$$

The structure of the obtained control law is generic, hence being able to handle an arbitrary number of nonlinearities and frequencies through the definition of suitable scheduling functions; unfortunately implying that each function should describe a mapping from a q-dimensional space, where q is the number of the nonlinearities and frequencies, namely $q = p + a$, into a 1-dimensional space. Although such mapping is obtainable by for example neural networks, the data set used for the network training would be a q-dimensional mesh of parameter values obtained for each possible combination of $\boldsymbol{\omega}_{hz}$ and $\mathbf{a}$. Clearly, this is not a feasible approach although being theoretically valid.

Fortunately, the problem can be significantly simplified by taking into account some properties of the physical systems where the vibrations occur. First, the disturbance frequencies perceived in a process are, in most cases, described by a main tone and its higher and lower harmonics and subharmonics. In essence, the information on a single tone can be used to describe all disturbance characteristics of the plant. Second, most of the processes, although nonlinear, typically operate in the close vicinity of a certain operation point, allowing the use linear process models. Even if the process is truly nonlinear, the dominating nonlinearity can typically be described with a single variable. By making such additional assumptions, the number of required description variables for the nonlinear controller is in the worst case two. Hence, implying that the functions describing the elements are mappings $f(\cdot):\mathbb{R}^2 \rightarrow \mathbb{R}^1$, which is essentially a problem of surface fitting and is rather readily realisable in practice. For simplicity, the assumption of the linearity of the underlying process is made in the sequel. Now the nonlinear controller for multi-tonal disturbance mitigation in a linear process subject to frequency varying disturbances, related to the variation of a main tone, is given as:

$$\begin{cases} \dot{\mathbf{x}}_c(t,\omega_{hz}) = \mathbf{A}_c(\omega_{hz})\mathbf{x}_c(t,\omega_{hz}) + \mathbf{B}_c(\omega_{hz})\mathbf{y}(t) \\ \mathbf{u}(t,\omega_{hz}) = \mathbf{C}_c(\omega_{hz})\mathbf{x}_c(t,\omega_{hz}) \end{cases}, \tag{4.47}$$

where ω_{hz} is the frequency of the main tone, with the related system matrices defined as:

$$\begin{aligned} &\mathbf{A}_c(\omega_{hz}) = \mathbf{A}(\omega_{hz}) - \mathbf{K}(\omega_{hz})\mathbf{C} - \mathbf{B}\mathbf{L}(\omega_{hz}) \\ &\mathbf{B}_c(\omega_{hz}) = \mathbf{K}(\omega_{hz}) \\ &\mathbf{C}_c(\omega_{hz}) = -\mathbf{L}(\omega_{hz}) \end{aligned}, \tag{4.48}$$

where the feedback matrices are given as:

$$\mathbf{K}(\omega_{hz}) = \begin{bmatrix} f_{11}(\omega_{hz}) & f_{12}(\omega_{hz}) & \cdots & f_{1n}(\omega_{hz}) \\ f_{21}(\omega_{hz}) & f_{22}(\omega_{hz}) & & f_{2n}(\omega_{hz}) \\ \vdots & & \ddots & \vdots \\ f_{r1}(\omega_{hz}) & f_{r2}(\omega_{hz}) & \cdots & f_{rn}(\omega_{hz}) \end{bmatrix} \tag{4.49}$$

and

$$\mathbf{L}(\omega_{hz}) = \begin{bmatrix} g_{11}(\omega_{hz}) & g_{12}(\omega_{hz}) & \cdots & g_{1r}(\omega_{hz}) \\ g_{21}(\omega_{hz}) & g_{22}(\omega_{hz}) & & g_{2r}(\omega_{hz}) \\ \vdots & & \ddots & \vdots \\ g_{m1}(\omega_{hz}) & g_{m2}(\omega_{hz}) & \cdots & g_{mr}(\omega_{hz}) \end{bmatrix}, \tag{4.50}$$

where $f_{rn}(\cdot)$ and $g_{mr}(\cdot)$ are arbitrary functions of the main disturbance frequency.

4.2.2 Determination of the weighting matrices

The weighting matrices used in the nonlinear control design consist of the arbitrary functions of the main disturbance frequency. These functions describe the variation of the gain element over the frequency domain of interest. Although the variation is continuous, implying that there may exist a single function describing the variation, in practice finding such function candidate is nearly impossible. Hence, functions approximating the variation are used. Regardless of the applied approximation method, the first step in the procedure is to define a finite set of element values over the frequency range of interest. Such set is obtained by first defining a finite frequency grid and then designing a linear controller for its every distinct point, resulting in a set of *N* distinct controllers. The feedback matrices of the resulting controllers are then extracted and stacked, forming two *rank three*-tensors, with the elements in the direction of the frequency axis given as vectors of element values $\mathbf{k}_{rn}$ and $\mathbf{l}_{mr}$ for observer weighting and state-feedback, respectively.

After the vectors of data points describing the element variations have been obtained, fit a suitable function is fitted for the approximation. One possible candidate for such function is a neural network, which can be readily used to describe complex nonlinear functions. Although the network training is simple, they are not very preferable for a real-time implementation due to potentially high on-line computational load and problems related to the actual implementation. For example, MATLAB© Real-time workshop does not support the neural networks at this time. A more straightforward approach is to use polynomial approximations, resulting in the functions of the form:

$$\begin{aligned} f_{rn}(\omega_{\text{hz}}) &= a_{rn1}\omega_{\text{hz}}^{p} + a_{rn2}\omega_{\text{hz}}^{p-1} + \cdots + a_{rn(p-1)}\omega_{\text{hz}}^{1} + a_{rnp} \\ &= \begin{bmatrix} a_{rn1} & a_{rn2} & \cdots & a_{rnp} \end{bmatrix}\begin{bmatrix} \omega_{\text{hz}}^{p} & \omega_{\text{hz}}^{p-1} & \cdots & \omega_{\text{hz}}^{0} \end{bmatrix}^{T} = \mathbf{a}_{rn}\boldsymbol{\omega}_{\text{hz}}^{T} \end{aligned} \tag{4.51}$$

and

$$\begin{aligned} g_{mr}(\omega_{\text{hz}}) &= b_{mr1}\omega_{\text{hz}}^{p} + b_{mr2}\omega_{\text{hz}}^{p-1} + \cdots + b_{mr(p-1)}\omega_{\text{hz}}^{1} + b_{mrp} \\ &= \begin{bmatrix} b_{mr1} & b_{mr2} & \cdots & b_{mrp} \end{bmatrix}\begin{bmatrix} \omega_{\text{hz}}^{p} & \omega_{\text{hz}}^{p-1} & \cdots & \omega_{\text{hz}}^{0} \end{bmatrix}^{T} = \mathbf{b}_{mr}\boldsymbol{\omega}_{\text{hz}}^{T}, \end{aligned} \tag{4.52}$$

where the coefficient vectors $\mathbf{a}_{rn}$ and $\mathbf{b}_{mr}$ are chosen such that they minimise the approximation error in the least squares sense, in essence:

$$\mathbf{a}_{rn} = \mathbf{k}_{rn}\boldsymbol{\Omega}^{T}\left(\boldsymbol{\Omega}\boldsymbol{\Omega}^{T}\right)^{-1} \tag{4.53}$$

and

$$\mathbf{b}_{mr} = \mathbf{l}_{mr}\boldsymbol{\Omega}^{T}\left(\boldsymbol{\Omega}\boldsymbol{\Omega}^{T}\right)^{-1}, \tag{4.54}$$

where $\boldsymbol{\Omega} = \left[\boldsymbol{\omega}_{\text{hz}}^{T}(1) \mid \boldsymbol{\omega}_{\text{hz}}^{T}(2) \mid \cdots \mid \boldsymbol{\omega}_{\text{hz}}^{T}(k)\right]$ with k denoting the index of the frequency related to the k:th element of $\mathbf{k}_{rn}$ or $\mathbf{l}_{mr}$.

With the polynomial approximation being applied, the frequency varying weighing matrices in Eqs. (4.49) and (4.50) are given as:

$$\mathbf{K}(\omega_{\text{hz}}) = \left[\begin{array}{c|c|c|c} \mathbf{a}_{11} & \mathbf{a}_{12} & \cdots & \mathbf{a}_{1n} \\ \hline \mathbf{a}_{21} & \mathbf{a}_{22} & & \mathbf{a}_{2n} \\ \hline \vdots & & \ddots & \vdots \\ \hline \mathbf{a}_{r1} & \mathbf{a}_{r2} & \cdots & \mathbf{a}_{rn} \end{array}\right] \otimes \boldsymbol{\omega}_{\text{hz}}^T = \mathbf{K}_{\mathbf{a}} \otimes \boldsymbol{\omega}_{\text{hz}}^T \tag{4.55}$$

and

$$\mathbf{L}(\omega_{\text{hz}}) = \left[\begin{array}{c|c|c|c} \mathbf{b}_{11} & \mathbf{b}_{12} & \cdots & \mathbf{b}_{1r} \\ \hline \mathbf{b}_{21} & \mathbf{b}_{22} & & \mathbf{b}_{2r} \\ \hline \vdots & & \ddots & \vdots \\ \hline \mathbf{b}_{m1} & \mathbf{b}_{m2} & \cdots & \mathbf{b}_{mr} \end{array}\right] \otimes \boldsymbol{\omega}_{\text{hz}}^T = \mathbf{L}_{\mathbf{b}} \otimes \boldsymbol{\omega}_{\text{hz}}^T . \tag{4.56}$$

An example of such continuously scheduled gain element is given in Fig. 4.5, where a fourth order polynomial is used for the approximation. It is apparent that the polynomial approximation describes the variation of the element with adequate accuracy.

Remark 4.5. The Eqs. (4.53) and (4.54) assume the existence of the inverse $\left(\boldsymbol{\Omega\Omega}^T\right)^{-1}$, which is inherently guaranteed if all element values are obtained for separate frequencies. For increased numerical accuracy, it is advisable to normalise the regressors (frequency vectors) to zero mean and unit variance.

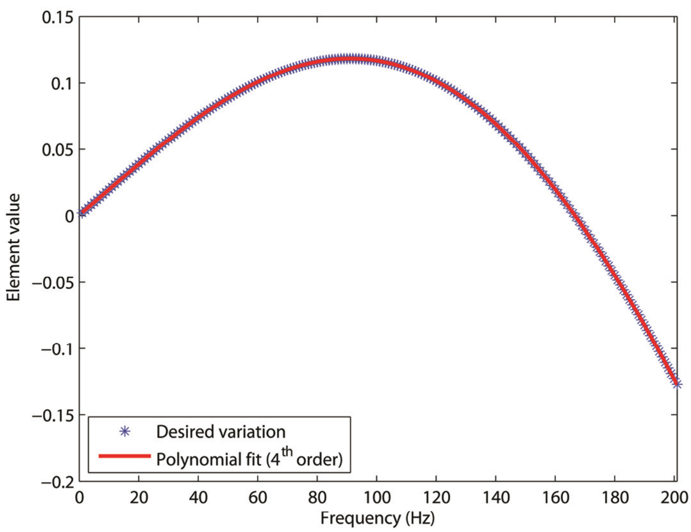

Figure 4.5. The polynomial approximation of the gain element variation vs. the desired element variation.

4.2.3 On the stability and optimality of the nonlinear controller

The guaranteed stability of the closed-loop system is of utmost importance in a practical implementation. The linear controllers used in the design of the nonlinear controller are guaranteed to yield an asymptotically stable closed-loop system under the assumption of an unbiased model. Even if the model is biased, the design still provides acceptable gain and phase margins. As the nonlinear control law is essentially a set of gain-scheduled linear controllers, the designer is tempted to assume that the extended control law has guaranteed stability thereof. Unfortunately, this is not the case as some of the elements of the system matrices are varied according to the process operation point and the state feedback matrix is a nonlinear function of the disturbance frequency. Hence the overall controller has become nonlinear parameter varying, and therefore the stability of the system can no longer be determined through linear stability analysis but more sophisticated methods have to be utilised. The stability of nonlinear systems can be evaluated by using Lyapunov stability criteria (Slotine and Weiping, 1991). Unfortunately, the analytical determination of the stability for the given system is infeasible as it would require the analysis of a Lyapunov-function in terms of the time, the operation point and the disturbance frequency, resulting in a set of complex high order partial differential equations.

Although the analytical analysis of the stability is not possible, there are results, which can be used to verify the closed-loop stability of the system. It has been previously shown by (Desoer, 1969; Rugh, 1991; Guo and Rugh, 1995) that a gain-scheduled control law stabilises the system if the closed-loop system is stable whenever the gain-scheduling is frozen and the variation of the parameters is smooth. These requirements are readily shown to be fulfilled when considering the system under study. First, the nonlinear controller is formed from a set of gain-scheduled LQ-controllers, implying that whenever the scheduling is frozen, the closed-loop system is restored into a process controlled with a linear feedback law; hence having the guaranteed gain and phase margins. However, as the gain elements are defined through polynomial approximations, which are to some extent inaccurate, the stability of the controller has to be re-evaluated at each discrete frequency point in order to verify that the closed-loop stability is indeed preserved. Second, the processes being considered in the applications are physical systems, with the disturbance frequency somehow related to their operation, for example the rotation of a shaft. Hence, the processes always contain some inertia, implying that the disturbance frequency, the scheduled variable, is at least twice differentiable. This guarantees that the frequency can never have instantaneous changes and its variation is smooth.

The controller uses information on the disturbance frequency as its scheduling variable. Even if this quantity is measured, it may be biased and subject to measurement noise. It is therefore crucial to evaluate the stability of the closed-loop system in the presence of biased scheduling variable. Fortunately, for the given design, the erroneous scheduling variable has no impact on the closed-loop stability. This is a direct result of the property of the underlying linear sub-controllers that were designed such that they produce no control effort outside the disturbance frequency, see Chapter 5. Hence, it follows that the biased frequency signal results in a use of a linear controller outside the true disturbance frequency, which in turn provides no control effort besides some minor deviation due to process noise. The resulting closed-loop system is then inherently stable although yielding no vibration mitigation.

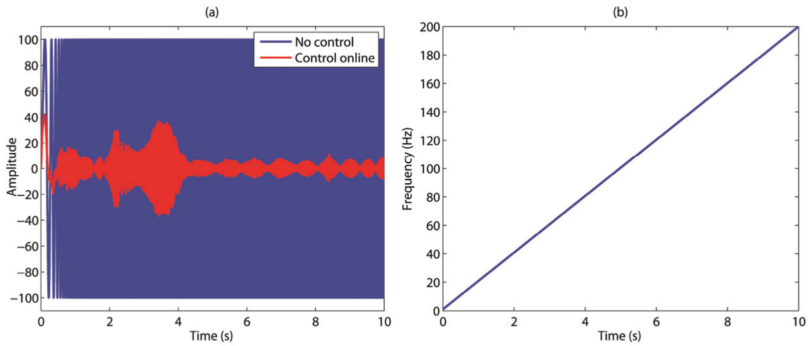

Figure 4.6. The performance of the nonlinear controller in a process subject to a disturbance with linearly changing frequency. (a) Measured process output. (b) Variation of the disturbance frequency.

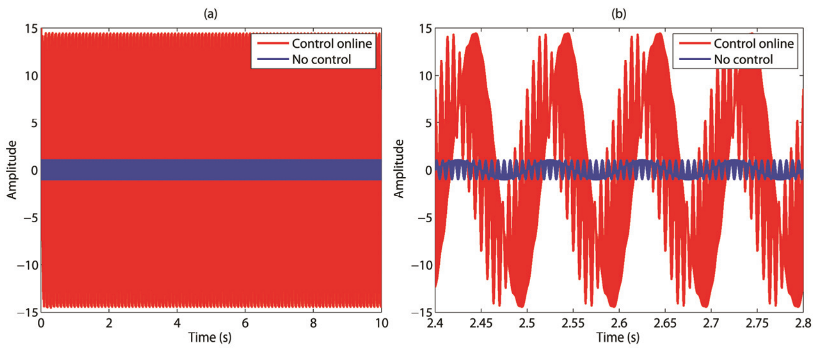

Figure 4.7. The performance of the nonlinear controller in a process subject to a disturbance with frequency subject to discrete switching. (a) Measured process output. (b) Close-up of the process output.

In order to verify the preceding claims, the stability is analysed in several simulations. The first simulation represents the worst case scenario of the acceptable frequency variation where the disturbance frequency is assumed to be a sinusoidal signal subject to a fast linear frequency variation from 0 Hz to 200 Hz in 10 seconds. The result of the test is given in Fig. 4.6. Even as the system evidently remains stable when the smoothness requirements are met, it is also important to evaluate the performance in a scenario where the smoothness assumptions are violated. This is easily realisable in simulations, where the sinusoidal disturbance is subject to discrete frequency changes; in essence the frequency is switched between two frequencies, namely 10 Hz and 150 Hz, on every sample instant. The results corresponding to this test are shown in Figs. 4.7 and 4.8. It is interesting to note that even as the smoothness assumptions are violated, the closed-loop system still remains stable although yielding very bad performance. By closer study it is evident that the system has ended up in a limit cycle, which is a typical result for nonlinear systems. It is important to bear in mind that even as the process studied herein remained stable, the result cannot be extended to all processes and hence nothing can be determined for the stability of the control scheme when subject to constant discrete changes in the frequency.

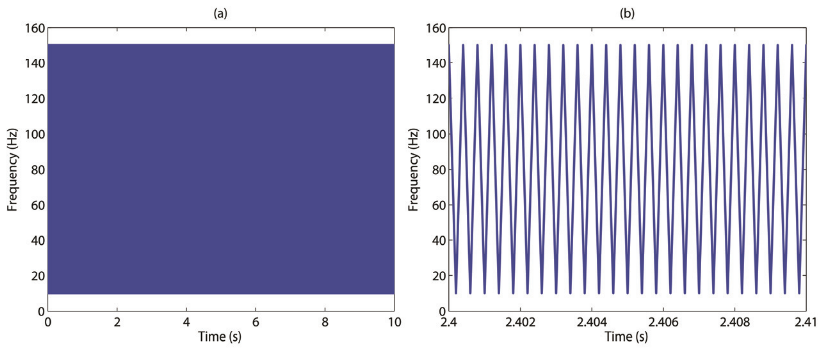

Figure 4.8. (a) Variation of the disturbance frequency. (b) Close-up of the frequency variation.

Previously, the nonlinear controller synthesised in the preceding sections is referred to as optimal, which is, in fact, a violation of the definition. Although the linear sub-controllers are indeed optimal, there is no guarantee that the nonlinear controller is such. In order to obtain an optimal nonlinear controller, the design would have to be made directly for that given system for example by using the calculus of variations. Unfortunately, as already discussed in the linear control design section, the resulting control law is time varying and time dependent. In addition, the optimal solution is obtained as a solution of a complex two-point boundary-value problem, which in general does not have analytical solution. Finally, the optimal control effort would require exact *a priori* information on the variation of the disturbance frequency, which is, in general, unavailable. Under these facts, it is improbable that a general optimal control law for nonlinear systems is ever available. Hence, the control law presented in this work is referred to as 'optimal' as it is such whenever the gain-scheduling is frozen. However, it should be borne in mind that it is not necessarily such in the transients of the disturbance frequency.

4.3 Frequency estimation

The nonlinear controller derived in the preceding section requires some measurement of the frequency of the main disturbance tone. In some processes, this information is directly available or some additional sensors can be installed to obtain it. Whenever the frequency can be measured, these measurements should be used for the controller frequency input. However, there are several scenarios where the direct disturbance measurement is either not possible at all or inclusion of additional sensors is not a cost-efficient approach. In such circumstances, the frequency information can be extracted from the measured process output. The benefit of such approach is that the information is obtained from the quantity, which is to be minimised through control, implying that the measurements are already readily available. The procedure of the frequency extraction is described in the following sub-sections.

4.3.1 RLS-based approach to frequency extraction

The problem of frequency extraction from a signal is a very active field of study. Already there are several very effective approaches such as (Savaresi *et al.*, 2003; Pai, 2009; Pai, 2010), which can be applied to obtain unbiased frequency estimates from a signal containing multiple tonal frequencies. As the field of study is rather vast, somewhat outside of the scope of this work and the frequency estimation is an independent problem from the controller design, these methods are not considered in further detail. However, a specific approach suitable for the frequency extraction in the given problem formulation, which is also used in PUB. IV is presented in detail. This RLS-based algorithm is rather trivial and computationally light and the most suitable for systems where the process is subject to a single significantly dominating tonal disturbance (Zazas *et al.*, 2010).

Consider a measured signal:

$$d(k) = A(k)\sin\left(\omega_d(k)kh + \varphi\right) + n(k)\,, \tag{4.57}$$

where $A(k)$ and $\omega_d(k)$ are a time-varying amplitude and frequency, respectively, φ is an arbitrary constant phase, k is the sample instant, h is the sampling rate and $n(k)$ is signal corresponding to the background noise.

The time-varying frequency can be decomposed as:

$$\omega_d(k) = \omega_{\text{ref}} + \omega_e(k)\,, \tag{4.58}$$

where ω_{ref} is a freely chosen constant reference frequency and $\omega_e(k)$ is a time-varying deviation from the reference.

By substituting Eq. (4.58) into Eq. (4.57), the disturbance signal can be rewritten as:

$$d(k) = A(k)\sin\left(\omega_{\text{ref}}kh + \Phi(k)\right) + n(k)\,, \tag{4.59}$$

where

$$\Phi(k) = \omega_e(k)kh + \varphi \tag{4.60}$$

is the time varying phase of the disturbance signal.

By utilising the sine addition formula, the Eq. (4.59) can be expanded and rewritten in a regression form as:

$$d(k) = \boldsymbol{\theta}^T(k)\mathbf{r}(k) + n(k), \tag{4.61}$$

where

$$\boldsymbol{\theta}(k) = \begin{bmatrix} \theta_1(k) & \theta_2(k) \end{bmatrix}^T = \begin{bmatrix} A(k)\cos(\Phi(k)) & A(k)\sin(\Phi(k)) \end{bmatrix}^T \tag{4.62}$$

and

$$\mathbf{r}(k) = \begin{bmatrix} \sin(\omega_{\text{ref}} kh) & \cos(\omega_{\text{ref}} kh) \end{bmatrix}^T. \tag{4.63}$$

The reference vector in Eq. (4.63) is a pair of sine and cosine signals acting on a static frequency chosen by the designer. The choice for the reference frequency is arbitrary and not necessary for the convergence of the algorithm. However, the closer the reference frequency is to the true frequency, the faster the convergence of the algorithm is; hence enabling the use of possible *a priori* information of the disturbance characteristics. It is obvious that the Eq. (4.61) is in a standard regression form; hence the parameter vector $\boldsymbol{\Phi}(k)$ can be estimated with any RLS-algorithm, such as presented in (Åström and Wittenmark, 1995).

The extraction of the signal properties from the estimated parameter vector Eq. (4.62) is a straightforward procedure, with the estimated phase and frequency obtained as:

$$\hat{A}(k) = \sqrt{\hat{\theta}_1^2(k) + \hat{\theta}_2^2(k)} \tag{4.64}$$

and

$$\hat{\Phi}(k) = \tan^{-1}\left(\frac{\hat{\theta}_2(k)}{\hat{\theta}_1(k)}\right), \forall \hat{\theta}_1(k) \neq 0. \tag{4.65}$$

Finally, the estimated disturbance frequency on a sample instant is obtained by first differentiating Eq. (4.60) in discrete time, yielding:

$$\left(1 - z^{-1}\right)\Phi(k) = \omega_e(k)kh + \varphi - \left(\omega_e(k)(k-1)h + \varphi\right) = \omega_e(k)h, \tag{4.66}$$

where z^{-1} denotes a shift operation backward in time. Also, the assumption of slow frequency variation, in essence $\omega_e(k) \approx \omega_e(k-1)$, was used.

The estimated frequency is now obtained by solving Eq. (4.66) for $\omega_e(k)$ and substituting it to Eq. (4.58), yielding:

$$\hat{\omega}_d(k) = \omega_{\text{ref}} + \frac{\left(1 - z^{-1}\right)\hat{\Phi}(k)}{h}. \tag{4.67}$$

Remark 4.6. By studying the Eq. (4.61) it is apparent that the preceding frequency estimator yields unbiased estimated only if $n(k)$ is a white noise sequence. Although this assumption is not feasible in practice, the estimator provides satisfactory accuracy when the signal is dominated by a single tone. In the presence of significant deterministic background noise or multiple tones, more elaborate estimator designs should be used.

4.3.2 Disturbance signal reconstruction

The frequency estimation in processes subject to active vibration mitigation has one significant disadvantage compared with the standard estimation schemes. Namely, the signal used for the estimation of the disturbance frequency is the very same signal which is being mitigated. This becomes a problematic property at the time when the controller is turned on. Essentially, the control action aims to completely compensate the tonal disturbance. At the time, that this occurs the frequency estimator cannot extract the true disturbance frequency as the measured signal no longer contains any significant energy at that particular frequency. The result of this interference is a control action, which first starts to converge to zero. At the time the disturbance signal amplitude falls below the background noise level, the frequency estimate becomes biased resulting in ineffective control action. Now, the disturbance signal becomes present again in the measured signal and the cycle starts all over again. The shadow curve of the measured output of the controlled process varies from the amplitude of perfect disturbance mitigation to the amplitude of the disturbance excitation.

This fundamental problem present in any active vibration control scheme is easily overcome by using signal reconstruction. As the process model is known, the output signal can be reconstructed by subtracting the expected control effort from the measured process output, resulting in a structure shown in Fig. 4.9, which is similar to those used in the IMC.

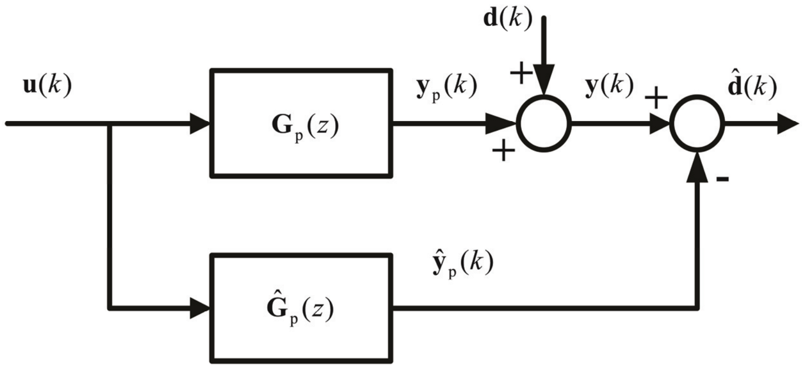

Figure 4.9. The structure of the frequency reconstruction scheme.

If the process model is an exact representation of the true system, the reconstructed signal is unbiased, which is obvious from:

$$\hat{\mathbf{d}}(k) = \mathbf{d}(k) + \mathbf{y}_{\mathrm{p}}(k) - \hat{\mathbf{y}}_{\mathrm{p}}(k) = \mathbf{d}(k) + \left(\mathbf{G}_{\mathrm{p}}(z) - \hat{\mathbf{G}}_{\mathrm{p}}(z)\right)\mathbf{u}(k)\,, \qquad (4.68)$$

where $\hat{\mathbf{d}}(k)$ is the reconstructed disturbance signal, $\hat{\mathbf{y}}_{\mathrm{p}}(k)$ and $\mathbf{y}_{\mathrm{p}}(k)$ are the model predicted and true process outputs, $\mathbf{G}_{\mathrm{p}}(z)$ and $\hat{\mathbf{G}}_{\mathrm{p}}(z)$ represent the true and modelled process dynamics.

However, because of the modelling errors this is unlikely to occur in practice, resulting in a reconstructed signal which is a sum of the residual of the true disturbance and the expected control. Fortunately, these biases affect only the phase and amplitude of the reconstructed signal, not the disturbance frequency. Hence, the biased reconstructed signal can be used for the frequency estimation. It is notable, that when the reconstruction scheme is being utilised, the amplitude of the disturbance is never zero in the reconstructed signal (unless, of course, there is no disturbance), preventing the time variation of the amplitude in the controlled process output thereof.

5. Performance evaluation

A crucial part in the controller synthesis is the evaluation of its performance and applicability for a given process. This theoretical study takes place before the practical implementation and yields valuable information whether an acceptable control performance can be expected even for an ideal process. Should the analysis give dissatisfactory results, the practical performance would be none the better, in general. In this chapter, the necessary analyses for an extensive performance evaluation are done. In Section 5.1, the theoretical performance of the linear control law derived in the preceding chapter is evaluated. The cross-comparison of the proposed method against the existing control approaches is given in Section 5.2; hence putting the effectiveness of the proposed control algorithm in the perspective and enabling the evaluation of its usability. Finally, in Section 5.3, the feasibility of the control scheme is evaluated by studying the requirements for the actuators in terms of the perfect vibration mitigation.

5.1 Performance and robustness analysis

An important phase of the control design is the performance and robustness analysis. Unfortunately, such analysis is often being overlooked, which is the reason why it is now stressed in this work. For any practical implementation, it is of utmost importance to verify that the resulting closed-loop process is stable. In addition to the stability requirement, it is good practice to evaluate the robust stability margins of the resulting system as the process models are known to be biased and vary over time, for example due to the wear and tear of the process components. In order to successfully implement a controller into a process, it is important that these margins are adequate, that is, the process remains stable regardless of the modelling inaccuracies. Finally, the performance of the closed-loop system is to be evaluated. Although this part is not necessary for the safety (stability) of the system, it is important to evaluate whether the controller provides a satisfactory control effort and meets the goals set by the designer. A general control configuration from which all preceding qualities can be derived is illustrated in Fig. 5.1. The signals of the interest are the input disturbance denoted by $\mathbf{d}_1(t) \in \mathbb{R}^m$, the output disturbance denoted by

$\mathbf{d}(t) \in \mathbb{R}^n$, the measurement noise denoted by $\mathbf{n}(t) \in \mathbb{R}^n$, the realised control effort denoted by $\mathbf{u}(t) \in \mathbb{R}^m$, the actuator (process) input denoted by $\mathbf{u}_\mathrm{p}(t) \in \mathbb{R}^m$ and the actuator (process) output denoted by $\mathbf{y}_\mathrm{p}(t) \in \mathbb{R}^n$.

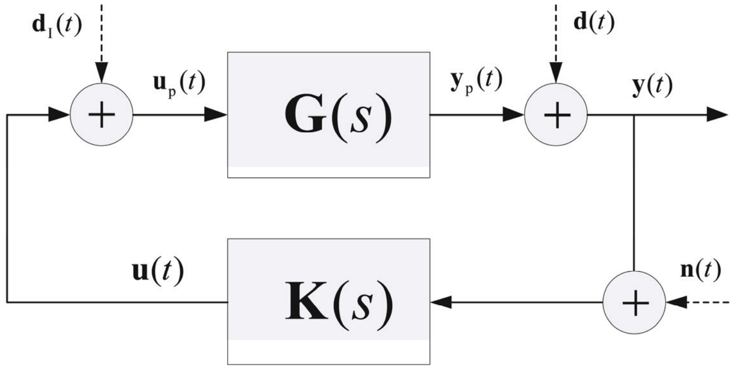

Figure 5.1. The general control configuration used in the performance analysis.

This section is structured as follows. In Subsection 5.1.1, the necessary quantities for the performance evaluation are derived. The performance analysis of the proposed control approach is carried out in Subsection 5.1.2, and finally some further aspects related to the analysis in terms of the practical implementation are discussed in Subsection 5.1.3.

5.1.1 Essential tools for the stability and robustness analysis

The essential tools for the stability and robustness analysis are derived in this section. The derivation is made for general systems, in essence, for a MIMO-process and a controller with possible feed-through terms. Although the feed-through elements significantly complicate the analysis, this extension is feasible as it enables the use of these methods for general control schemes, not solely for the one studied herein. In the analysis, the functions describing the dynamics are first given in the transfer function form, in which they are usually presented in the literature. Most of the analysis functions discussed in the sequel are generally well-known results and can be found for example in (Skogestad and Postlethwaite , 2005). The transfer function representations of the sensitivity functions are problematic when the MIMO-processes are considered. This is due to the possibility of very ill-conditioned loop transfer functions, whose inverses are required in most of the derivations. Such matrices with very high condition numbers yield unstable numerical results. Hence, the derivations are ultimately given in the state-space form, where all of these issues are avoided. The system matrices of the state-space representations describing the controller and the process are denoted by $(\mathbf{A}_\mathrm{p}, \mathbf{B}_\mathrm{p}, \mathbf{C}_\mathrm{p}, \mathbf{D}_\mathrm{p})$ and $(\mathbf{A}_\mathrm{c}, \mathbf{B}_\mathrm{c}, \mathbf{C}_\mathrm{c}, \mathbf{D}_\mathrm{c})$, respectively and obtained in the obvious way.

Prior to the derivation of the performance functions, two important identities of the controlled process are defined. The output open-loop transfer function, given as:

$$\mathbf{G}_{\mathrm{OL}}(s)=\mathbf{G}(s)\mathbf{K}(s)\,, \tag{5.1}$$

and the input open-loop transfer function, given as:

$$\bar{\mathbf{G}}_{\mathrm{OL}}(s)=\mathbf{K}(s)\mathbf{G}(s)\,, \tag{5.2}$$

where $\mathbf{G}(s)$ and $\mathbf{K}(s)$ are the transfer function matrices of the process and controller models, respectively.

5.1.1.1 Sensitivity analysis

The first quantity of interest is the net process output sensitivity to the output disturbances. This is described by a quantity referred in the literature as the *sensitivity function*, denoted by $\mathbf{S}(s)$ and given by:

$$\mathbf{y}(s)=\left(\mathbf{I}-\mathbf{G}_{\mathrm{OL}}(s)\right)^{-1}\mathbf{d}(s)=\mathbf{S}(s)\mathbf{d}(s)\,, \tag{5.3}$$

with the corresponding state-space representation given as:

$$\begin{cases}\dot{\mathbf{x}}_{\mathrm{sen}}(t)=\left[\begin{array}{c|c}\mathbf{A}_{\mathrm{p}}+\mathbf{B}_{\mathrm{p}}\bar{\mathbf{D}}\mathbf{D}_{\mathrm{c}}\mathbf{C}_{\mathrm{p}} & \mathbf{B}_{\mathrm{p}}\bar{\mathbf{D}}\mathbf{C}_{\mathrm{c}}\\ \hline \mathbf{B}_{\mathrm{c}}\left(\mathbf{I}+\mathbf{D}_{\mathrm{p}}\bar{\mathbf{D}}\mathbf{D}_{\mathrm{c}}\right)\mathbf{C}_{\mathrm{p}} & \mathbf{A}_{\mathrm{c}}+\mathbf{B}_{\mathrm{c}}\mathbf{D}_{\mathrm{p}}\bar{\mathbf{D}}\mathbf{C}_{\mathrm{c}}\end{array}\right]\mathbf{x}_{\mathrm{sen}}(t)\\ \qquad\qquad+\left[\begin{array}{c}\mathbf{B}_{\mathrm{p}}\bar{\mathbf{D}}\mathbf{D}_{\mathrm{c}}\\ \hline \mathbf{B}_{\mathrm{c}}\left(\mathbf{I}+\mathbf{D}_{\mathrm{p}}\bar{\mathbf{D}}\mathbf{D}_{\mathrm{c}}\right)\end{array}\right]\mathbf{d}(t)\\ \mathbf{y}(t)=\left[\left(\mathbf{I}+\mathbf{D}_{\mathrm{p}}\bar{\mathbf{D}}\mathbf{D}_{\mathrm{c}}\right)\mathbf{C}_{\mathrm{p}}\;\middle|\;\mathbf{D}_{\mathrm{p}}\bar{\mathbf{D}}\mathbf{C}_{\mathrm{c}}\right]\mathbf{x}_{\mathrm{sen}}(t)+\left[\mathbf{I}+\mathbf{D}_{\mathrm{p}}\bar{\mathbf{D}}\mathbf{D}_{\mathrm{c}}\right]\mathbf{d}(t)\end{cases}, \tag{5.4}$$

where $\bar{\mathbf{D}}=\left(\mathbf{I}-\mathbf{D}_{\mathrm{c}}\mathbf{D}_{\mathrm{p}}\right)^{-1}$ and $\mathbf{x}_{\mathrm{sen}}(t)=\left[\mathbf{x}_{\mathrm{p}}(t)^{T}\;\middle|\;\mathbf{x}_{\mathrm{c}}(t)^{T}\right]^{T}$ with $\mathbf{x}_{\mathrm{p}}(t)\in\mathbb{R}^{k}$ and $\mathbf{x}_{\mathrm{c}}(t)\in\mathbb{R}^{r}$ being the state vectors for the process and controller dynamics, respectively.

The sensitivity function describes the controller capability to mitigate the output disturbances and is hence essential for the analysis of the problems considered in this work.

The second quantity of interest is the process input sensitivity to the input disturbances. This is described by a quantity referred to as the *input sensitivity function*, denoted by $\mathbf{S}_{\mathrm{I}}(s)$ and given by:

$$\mathbf{u}_{\mathrm{p}}(s)=\left(\mathbf{I}-\bar{\mathbf{G}}_{\mathrm{OL}}(s)\right)^{-1}\mathbf{d}_{\mathrm{I}}(s)=\mathbf{S}_{\mathrm{I}}(s)\mathbf{d}_{\mathrm{I}}(s)\,, \tag{5.5}$$

which is given in the state-space form as:

$$\begin{cases}\dot{\mathbf{x}}_{\mathrm{sen}}(t)=\left[\begin{array}{c|c}\mathbf{A}_{\mathrm{p}}+\mathbf{B}_{\mathrm{p}}\bar{\mathbf{D}}\mathbf{D}_{\mathrm{c}}\mathbf{C}_{\mathrm{p}} & \mathbf{B}_{\mathrm{p}}\bar{\mathbf{D}}\mathbf{C}_{\mathrm{c}}\\ \hline \mathbf{B}_{\mathrm{c}}\left(\mathbf{I}+\mathbf{D}_{\mathrm{p}}\bar{\mathbf{D}}\mathbf{D}_{\mathrm{c}}\right)\mathbf{C}_{\mathrm{p}} & \mathbf{A}_{\mathrm{c}}+\mathbf{B}_{\mathrm{c}}\mathbf{D}_{\mathrm{p}}\bar{\mathbf{D}}\mathbf{C}_{\mathrm{c}}\end{array}\right]\mathbf{x}_{\mathrm{sen}}(t)+\left[\begin{array}{c}\mathbf{B}_{\mathrm{p}}\\ \hline \mathbf{B}_{\mathrm{c}}\mathbf{D}_{\mathrm{p}}\end{array}\right]\mathbf{d}_{\mathrm{I}}(t)\\ \mathbf{u}_{\mathrm{p}}(t)=\left[\mathbf{D}_{\mathrm{p}}\bar{\mathbf{D}}\mathbf{D}_{\mathrm{c}}\;\middle|\;\bar{\mathbf{D}}\mathbf{C}_{\mathrm{c}}\right]\mathbf{x}_{\mathrm{sen}}(t)+\mathbf{d}_{\mathrm{I}}(t)\end{cases}. \tag{5.6}$$

The input sensitivity function describes the process input sensitivity to the input disturbances. This is the quantity that is to be minimised in the input disturbance mitigation problems. For the processes, where the same actuator is used to realise both the external control signals and those produced by the controller, this function explicitly defines how the impact of such external control signal is altered and gives insight on the precompensator characteristics required for the recovery of the closed-loop dynamics.

The third quantity of interest is the process output sensitivity to the measurement noise. This is described by a quantity referred to as the *complementary sensitivity function*, denoted by $\mathbf{T}(s)$ and given as:

$$\mathbf{y}_{\mathrm{p}}(s) = \left(\mathbf{I} - \mathbf{G}_{\mathrm{OL}}(s)\right)^{-1} \mathbf{G}_{\mathrm{OL}}\mathbf{n}(s) = \mathbf{T}(s)\mathbf{n}(s), \tag{5.7}$$

which is given in a state-space form as:

$$\begin{cases} \dot{\mathbf{x}}_{\mathrm{sen}}(t) = \left[\begin{array}{c|c} \mathbf{A}_{\mathrm{p}} + \mathbf{B}_{\mathrm{p}}\bar{\mathbf{D}}\mathbf{D}_{\mathrm{c}}\mathbf{C}_{\mathrm{p}} & \mathbf{B}_{\mathrm{p}}\bar{\mathbf{D}}\mathbf{C}_{\mathrm{c}} \\ \hline \mathbf{B}_{\mathrm{c}}\left(\mathbf{I} + \mathbf{D}_{\mathrm{p}}\bar{\mathbf{D}}\mathbf{D}_{\mathrm{c}}\right)\mathbf{C}_{\mathrm{p}} & \mathbf{A}_{\mathrm{c}} + \mathbf{B}_{\mathrm{c}}\mathbf{D}_{\mathrm{p}}\bar{\mathbf{D}}\mathbf{C}_{\mathrm{c}} \end{array}\right]\mathbf{x}_{\mathrm{sen}}(t) \\ \qquad\qquad + \left[\begin{array}{c} \mathbf{B}_{\mathrm{p}}\bar{\mathbf{D}}\mathbf{D}_{\mathrm{c}} \\ \hline \mathbf{B}_{\mathrm{c}}\left(\mathbf{I} + \mathbf{D}_{\mathrm{p}}\bar{\mathbf{D}}\mathbf{D}_{\mathrm{c}}\right) \end{array}\right]\mathbf{n}(t) \\ \mathbf{y}_{\mathrm{p}}(t) = \left[\left(\mathbf{I} + \mathbf{D}_{\mathrm{p}}\bar{\mathbf{D}}\mathbf{D}_{\mathrm{c}}\right)\mathbf{C}_{\mathrm{p}} \;\middle|\; \mathbf{D}_{\mathrm{p}}\bar{\mathbf{D}}\mathbf{C}_{\mathrm{c}}\right]\mathbf{x}_{\mathrm{sen}}(t) + \left[\mathbf{D}_{\mathrm{p}}\bar{\mathbf{D}}\mathbf{D}_{\mathrm{c}}\right]\mathbf{n}(t) \end{cases}. \tag{5.8}$$

The complementary sensitivity function describes the closed-loop system sensitivity to the measurement noise. From the performance point of view it is desirable that the controller is as insensitive to this noise as possible, preventing its amplification thereof. This implies that the controller should be designed such that the magnitude of $\mathbf{T}(s)$ is as low as possible over the whole frequency space. Unfortunately, the design is restricted by one of the most fundamental limitations in linear control theory, namely by $\mathbf{S}(s) + \mathbf{T}(s) = \mathbf{I}$ (Skogestad and Postlethwaite , 2005). This limitation implies that the less sensitive the system is to the measurement noise the less effective it is in the cancellation of the output disturbances; a property which is very problematic from the active vibration control point of view.

The fourth and the final quantity of interest is the sensitivity of the realised control signals to the input disturbances. This is described by a quantity referred to as the *input complementary sensitivity function* in the literature, which is usually denoted by $\mathbf{T}_{\mathrm{I}}(s)$ and given as:

$$\mathbf{u}(s) = \left(\mathbf{I} - \bar{\mathbf{G}}_{\mathrm{OL}}(s)\right)^{-1} \bar{\mathbf{G}}_{\mathrm{OL}}(s)\mathbf{d}_{\mathrm{I}}(s) = \mathbf{T}_{\mathrm{I}}(s)\mathbf{d}_{\mathrm{I}}(s), \tag{5.9}$$

with the corresponding state-space representation given as:

$$\begin{cases} \dot{\mathbf{x}}_{\text{sen}}(t) = \left[\begin{array}{c|c} \mathbf{A}_\text{p} + \mathbf{B}_\text{p}\bar{\mathbf{D}}\mathbf{D}_\text{c}\mathbf{C}_\text{p} & \mathbf{B}_\text{p}\bar{\mathbf{D}}\mathbf{C}_\text{c} \\ \hline \mathbf{B}_\text{c}\left(\mathbf{I}+\mathbf{D}_\text{p}\bar{\mathbf{D}}\mathbf{D}_\text{c}\right)\mathbf{C}_\text{p} & \mathbf{A}_\text{c} + \mathbf{B}_\text{c}\mathbf{D}_\text{p}\bar{\mathbf{D}}\mathbf{C}_\text{c} \end{array}\right]\mathbf{x}_{\text{sen}}(t) \\ \qquad\qquad + \left[\begin{array}{c} \mathbf{B}_\text{p}\left(\mathbf{I}+\bar{\mathbf{D}}\mathbf{D}_\text{c}\mathbf{D}_\text{p}\right) \\ \hline \mathbf{B}_\text{c}\left(\mathbf{I}+\mathbf{D}_\text{p}\bar{\mathbf{D}}\mathbf{D}_\text{c}\right)\mathbf{D}_\text{p} \end{array}\right]\mathbf{d}_\text{I}(t) \\ \mathbf{u}(t) = \left[\begin{array}{c|c} \bar{\mathbf{D}}\mathbf{D}_\text{c}\mathbf{C}_\text{p} & \bar{\mathbf{D}}\mathbf{C}_\text{c} \end{array}\right]\mathbf{x}_{\text{sen}}(t) + \left[\bar{\mathbf{D}}\mathbf{D}_\text{c}\mathbf{D}_\text{p}\right]\mathbf{d}_\text{I}(t) \end{cases} . \tag{5.10}$$

The input complementary sensitivity function describes the amount of amplification (or mitigation) of the control signal due to the input disturbance as it passes through the loop. In the ideal case, the input disturbance should have no impact on the realised control signal. This sensitivity has a major impact on the robustness properties of the closed-loop system as will be shown subsequently.

Remark 5.1. It is worth noticing that for the SISO-systems the complementary sensitivity and the input complementary sensitivity functions coincide, in essence $\mathbf{T}(s) = \mathbf{T}_\text{I}(s)$.

5.1.1.2 Stability analysis

The stability analysis of a SISO-system is a straightforward procedure. The necessary and sufficient condition for the asymptotic stability is satisfied simply by verifying that all poles of the closed-loop system are on the negative half-plane, under the assumption of no pole-zero cancellations. However, when the MIMO-systems are considered, the stability condition becomes significantly more complex as it is required that the system is also internally stable. In essence, the internal stability can be verified only by studying all systems related to the input-output behaviour from the external disturbance signals to the realised control effort and the measured process output; namely the relations $\mathbf{T}(s) = \mathbf{T}_\text{I}(s)$, $\mathbf{d}(t) \to \mathbf{y}(t)$, $\mathbf{d}_\text{I}(t) \to \mathbf{u}(t)$ and $\mathbf{d}_\text{I}(t) \to \mathbf{y}(t)$ (Skogestad and Postlethwaite, 2005). Clearly, this becomes a rather tedious process and even as the results are obtained, they give very little information of the tolerable gain margins.

Another and a more visual approach to defining the stability of a system is based on the Nyquist-stability criterion (Skogestad and Postlethwaite, 2005). This method can be used to guarantee both the closed-loop and the internal stability of the system, again, assuming no pole-zero cancellations. In order for the method to be applicable to the MIMO-system, the stability criterion is extended, resulting in a method utilising the *generalised Nyquist-criterion* (Maciejowski, 1989). The generalised Nyquist diagram, used in the stability evaluation, is formed by drawing the characteristic loci $\lambda(\omega)$ of the open-loop system over the whole frequency domain, in essence:

$$\det\left(\mathbf{G}_\text{OL}(j\omega) - \lambda(\omega)\mathbf{I}\right) = 0, \forall \omega \in \left]-\infty, \infty\right[. \tag{5.11}$$

In order for the closed-loop system to be stable, it is required that there are as many encirclements of the point -1 as there are unstable open-loop (Smith-MacMillan) poles. For a stable process and a controller it suffices to verify that there are no encirclements of this point. The general gain margin of the MIMO-process is obtained from the diagram as the shortest distance from the point -1 to the point where the curve intersects the negative real axis. However, for the MIMO-systems, the gain margin is rather conservative and only covers the scenario where all input channels are amplified (or diminished) simultaneously (Gasparyan, 2008). Also, unlike in the SISO-systems, the diagram gives no information on the phase margins of the system. In the case of SISO-systems, the generalised criterion simplifies to the traditional Nyquist-criterion.

5.1.1.3 Robustness analysis

The analysis described in the previous subsection guarantees the nominal stability of the system. However, as the models are always inaccurate and some of the process dynamics may have been purposefully omitted from the model, it is necessary to evaluate the controller robustness to such changes in the process. This evaluation is done by studying the robust stability properties of the system. The generic unstructured modelling errors can be described by multiplicative uncertainty dynamics, which give better coverage than the summative uncertainties. For the SISO-systems, the position of the modelling error is interchangeable; hence the analysis in either location is sufficient. However, for the MIMO-systems, the location of the modelling error is of significance. Hence, two different possibilities for the modelling errors are considered. These are either the output multiplicative error, given as:

$$\mathbf{G}_{\mathrm{e}}(s) = \left(\mathbf{I} + \mathbf{\Delta}_{\mathrm{o}}(s)\right)\mathbf{G}_0(s)\,, \tag{5.12}$$

or the input multiplicative error, given as:

$$\mathbf{G}_{\mathrm{e}}(s) = \mathbf{G}_0(s)\left(\mathbf{I} + \mathbf{\Delta}_{\mathrm{I}}(s)\right)\,, \tag{5.13}$$

where $\mathbf{G}_0(s)$ is the nominal process model, $\mathbf{G}_{\mathrm{e}}(s)$ is the perturbed model, $\mathbf{\Delta}_{\mathrm{o}}(s)$ and $\mathbf{\Delta}_{\mathrm{I}}(s)$ are the transfer functions representing the output and input errors, respectively.

The multiplicative uncertainty is very usable to cover most of the possible process perturbations; unfortunately this comes with the price of the approach being very conservative and with covering scenarios which may never be realised (Skogestad and Postlethwaite , 2005). This property should be borne in mind when making conclusions on the results. The limits of the stability bounds could be tightened by introducing structured uncertainties and using μ-analysis (Zhou and Doyle, 1998). This however increases the design complexity and is not considered herein. It should also be noted that the above formulations do not consider simultaneous errors in both the input and the output of the model; hence leaving some margin for error in the analysis.

The derivation of the bounds for the tolerable modelling errors is a straightforward procedure. The upcoming derivation loosely follows the original work by (Maciejowski, 1989). The derivation starts from the generalised Nyquist-stability criterion, stating that the characteristic loci of an internally stable system may not pass through the point -1, which can be expressed as:

$$\det\left(\mathbf{I}+\mathbf{G}_{\mathrm{OL}}(j\omega)\right)\neq 0, \forall \omega \in \left]-\infty,\infty\right[. \tag{5.14}$$

In the case of the output modelling errors, this is the same as:

$$\underline{\sigma}\left(\mathbf{I}+\mathbf{G}_{\mathrm{OL}}(j\omega)\right)>0, \tag{5.15}$$

where $\underline{\sigma}(\bullet)$ denotes the smallest singular value of a matrix.

By substituting the identity in Eq. (5.12), the Eq. (5.15) can be rewritten as (with the argument $j\omega$ omitted in the sequel):

$$\underline{\sigma}\left(\mathbf{I}+\mathbf{G}_0\mathbf{K}+\boldsymbol{\Delta}_{\mathrm{o}}\mathbf{G}_0\mathbf{K}\right)=\underline{\sigma}\left(\left[\left(\mathbf{G}_0\mathbf{K}\right)^{-1}\boldsymbol{\Delta}_{\mathrm{o}}^{-1}+\boldsymbol{\Delta}_{\mathrm{o}}^{-1}+\mathbf{I}\right]\boldsymbol{\Delta}_{\mathrm{o}}\mathbf{G}_0\mathbf{K}\right)>0 . \tag{5.16}$$

Next, by exploiting the triangle inequality properties of the singular values, it follows:

$$\begin{aligned}&\underline{\sigma}\left(\left[\left(\mathbf{G}_0\mathbf{K}\right)^{-1}\boldsymbol{\Delta}_{\mathrm{o}}^{-1}+\boldsymbol{\Delta}_{\mathrm{o}}^{-1}+\mathbf{I}\right]\boldsymbol{\Delta}_{\mathrm{o}}\mathbf{G}_0\mathbf{K}\right)\\ &\geq\underline{\sigma}\left(\left(\mathbf{G}_0\mathbf{K}\right)^{-1}\boldsymbol{\Delta}_{\mathrm{o}}^{-1}+\boldsymbol{\Delta}_{\mathrm{o}}^{-1}+\mathbf{I}\right)\underline{\sigma}\left(\boldsymbol{\Delta}_{\mathrm{o}}\mathbf{G}_0\mathbf{K}\right)>0\end{aligned} . \tag{5.17}$$

The right-hand side of equality is violated only if either of the terms is identically zero. Hence, under the assumption of nominally asymptotically stable open-loop system and non-zero uncertainty, it suffices to study the left-hand side multiplier, in essence:

$$\underline{\sigma}\left(\left(\mathbf{G}_0\mathbf{K}\right)^{-1}\boldsymbol{\Delta}_{\mathrm{o}}^{-1}+\boldsymbol{\Delta}_{\mathrm{o}}^{-1}+\mathbf{I}\right)=\underline{\sigma}\left(\left[\left(\mathbf{G}_0\mathbf{K}\right)^{-1}+\mathbf{I}\right]\boldsymbol{\Delta}_{\mathrm{o}}^{-1}+\mathbf{I}\right)>0, \tag{5.18}$$

which, by exploiting the additive properties of the eigenvalues, can be rewritten as:

$$\underline{\sigma}\left(\left[\left(\mathbf{G}_0\mathbf{K}\right)^{-1}+\mathbf{I}\right]\boldsymbol{\Delta}_{\mathrm{o}}^{-1}+\mathbf{I}\right)>0\Rightarrow\underline{\sigma}\left(\left[\left(\mathbf{G}_0\mathbf{K}\right)^{-1}+\mathbf{I}\right]\boldsymbol{\Delta}_{\mathrm{o}}^{-1}\right)>1. \tag{5.19}$$

By exploiting the triangle inequality once again and expanding, we get:

$$\underline{\sigma}\left(\left[\left(\mathbf{G}_0\mathbf{K}\right)^{-1}+\mathbf{I}\right]\boldsymbol{\Delta}_{\mathrm{o}}^{-1}\right)\geq\underline{\sigma}\left(\boldsymbol{\Delta}_{\mathrm{o}}^{-1}\right)\underline{\sigma}\left(\left(\mathbf{G}_0\mathbf{K}\right)^{-1}\left[\mathbf{I}+\mathbf{G}_0\mathbf{K}\right]\right)>1, \tag{5.20}$$

which is essentially the same as:

$$\bar{\sigma}\left(\boldsymbol{\Delta}_{\mathrm{o}}^{-1}\right)\bar{\sigma}\left(\left[\mathbf{I}+\mathbf{G}_0\mathbf{K}\right]^{-1}\mathbf{G}_0\mathbf{K}\right)<1, \tag{5.21}$$

where the property $\bar{\sigma}\left([\cdot]^{-1}\right)=\underline{\sigma}\left([\cdot]\right)^{-1}$ is utilised.

Finally, by substituting the identity in Eq. (5.7) into Eq. (5.21) and expanding for all singular values, the following identity is obtained:

$$\sigma(\mathbf{\Delta}_{\mathrm{o}})\sigma(\mathbf{T}) < \mathbf{I}, \tag{5.22}$$

yielding the final relation:

$$\sigma(\mathbf{\Delta}_{\mathrm{o}}(j\omega)) < \sigma\left(\mathbf{T}^{-1}(j\omega)\right), \forall \omega \in \left]-\infty, \infty\right[. \tag{5.23}$$

By performing similar treatment for the input multiplicative uncertainties, another identity is obtained:

$$\sigma(\mathbf{\Delta}_{\mathrm{I}}(j\omega)) < \sigma\left(\mathbf{T}_{\mathrm{I}}^{-1}(j\omega)\right), \forall \omega \in \left]-\infty, \infty\right[. \tag{5.24}$$

According to the Eqs. (5.23) and (5.24), the closed-loop tolerance to modelling errors is directly related to the inverses of the complementary and input complementary sensitivity functions; in essence the sensitivity to the measurement noise and input disturbances. The implication of these results is immediate; in order to obtain good robustness, the process must be insensitive to the measurement and the input noises. However, the performance of the system is restricted by the equality $\mathbf{S}(s) = \mathbf{I} - \mathbf{T}(s)$, implying a trade-off between the obtainable output disturbance mitigation and the robustness, which is in a sense a natural result. For problems related to the active vibration mitigation, the 'optimal' approach would now be to have very high damping at the disturbance frequencies and none outside them. It will become apparent in the following section, that this is exactly the impact of the proposed control law; in essence yielding an optimal approach to vibration control in terms of closed-loop robustness.

5.1.2 Performance of the proposed control law

In this subsection, the theoretical performance of the proposed control law is evaluated by utilising the tools presented in the preceding subsection. The analysis covers the most crucial parts of the performance evaluation, which should be performed for any controller prior to the implementation. The designer should be careful when interpreting the results as they yield only the theoretical performance but not the transient time behaviour. A common characteristic of the transient behaviour in the vibration control is a non-minimum-phase like behaviour, that is, the disturbances get first amplified prior to the convergence. This unwanted phenomenon can be minimised in many approaches by retuning control design the parameters. Hence, in order to fully validate the controller performance, simulations should be done in order to identify the possible transient time issues.

The following analysis is focused on the analysis of the linear control law in a MIMO-process with two inputs and two outputs, subject to two tonal disturbances acting at the frequencies 66 Hz and 88 Hz, respectively. The performance analysis of the nonlinear controller is rather complicated and the results are not very visual due to the dimensionality. Hence, such analysis is excluded from this study. In practice, the analysis consists of independent analyses of the linear controllers over some frequency range, which are then combined. In essence, a descriptive surface is formed instead of a curve. An example of such graph, describing the controller robustness to output modelling errors is given in Fig. 5.2. In essence, the figure shows that the obtained gain margin depends on the disturbance frequency and the scheduling frequency used for the controller parameterisation. A cross-section of the graph in xz-plane defines the gain margin at an operation point of the controller.

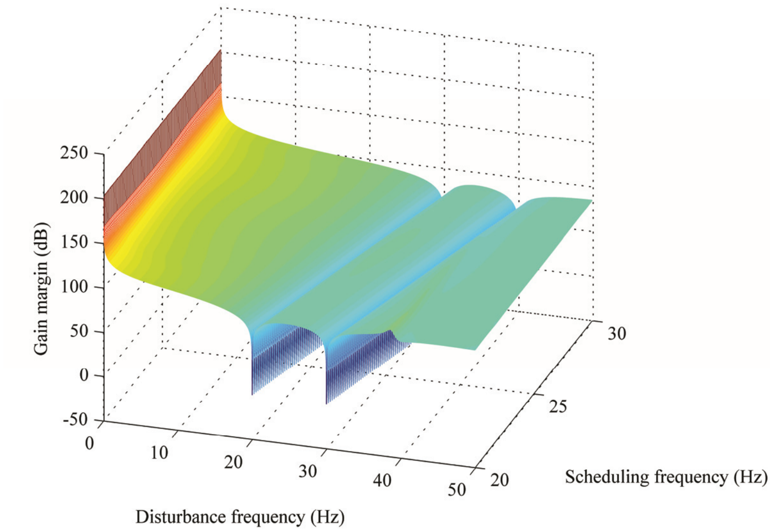

Figure 5.2. A surface describing the robustness margins to output modelling errors as a function of the scheduling variable.

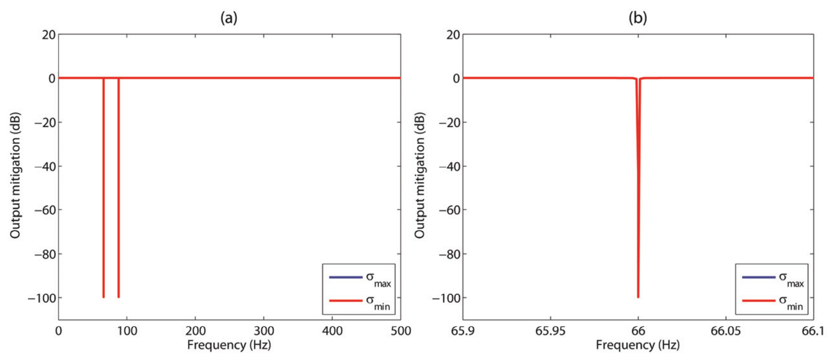

Figure 5.3. (a) The closed-loop sensitivity to the output disturbances. (b) A close-up of the 66Hz tone.

The sensitivities of the linear controller to the input and output disturbances are shown in Figs. 5.3 and 5.4, respectively. According to the graphs, the controller is capable of providing a very high rate of mitigation of approximately 100 dB on both disturbance tones. It is also notable that the largest and the smallest singular spectra coincide. Also, the controller is totally insensitive to the disturbances outside the particular tones, which is one of the desired controller properties set in the control goals. The control impact on both the input and the output disturbances is rather similar, which is an expected result for square systems. In certain non-square systems the difference between these sensitivities may be significant. In such scenarios, the control goal, in essence whether the point of excitation of the disturbance is assumed at the process input or output, should be set according to the application.

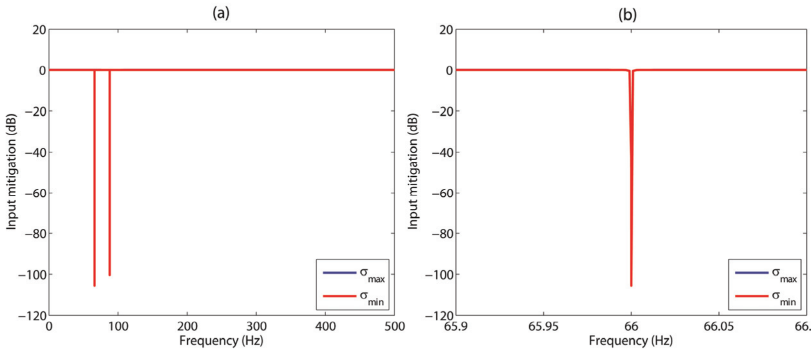

Figure 5.4. (a) The closed-loop sensitivity to the input disturbances. (b) A close-up of the 66Hz tone.

The closed-loop sensitivity to the measurement noise is shown in Fig. 5.5. According to the results, the controller is in practice completely insensitive to any noise outside the disturbance frequencies. Although such feature is considered very good when the controlled process is subject to high levels of noise, the drawback is the complete inability to follow any external references. This is a particularly problematic feature in processes where the same actuator is used for both the active vibration compensation and the higher level control of the process operation, typically implying that the process should follow some given reference trajectory. However, these problems can be somewhat alleviated by pre-compensating the reference signal prior to the excitation in the system. The required precompensation is explicitly given by the Fig. 5.5.

The closed-loop robustness to the input and the output modelling errors are assessed in Figs. 5.6 and 5.7. According to the results, the system is able to withstand at least an average of 75 dB input and 110 dB output gain-errors, respectively, at any frequency. Hence, it is obvious that the controller is very robust to modelling errors outside the disturbance frequencies which are to be compensated. The true tolerable modelling errors may be even higher as the singular values provide only the lower and higher bounds for these quantities. In the given design, the tolerance to modelling errors is a very important feature, as the process models are derived to be accurate only over a certain frequency band, hence implying potentially high model errors outside this band. Therefore, the designer must verify that the omitted process dynamics are indeed below the tolerable error margins.

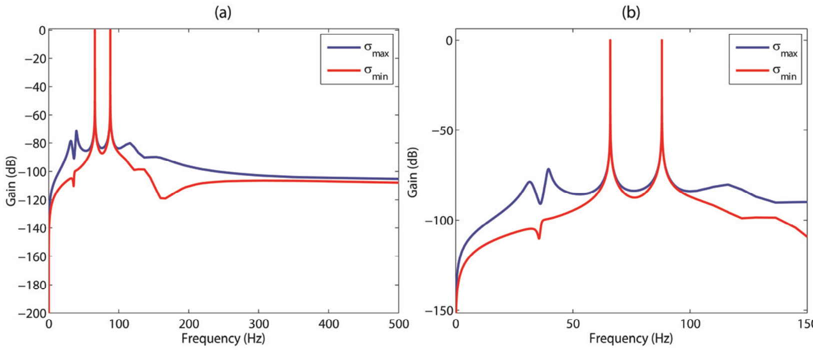

Figure 5.5. (a) The closed-loop sensitivity to the measurement noise. (b) A close-up of the frequency band containing the disturbance tones.

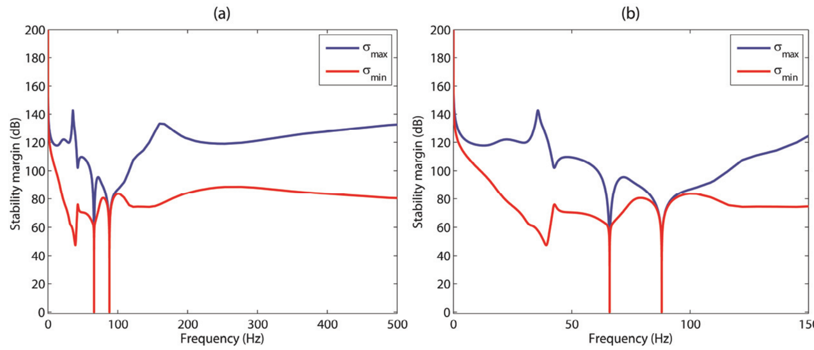

Figure 5.6. (a) The closed-loop robustness to the input modelling errors. (b) A close-up of the frequency band containing the disturbance tones.

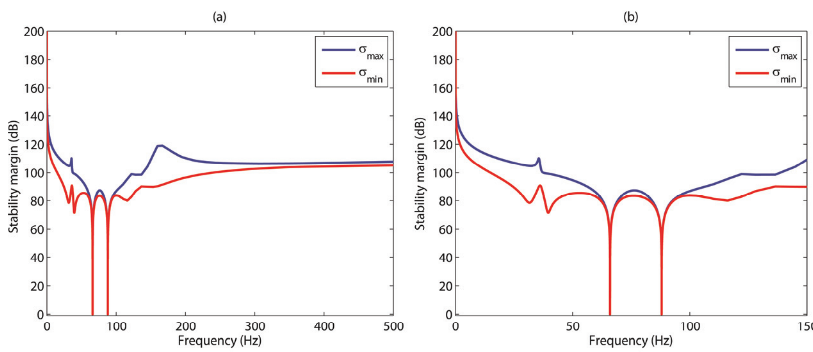

Figure 5.7. (a) The closed-loop robustness to the output modelling errors. (b) A close-up of the frequency band containing the disturbance tones.

Finally, the nominal stability of the closed-loop system is verified from the generalised Nyquist-diagram, given in Fig. 5.8. According to the results, the process is stable with a very high gain margin of 83dB.

According to the preceding analysis, the controller is able to provide very high suppression on the tonal disturbances with very high gain margins and tolerance to the modelling errors. The closed-loop system is also practically unaffected by any measurement noise. Hence, the proposed control approach can be considered fulfilling all control goals set for it.

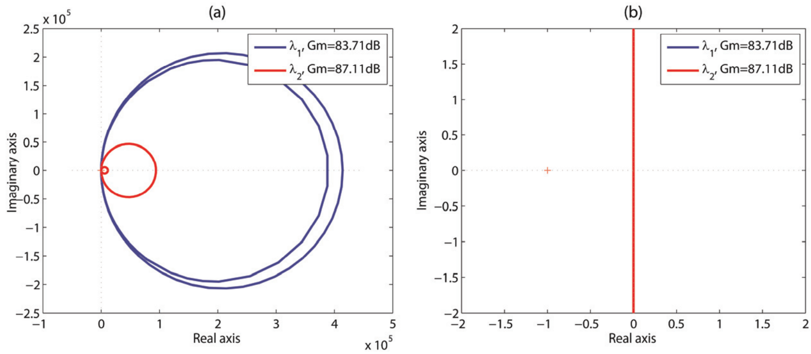

Figure 5.8. (a) The generalised Nyquist-curve of the open-loop system. (b) A close-up in the proximity of the point -1.

5.1.3 Enhanced analysis for practical implementation

Most of the time, the theoretical performance and stability analysis based on the identified process model is sufficient for the verification of the controller applicability. However, in certain cases where the model is less accurate and there are significant dynamics being excluded from the model, it is worth the effort to study the performance in terms of the true process dynamics. This study is made by carrying out the analyses presented in Subsection 5.1.2, with the exception that instead of using the identified model, the process dynamics are described directly by the measured input-output data used for the identification. In essence, the process characteristics at every frequency are obtained through the DFT:

$$\bar{\mathbf{G}}_m\left(e^{jqh}\right)=\frac{\bar{\mathbf{Y}}_m(q)}{\bar{U}_m(q)},q=\omega_0,\omega_1,\cdots,\omega_N\,, \tag{5.25}$$

where j denotes the imaginary unit, $\bar{U}_m(n)$ and $\bar{\mathbf{Y}}_m(n)$ are the Fourier transformed input and output signals over the frequency grid q, respectively, when only the m:th input channel is excited. The $\mathbf{G}_m(jq)$ is the column vector representing the process subdynamics related to the input m, where the process is defined as $\bar{\mathbf{G}}(jq)=\left[\mathbf{G}_1(jq) \quad \cdots \quad \mathbf{G}_m(jq)\right]$.

In order to minimise the effect of the spectral leakage, a suitable windowing, such as Hamming (Oppenheim *et al.*,1999), should be applied in the Fourier-transformation. The FRF of the controller is obtained by computing its frequency responses over the given frequency grid. The open-loop system is then readily obtained by post- or premultiplying the controller FRF with the process FRF in Eq. (5.25). Then the sensitivity functions are obtained in the obvious way. The resulting functions are slightly noisier, but providing that the process model is linear, they can be used to guarantee the performance in practice, unlike which is the case when the analysis is based on the estimated process model with omitted dynamics.

5.2 Performance comparison against the existing controllers

Active vibration mitigation has been an actively and rigorously studied field for a couple of decades and has resulted in many rather complete and effective solutions for the problem. Hence, it is necessary to put the approach proposed here into the perspective with the existing methods in order to assess whether the proposed approach brings any further value to the field. The comparison is done for the linear controller performance evaluation only, excluding the performance comparison of the nonlinear controller. This choice is made due to several factors. First, some of the existing nonlinear controllers are based on extensions to the linear controllers evaluated here; hence the difference in the performance can be approximated by the comparison of the underlying linear controllers. Secondly, the design approach and methodology for the nonlinear controllers vary significantly, making it almost impossible to do the comparison in a unified framework. This would result in the evaluation based solely on the simulations, which, in general, does not allow a fair and complete assessment.

As the study field is mature and the number of proposed solutions is rather vast, only the seemingly most popular approaches are chosen for the comparison. Hence, it should be borne in mind that there are very applicable and effective approaches other than those considered herein. All chosen algorithms are linear designs; hence excluding the whole family of the adaptive approaches, which are also rather popular, some of which can be found for example in (Sommerfeldt and Tichy, 1988; Knospe *et al.*, 1997b; Hätönen *et al.*, 2004). An extensive comparison of the chosen methods in the scenarios covering the most of the problem setups is given in PUB. 5 and only the main results and their implications are presented in this summary.

The comparison covers four methods in addition to the approach considered herein. The first method was originally proposed by (Gupta, 1980) and later revised by (Sievers *et al.*, 1991), where the control goal is to suppress tonal output disturbances through the optimal state-feedback. The method is based on the minimisation of a cost function with frequency dependent weighting matrices, from which it has its name as the method of the *frequency shaped cost functionals* referred to as (FSCF) in this context. The second approach is a simplification of the FSCF-method referred to as (SFSCF) proposed by the author of this thesis. The third method was originally proposed by (Sievers and von Flotow, 1988) and later revised and modified by (Bittanti *et al.*, 1996). This method is essentially based on a mixture of optimal feedback and feedforward control strategies. The point of excitation of the tonal disturbances is assumed at the process input, which are compensated by the feedforward control and the stability of the plant is provided through the optimal state-feedback. This method is referred to as the *input disturbance cancellation* (IDC).The fourth approach is called the *instantaneous harmonic control* (IHC) or the *convergent control* (CC), which was first proposed as an adaptive frequency domain approach by (Knospe *et al.*, 1997a) and later revised with some modifications into a LTI control law by (Tammi, 2007; Daley *et al.*, 2008). This approach originates from the standard harmonic control by (Fuller *et al.*, 1995), whose slow convergence properties are addressed in the IHC-approach. Essentially, the method is based on suitably tuned notch filters, providing the compensating control effort. The last method is the one proposed herein and referred to as the *direct optimal feedback compensation* (DOFC). The major differences of the methods are related to the number of required design parameters, the order of the resulting controller, performance in the MIMO-systems, performance under several distinct tonal disturbances, the generality of the design parameters and the performance in processes with unequal input-output dimensions. Most of the encountered problems are related to the position of the point of excitation of the expected disturbance, which causes problems in non-square plants. Also, with some controllers, there are some additional problems related to the closed-loop stability in the MIMO-systems and in the presence of multiple disturbance tones. All these issues are evaluated in the following summary where the results are collected as decision tables.

Table 5.1. The order and the number of the design parameters of the controllers in different processes, where the variables *m*, *n*, *r*, and *p* denote the number of process inputs, outputs, states and disturbance tones, respectively.

	SISO		**MIMO**	
Method	**Order of the controller**	**Number of design parameters**	**Order of the controller**	**Number of design parameters**
FSCF	r+2p	3+r	r+2pn	2n+m+r
SFSCF	2p	3+r	2pn	2n+m+r
IDC	r+2p	3+p	r+2pm	(p+1)m+2n
IHC	2p	2p	2pn	2p
DOFC	r+2p+1	6	r+(2p+1)n	2n+m+3
	MISO		**SIMO**	
FSCF	r+2p	2+m+r	r+2pn	2n+r+1
SFSCF	2p	2+m+r	2pn	2n+r+1
IDC	r+2pm	(p+1)m+2	r+2p	2n+p+1
IHC	2p	2p	2pn	2p
DOFC	r+2p+1	m+5	r+(2p+1)n	2n+4

The number of the required design parameters and the order of the resulting controller are presented in Table 5.1. According to the results, the lowest order controllers are obtained by the IHC and the SFSCF methods, being proportional to the number of disturbance tones and outputs. The DOFC, FSCF and IDC designs provide higher order controllers with the order proportional to the number of process states, the number of disturbance tones and the number of inputs or outputs. On the other hand, the lowest number of design parameters is obtained by the DOFC, IDC and IHC methods, being proportional to either the number of inputs and outputs or the number of disturbance tones. With the FSCF and SFSCF methods, the number of design parameters is proportional to the number of states, inputs and outputs.

Table 5.2. The performances of the controllers in the SISO-systems.

	1 disturbance tone				
Method	**Time domain convergence**	**Stability margins**	**Disturbance mitigation**	**Sensitivity to measurement noise**	**Sensitivity to model errors**
FSCF	very good	very high	very good	very good	very good
SFSCF	good	very high	very good	very good	very good
IDC	very good	very high	very good	good	good
IHC	very good	very high	very good	very good	very good
DOFC	very good	very high	very good	good	good
	2 disturbance tones				
FSCF	very good	low	good	bad	very bad
SFSCF	very good	very low	good	very bad	very bad
IDC	very good	high	very good	good	good
IHC	very good	low	good	bad	bad
DOFC	very good	high	very good	good	good

Table 5.3. The performances of the controllers in the MIMO-systems.

	1 disturbance tone					
Method	**Time domain convergence**	**Stability margins**	**Disturbance mitigation**	**Sensitivity to measurement noise**	**Sensitivity to input model errors**	**Sensitivity to output model errors**
FSCF	bad	very high	very good	very good	very good	very good
SFSCF	bad	high	very good	very good	very good	very good
IDC	bad	high	very good	good	bad	good
IHC	very good	very high	very good	very good	good	good
DOFC	very good	high	very good	good	bad	good
	2 disturbance tones					
FSCF	bad	low	very good	bad	good	bad
SFSCF	bad	low	very good	bad	good	bad
IDC	bad	very high	very good	good	bad	good
IHC	very good	low	very good	bad	bad	bad
DOFC	very good	high	very good	good	bad	good

The different performance criteria of the methods in several scenarios are collected in Tables 5.2-5.5, which clearly show that all methods yield very good performance in the most trivial case, namely a SISO-system subject to a single tonal disturbance. However, as the complexity increases, there are some rather evident differences.

By summarising, the different methods can be described as follows. The FSCF-method is a high order controller with a high number of free design parameters. The approach yields superb robustness to the modelling errors with a high rate of vibration mitigation while having poor stability margins in presence of multiple disturbance tones and poor convergence in MIMO-systems. The method is the best applicable to the SISO-, SIMO- and MISO-systems subject to a single disturbance tone.

Table 5.4. The performances of the controllers in the MISO-systems.

Method	Time domain convergence	Stability margins	Disturbance mitigation	Sensitivity to measurement noise	Sensitivity to input model errors	Sensitivity to output model errors
	1 disturbance tone					
FSCF	very good	very high	very good	very good	very good	very good
SFSCF	good	high	very good	very good	very good	very good
IDC	very good	very high	very good	good	bad	good
IHC	very good	high	good	very good	very good	very good
DOFC	very good	very high	very good	good	very good	good
	2 disturbance tones					
FSCF	very good	low	good	bad	very good	bad
SFSCF	very good	very low	good	bad	very good	bad
IDC	very good	very high	very good	good	bad	good
IHC	very bad	high	very bad	bad	very good	bad
DOFC	very good	very high	very good	good	very good	good

Table 5.5. The performances of the controllers in the SIMO-systems.

Method	Time domain convergence	Stability margins	Disturbance mitigation	Sensitivity to measurement noise	Sensitivity to input model errors	Sensitivity to output model errors
	1 disturbance tone					
FSCF	good	high	very good	very good	very good	very good
SFSCF	bad	high	very good	very good	very good	very good
IDC	good	high	very good	good	good	good
IHC	good	very high	very good	very good	very good	very good
DOFC	good	very high	very good	good	good	good
	2 disturbance tones					
FSCF	good	low	very good	good	good	bad
SFSCF	good	low	very good	good	bad	bad
IDC	good	high	very good	good	good	good
IHC	good	low	very good	bad	bad	very good
DOFC	good	high	very good	good	good	good

The SFSCF-method provides similar performance as the FSCF-method with some exceptions. The order of the controller is very low while being sensitive to measurement noise and yielding very poor stability margins in processes subject to multiple disturbance tones. Due to the low order of the controller, this method is the best applicable to the SISO- and MIMO-systems subject to a single tonal disturbance, especially when the available computational power is scarce.

The IDC-method is a high order controller with a low number of free design parameters. The control law yields very good vibration mitigation, stability margins and tolerance to output modelling errors and measurement noise with good convergence properties in SISO-, MISO- and SIMO-systems. In the MIMO-systems, the convergence and the tolerance to the input model errors are bad. Hence, the method is the best suitable for the SISO-, SIMO- and MISO-systems subject to any number of disturbance tones.

The IHC-method is a very low order controller with a low number of free design parameters, proportional to the product of the number of disturbance tones and outputs. The method does not require a full process model, but just the gain and phase information at the disturbance frequencies. The method provides excellent performance in all fields in processes subject to a single tonal disturbance. However, in the presence of multiple disturbance tones, the stability margins, the mitigation performance, and the tolerance to the modelling errors and the process noise are completely lost. The method is the best applicable to highly complex systems subject to a single tonal disturbance, especially if the available computational power is scarce.

The DOFC-method is a high order controller with a very low number of free design parameters. This approach is the only one, which provides similar performance with the same design parameters regardless of the process dimensions or the number of disturbance tones. The method yields the best overall performance while being slightly inferior to some of the other methods in certain scenarios. The controller is equally applicable to any process, providing that the process model and adequate computational power are available.

Based on the above analysis, there is no single control approach that could be considered superior. Hence, the choice for a suitable controller depends on the studied problem. However, it is also evident that the proposed control approach yields the best overall performance and has some clear benefits in certain scenarios. Hence, it can be considered to bring additional value to the field as a novel approach to the studied problem.

5.3 Feasibility analysis

The control design and all related performance analyses presented in the preceding sections are based on the assumption of absence of the control limitations. However, in practical implementations the available control energy is always limited. Hence, it is advisable to determine whether the actuators and their placement, in essence the whole physical control scheme, is capable of mitigating the disturbances even in theory. This analysis enables both the evaluation of the number of required actuators and the feasibility of the whole control scheme in the first place. Such information is obtained by studying the feasibility of the control scheme in terms of the perfect vibration mitigation. A control effort providing the perfect vibration mitigation, that is, complete disturbance cancellation or in case of the non-square plants the minimum obtainable cancellation in the least squares sense is given as:

$$\mathbf{U}(j\omega) = -\mathbf{M}(j\omega)\mathbf{W}_{\mathrm{d}}(\omega)\mathbf{D}(\omega), \forall \omega \in \mathbb{R}^{+}, \tag{5.26}$$

where $\mathbf{D}(\omega)=\mathbf{1}$ is a unity vector of appropriate dimensions, $\mathbf{W}_{\mathrm{d}}(\omega)$ is a frequency dependent scaling matrix taking the amplitudes and the relative phases of the separate disturbance signals into the account. $\mathbf{M}(j\omega)$ is a matrix describing the inverse process dynamics, defined for square plants as:

$$\mathbf{M}(j\omega)=-\mathbf{G}_{\mathrm{p}}^{-1}(j\omega) \tag{5.27}$$

and for the non-square plants as:

$$\mathbf{M}(j\omega)=\left(\mathbf{G}_{\mathrm{p}}^{T}(j\omega)\mathbf{G}_{\mathrm{p}}(j\omega)\right)^{-1}\mathbf{G}_{\mathrm{p}}^{T}(j\omega)\,. \tag{5.28}$$

The disturbance characteristics, namely the amplitude and the relative phases of the disturbance signals are obtained directly from the Fourier transformations of the measured process outputs, containing the disturbances, when no control action is present. This information is then used to define the matrix $\mathbf{W}_{\mathrm{d}}(\omega)$ used in the scaling of the disturbances.

Then, in order to avoid actuator saturation, it suffices to verify that

$$\sum_{\omega}\left|\mathbf{M}(j\omega)\mathbf{W}_{\mathrm{d}}(\omega)\right|\leq\mathbf{\Lambda},\forall\omega\in\mathbb{R}^{+},\left|\mathbf{D}(j\omega)\right|\neq 0 \tag{5.29}$$

holds where $\mathbf{\Lambda}$ is a vector with compatible dimensions, containing the saturation limits of each actuator.

If the inequality Eq. (5.29) holds, the control scheme is feasible. Additionally, if any of the required control efforts is close to zero, the corresponding actuator can most likely be removed from the control scheme without having any significant effect on the obtainable control performance. Similarly, if one or several of the actuator control efforts is close to the saturation, the relocation of the actuators may be advisable.

6. Case studies

In the preceding chapters, a linear control law was derived for active vibration mitigation. This control law was further extended into its nonlinear counter-part. Ultimately, a simple frequency estimator was included in the design. The performance of the resulting controller was validated by studying its theoretical damping capability and robustness to varying unidealities, such as modelling errors and process noise. In order to put the controller into perspective with respect to the existing control laws, an extensive comparison was made. Although the validation of the applicability has already been rather thorough, the most important validation step for any controller to be implemented in practice is still to be carried out; namely the performance evaluation in test-bed processes.

In this chapter, several case studies validating the applicability and the performance of the proposed control law in real process environment are presented. The applications are chosen such that they bear similarities with other processes where the vibrations are a problem, allowing the evaluation of the applicability of the control scheme to many different processes thereof. The detailed case studies are presented in PUBS. I-IV; hence only the main characteristics of the related problem and the main results are presented in the sequel.

In each of the cases, the required control effort is realised by using dSpace®-system. The control law is uploaded to the system as a code generated via MATLAB® Real-time-workshop® converted from basic Simulink® models. The controller is in discrete time; hence the continuous process measurements are fed through an AD-converter providing the zero-order-hold (ZOH) discretisation. Also, a suitable low-pass filtering is applied to the measured signals in every case study.

6.1 Case I: Suppression of radial rotor vibrations

The first case resembles the general problem related to the spatial deviation of axles or shafts rotating in confined spaces. The common factor for these processes is the absolute intolerance to the shaft displacement as it may collide with the surrounding structure, the stator in the case of the electric motors, which may have catastrophic consequences. In addition, these are a family of probably the most common pieces of equipment found in the industry today. The shaft vibrations are caused by its imbalances, resulting from poor machinery or defects. Even as these problems can be minimised through the means of fine-machining and rebalancing, the shaft can never be in complete balance and vibrations will always occur. The vibration related problems are the most severe when the rotating speed of a shaft approaches or crosses its natural bending frequency, resulting in significantly amplified vibrations. Traditionally, this problem is overcome by driving the process below its natural resonances, by making the structure stiffer or by changing the dynamics of the shaft in order to change its natural frequency. None of these approaches is very feasible as the trend is to make the shafts slimmer and longer in order to save both energy and resources, thus making the vibration problems worse in general. On the other hand, the avoidance of natural frequencies requires very specific overall plant design, which usually limits the overall efficiency of the process and practically prohibits the use of generically designed process components. According to the preceding evaluation of the encountered problems, it is evident that mitigation of the shaft vibrations may lead to significant benefits.

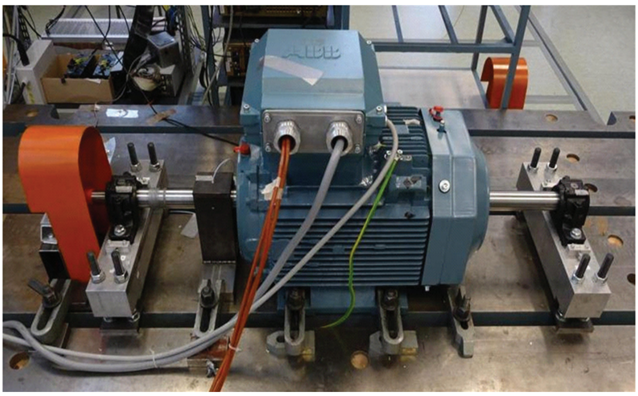

Figure 6.1. The 30 kW three-pole squirrel-cage motor used as the test-bed process.

The first case study, presented in detail in PUB. I, considers the suppression of radial rotor vibrations in an electric machine. Although there are also several other vibration problems related to the axial and torsional vibrations of the rotor shaft, the radial vibrations are the most harmful for the motor itself. The rotor vibrations cause severe wear and tear in the supportive structures of the rotor, especially in the bearings, resulting in increased maintenance effort and costs thereof. Additionally, the efficiency of the motor is roughly inversely proportional to the width of the air-gap between the rotor and the stator. One major issue resulting in an increase of the air-gap width is due to the safety margins, which are used to guarantee that the rotor may never collide with the stator, even in the presence of vibrations. In order to decrease the margins and to increase the motor efficiency, the rotor vibrations have to be minimised. For this purpose the means of active vibration control can be applied.

The studied motor is a 30 kW three-pole squirrel-cage motor shown in Fig. 6.1, which is considered small in industrial terms. The required control effort is generated by additional stator windings resulting in radial forces. The geometry of the extra windings is designed such that it has minimal interference with the actual driving windings (Laiho, 2009). The produced forces are then controlled by varying the voltage of these windings. There are several research studies made in this field, in which the forces are typically generated by magnetic bearings (Knospe *et al.*, 1997; Tammi, 2007). Also the actuators are usually current controlled (Chiba *et al.*, 1991). The actuator applied here can be interpreted as a voltage controlled built-in magnetic bearing.

Table 6.1. The specifications of the test-bed motor

Parameter	Value	Unit
supply frequency	50	Hz
rated voltage	400	V
connection	delta	-
rated current	50	A
rated power	30	kW
number of phases	3	-
number of poles	2	-
rated slip	1	%
rotor mass	55.8	kg
rotor shaft length	1560	mm
critical speed	37.5	Hz
width of the air-gap	1	mm
supply frequency	50	Hz

The shaft of the rotor is extended for test purposes in order to produce more severe vibrations. In addition, the rotor is curved, which would be considered defect and unusable in an industrial application. With such rotor, the motor cannot be run at its nominal speed for any time period. In order to prevent any fatal breakdowns, additional safety bearings are fitted in the original bearing housings. These bearings are measured such that they are in contact with the rotor only at the times when the rotor would otherwise collide with the stator, that is, it collides first with the bearings. The technical specifications of the modified motor are given in Table 6.1.

The control goal is to minimise the rotor displacement in a two-dimensional coordinate basis; hence implying that the control problem is a MIMO-system. The resulting control scheme is illustrated in Fig. 6.2. The position of the rotor is measured by eddy-current sensors in xy-direction, yielding the quantity to be minimised. The control signals are also defined in a two-dimensional coordinate system, allowing the simple formulation for ellipsoidal trajectories. It is noteworthy that, in general, the coordinate basis of the measurements and the control signals do not coincide. The control signals are fed to the motor as three-phase voltages; hence the two-phase control signals are converted into such signal. The resulting three-phase control signal is fed through a current amplifier prior to feeding into a frequency converter. The frequency range of interest is in the vicinity of 35 Hz; hence the controller is discretised with the sampling rate of 1 kHz.

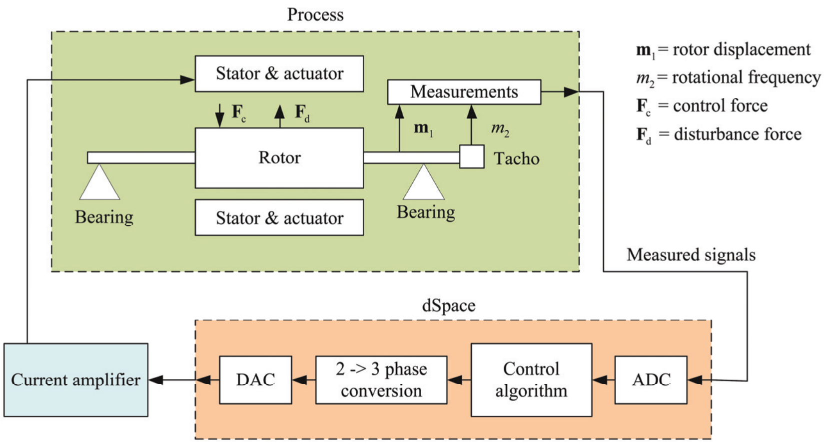

Figure 6.2. Layout of the control scheme for the suppression of radial rotor vibrations.

The applied controller is a combination of an earlier version of the control law presented herein, cascaded with an IHC-controller to produce better vibration mitigation and allowing the minimisation of the zero frequency component of the disturbance, caused by an unbalanced magnetic pull (UMP) (Sinervo and Arkkio, 2112). Similar results would be obtained with the enhanced controller considered in this thesis, apart from the elimination of the static offset, on which the controller has no impact.

In this study, only the mitigation of vibration with static frequency was considered. Hence, the linear control law was applied. The performance tests were divided into two parts. First, the vibrations were mitigated when the process was run at 32 Hz rotation speed. At this frequency, the motor could still be run without any control, enabling the evaluation of the obtained suppression rate when the controllers are turned on separately. According to the results given in Fig. 6.3, the shaft moves on an ellipsoidal trajectory with the average displacement of $300\ \mu\text{m}$ when no control is applied. As the DOFC-controller was turned on, the shaft was forced on a circular trajectory with the average displacement of $25\ \mu\text{m}$ obtained within one cycle of rotation. Finally, as the IHC-controller was turned online, the average displacement was further decreased into the average of $12\ \mu\text{m}$. It is obvious that the control action had a significant impact on the perceived disturbance levels. The DOFC-controller alone suppressed the vibrations by 21 dB, which was further increased to 28 dB at the time the IHC-controller was switched online.

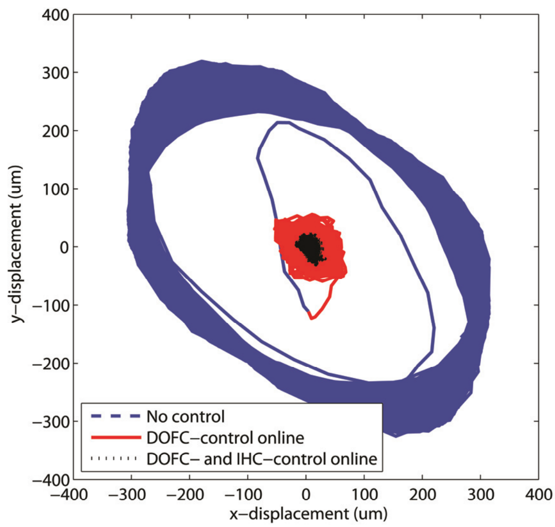

Figure 6.3. Measured shaft displacement with different control configurations when the motor is run at 32Hz.

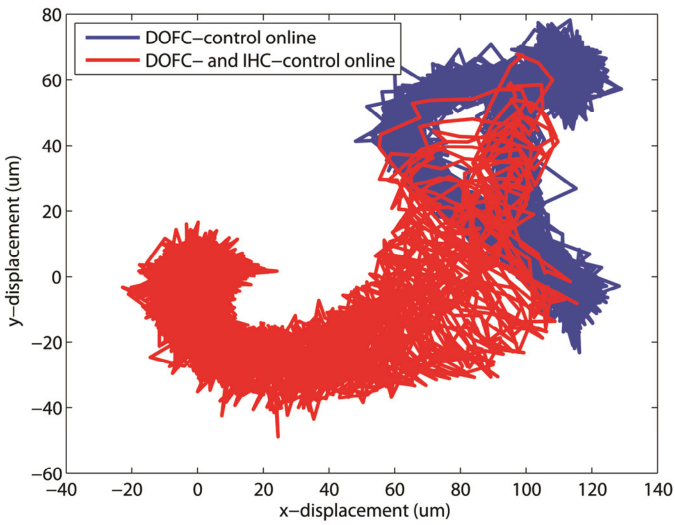

Figure 6.4. Measured shaft displacement with the DOFC-controller and both controllers online, separately.

After the acceptable control performance was verified at the sub-critical frequencies, the rotation frequency of the motor was increased to its critical frequency, namely 37.5 Hz. At this frequency, the motor could not be driven at all without a control action. Again, the controllers were turned on separately, making their performance distinguishable. Based on the results given in Fig. 6.4, the DOFC-controller is capable of stabilising the naturally unstable system. Although the level of obtained damping cannot be determined, the controller can be considered yielding good performance, providing the average displacement of $30\,\mu m$ with some rather significant deviation from zero. Unlike in the previous test, the trajectory of the shaft is now more complex than a simple ellipsoid. The impact of the IHC-controller is clearly distinguishable because after it was turned on, the shaft was centered about the zero static offset. The displacement due to the vibration was further suppressed into the average of $10\,\mu m$. It is noteworthy that the IHC-controller could not stabilise the process alone, while the DOFC-controller could.

Based on the tests, it is evident that the proposed control configuration provides a significant mitigation of vibrations with static frequency in the family of processes considered herein. It is also apparent that the DOFC-controller is capable to significant suppression alone. However, through the addition of IHC-controller, the rate of obtained suppression can be increased even further.

6.2 Case II: Blocking of mount force transmissions

The second case study considers the blocking of force transmissions through the mounts of a steel structure. Similar structures are found practically anywhere, for example in bridges, skyscrapers and ship hulls. Such structures share two common characteristics, namely the very low internal damping and high amplification at their natural frequencies thereof; implying that these structures are prone to vibrate whenever excited and the vibration decays very slowly. Depending on application, there are two separate control goals, either the minimisation of the vibration of the structure itself or blocking the force transmission to the surrounding structures at the mounts. The first case is more feasible for example in bridges, while the second is more feasible in mounted machinery be it a motor in a ship hull for example. The vibrations perceived in these structures rather often have varying frequency, thus making the impact of the vibrations even more severe. Because of the poor internal damping capability of the structure, the active vibration control is a natural approach to tackle the problem.

The particular problem taken as an example in this case study, presented in detail in PUB. II, is a minimisation of transmitted vibration in a steel bar rigidly mounted from its both ends. The scenario resembles a raft with some machinery placed on top, where the machinery and the raft are allowed to vibrate freely but no disturbance force transmissions to the surrounding structures are allowed. The mounts provide some passive damping over a certain effective bandwidth. Hence, the control goal is to enhance the blocking by mitigating the residual vibrations on the frequency band where the passive approach is ineffective. In addition, the source of the vibration is assumed to have unmeasurable time varying frequency; hence implying it has to be identified from the signal which is being minimised. The test-bed is realised in a laboratory environment as a steel beam mounted from both ends on a flexible table. An inertial mass shaker is placed in the middle of the beam, emulating a disturbance originating from some machinery. The minimised quantity is chosen as the acceleration measurements perpendicular to the mounts measured at the bottom of both mounts. The control effort is produced by a pair of inertial mass shakers placed on top of both mounts. The original MIMO-system is simplified by defining the sum of the acceleration measurements as the minimised quantity and by feeding the same control signal to both actuators. This is a feasible approach as the system is symmetric; hence having approximately the same disturbance levels in both ends and the impact of the actuators being approximately the same. A schematic diagram of the control scheme is given in Fig. 6.5.

As the problem includes frequency varying disturbances without direct frequency measurement available, the applied control law is a nonlinear controller with embedded frequency estimation. In the tests, the disturbances were assumed to be on the frequency band of 275 Hz-290 Hz; hence the sampling rate was chosen as 5 kHz in order to prevent aliasing. Again, the tests were divided into two parts both resembling slightly different scenarios.

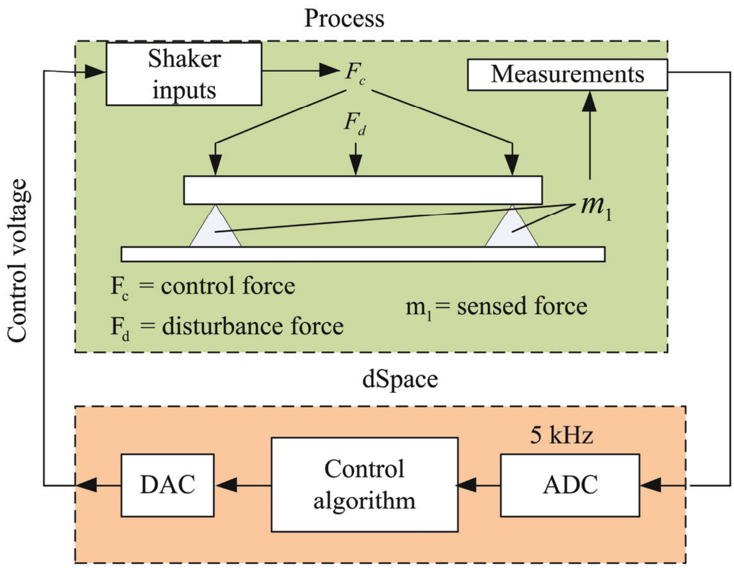

Figure 6.5. Illustration of the control scheme for blocking of mount transmitted disturbances.

In the first test, the disturbance was assumed to have static frequency, first at 278 Hz and at the time instant 7,5 s a discrete frequency change to 285 Hz was introduced (the rate of change is limited only by the actuator inertia). The obtained rate of mitigation is given in Fig. 6.6. According to the results it is obvious that the closed-loop system does not perform well when subject to a discrete change in the disturbance frequency. Although the transient response of the system was poor at the time of the frequency change, it converged very fast and the system remained indeed stable, as expected. The control effort provided very high vibration suppression up to 80 dB as the initial transients had decayed. Such rate of mitigation can be considered exceptional when obtained from practical tests.

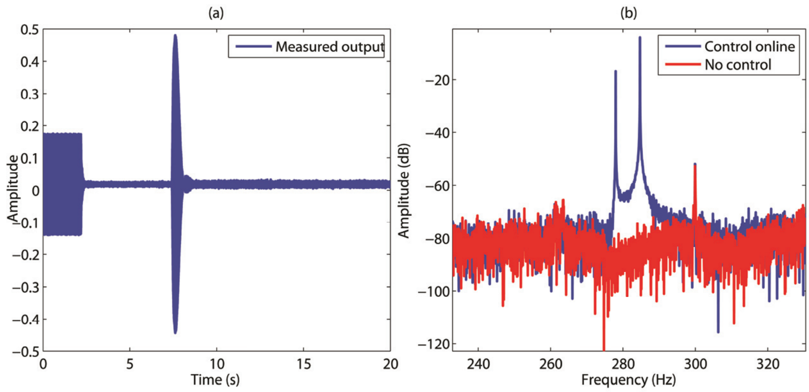

Figure 6.6. Perceived disturbance mitigation when the process is subject to a discrete frequency change. (a) Time domain performance. (b) The frequency spectra of the measured outputs.

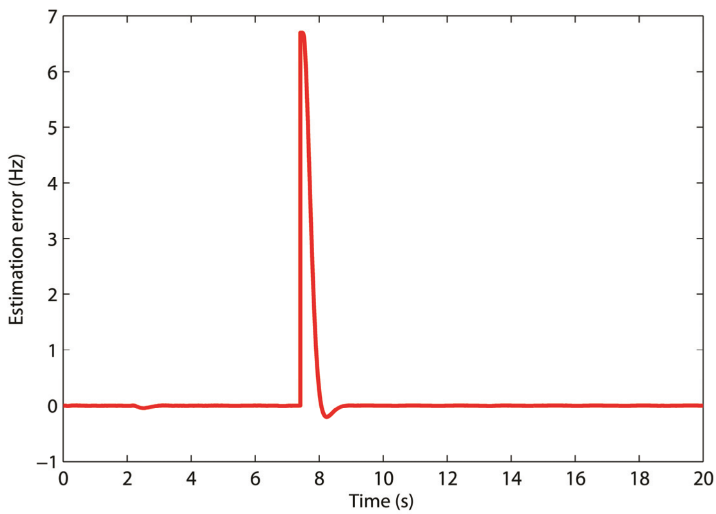

Figure 6.7. Performance of the frequency estimator when the process is subject to a discrete frequency change at t=7s.

The cause for the switching transient is evident when the error of the frequency estimate is studied. According to the Fig. 6.7 there was a significant 7 Hz estimation error at the time of the frequency switch, which resulted in the use of an ineffective control action, therefore deteriorating the perceived control performance.

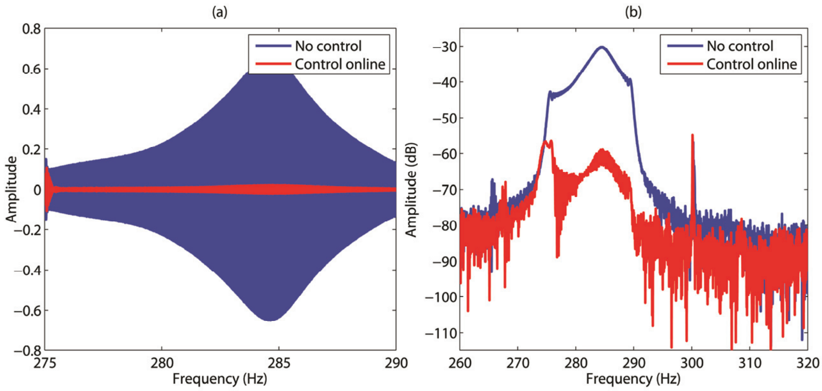

Figure 6.8. Perceived disturbance mitigation when the process is subject to a constant linear change in the frequency. (a) Time domain performance. (b) Frequency domain performance.

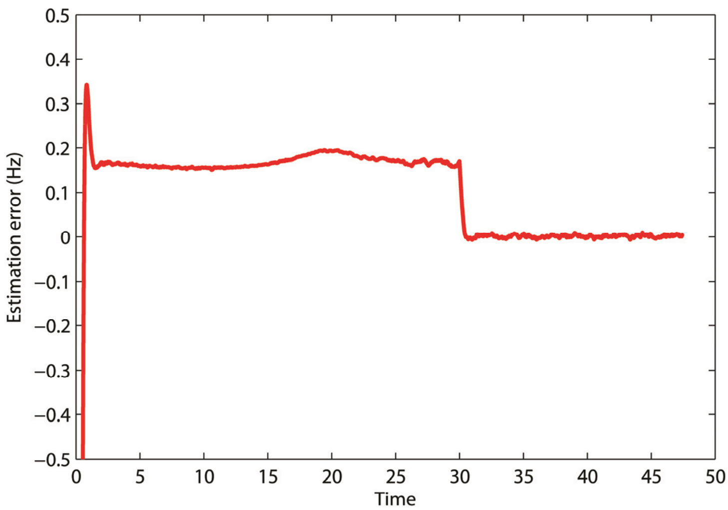

Figure 6.9. Performance of the frequency estimator when the process is subject to a constant linear change in the frequency.

In the second test the process was assumed to be subject to disturbance with linearly changing frequency, a phenomenon typically occurring in the process run-ups and run-downs. The frequency variation was chosen to be over the whole frequency band, namely 275 Hz to 290 Hz with the rate of change of $0.5\,\mathrm{Hz/s}$. The performance of the control action is shown in Figs. 6.8, where the impact of the control action is clearly distinguishable. In essence, the control effort provides over 25 dB vibration mitigation over the whole frequency range, which was still slightly less than expected based on the theoretical analysis.

The underlying reason for the slightly deteriorated control performance becomes evident when the frequency estimation error, given in Fig. 6.9, is studied. According to the figure, the frequency estimate is biased by 0.2 Hz during the whole frequency sweep. Although such an error may seem minimal, it had significant impact on the obtainable rate of suppression. This interpretation is readily verified when considering the theoretical performance of the controller, where the effective frequency range of suppression is indeed very narrow due to the desired robustness properties. Hence, a minor deviation of the frequency has severe deteriorating impact on the obtainable control performance.

Based on the results from the two tests, it is apparent that the nonlinear controller is capable of providing very high vibration mitigation in cases, in which the disturbance has either static or varying frequency. The major problem of the design is clearly related to the frequency estimate, which when biased, results in a poor yet stable control performance. This was an expectable result as the applied frequency estimation algorithm is very simple. Although the performance could have been better, it is also obvious that even with such frequency estimator the implemented control scheme provided more than acceptable results. Hence, the proposed control law can be considered applicable to the family of vibration mitigation problems considered in this case study.

6.3 Case III: Mitigation of vibrations in a rolling process

In the third case study, the problems related to varying industrial rolling processes are studied. These processes can be found in many different branches of industry, where the production of a final product is subject to rolling in the production line. Some typical examples of such processes can be found for example in steel industry, where the steel if reformed through rolling; in the paper industry where the paper is rolled on a reel. The main common factors in such processes are given as follows. The actual rolling speed is dependent on the speed of the product line, which is a factor typically set on higher level to optimise the overall process in some way. The actual rolling process typically involves the production line (the material) to be passed between one or several reels with certain nip forces tightening the line and reforming the material. The vibration problems occur when the reels rotate in the proximity of their natural frequencies; hence resulting in oscillating displacements and variations in the nip forces. The force oscillation passes on as an oscillation of the density and thickness of the end product. Such inconsistent products are considered being of a lower grade, reducing their sale value thereof. As the rolling processes are typically found in industry which produces continuous throughput, even a minor enhancement in the end product quality potentially generates a significant increase in the overall profits and revenue. A typical approach to minimise the impact of the vibration would be to set the rotating speed such that the natural frequency is never excited. Unfortunately, this is not a viable approach in processes that are part of a larger system. In essence, the line-speed defining the rotation frequency is determined by higher level specifications and changes in the speed may deteriorate the process performance and decrease in the overall throughput thereof.

The example taken for this study is an industrial rolling process described in detail in PUB. III. The process consists of an end-product roll pinned against a reel from the bottom and supported by a hydraulic actuator which provides the desired nip forces. The actuator is connected to a force sensor, which acts as a linkage to the surrounding structure. A schematic diagram of the process is given in Fig. 6.10.

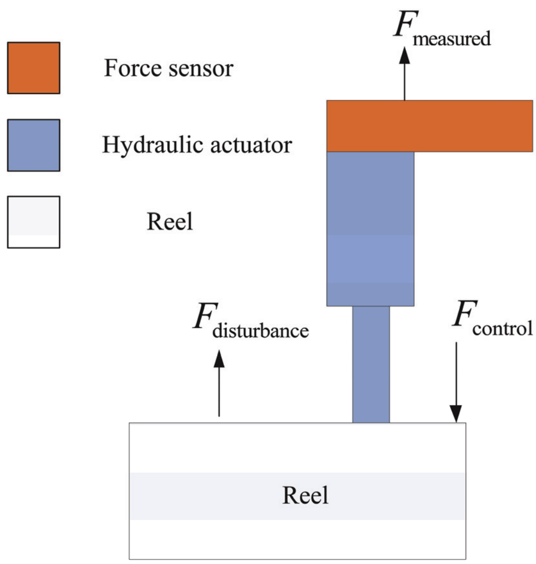

Figure 6.10. A schematic diagram of the studied industrial rolling process.

The roll rotates at a frequency specified by the line-speed of the rolled product, defined by higher level factors of the overall process. As the material is being rolled, the width of the roll increases while the line-speed is constant, resulting in a variation of the rolling frequency. High level vibrations are induced as the rolling frequency passes the natural frequencies of the combined system. The vibration causes variation in the thickness of the rolled material and ultimately results in a defect end product. The control goal can be stated as follows; minimise the force oscillations in the perceived force signals. Hence, the minimised quantity is the sensed force and the required control effort is generated by the hydraulic actuator. The resulting control scheme is illustrated in Fig. 6.11. The pressure of the hydraulic actuator is altered by a valve, whose stem position is controlled by a voltage signal. This voltage is used as the control quantity, ranging from -10 V to 10 V, which corresponds to $\pm100\%$ opening of the valve. The measured forces are proportional to a voltage signal, which is being measured. In addition, a measurement of the rolling frequency is available. The studied process is simplified by making an assumption of a constant roll width. Hence, the required frequency variation is produced by varying the roll speed directly. In practice the width is not constant, which introduces several additional problems. The dynamics of the process change both in terms of the frequency and the piston position of the hydraulic actuator, resulting in further nonlinearities. In addition, the process characteristics vary depending on the rolled material, ultimately leading into a very complex problem with several uncertainties. Such problem cannot be solved by the approach considered herein; hence the simplification is made.

In order to tackle the problem, the nonlinear control law is implemented into the process. The rolling frequency is known to be within the frequency range of 5 Hz to 50 Hz; hence the sampling frequency is chosen as 1 kHz. Due to the presence of the nip forces, the measured force is not zero mean. This force offset is set by the process operator and is not to be controlled; hence the control effort is allowed to be effective only at the disturbance frequency. The resulting control scheme is a SISO-system with voltages both as its inputs and outputs.

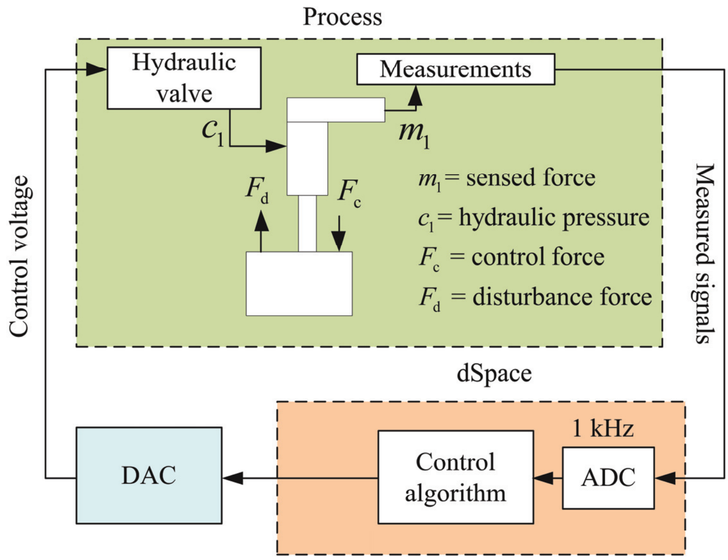

Figure 6.11. Layout of the control scheme for the mitigation of the perceived force vibrations in a rolling process.

In the test implementation, the disturbance frequency was varied linearly over the interval of 5 Hz to 50 Hz. The impact of the control action on the perceived force measurement is shown in Fig. 6.12. According to the results, the controller was capable of providing satisfactory mitigation over the whole frequency range with the average suppression rate of 20 dB. In addition, it is evident that the control action had no impact on the static force offset, which is crucial for the normal operation of the system. Therefore, the control approach can be considered capable of providing good vibration mitigation in the family of the processes considered in this case study when the roll or reel diameter is constant. For the more complex problems, another control approach has to be considered.

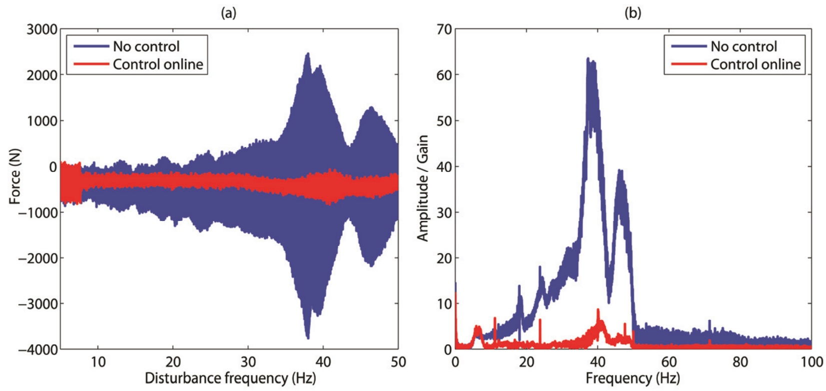

Figure 6.12. Measured force from the process subject to a frequency varying disturbance without control and with the controller online. (a) Time performance. (b) The frequency spectra of the measured forces.

6.4 Case IV: Mitigation of the engine induced vibrations

The fourth and the last case study considers the problems related to the engine induced vibrations. The problem can be further expanded into any system where some machinery is placed on a raft. These types of processes are commonly found in automotive, marine and work machine industry and they often share a similar characteristic. Namely, the machinery mounted on the raft is allowed to vibrate freely but no vibration transmissions are allowed to the structures where the raft is mounted. The dual of the problem can be readily formulated in a similar way, in which the problem is to block the exogenous vibrations from entering the raft. The typical examples of such processes are the assembly tables in fine machining industry and the chassis of a work machine in a heavy loader for example.

The problem considered in detail is related to the blocking of the transmitted engine induced vibrations at the raft mounting. The detailed problem formulation is presented in PUB V. The engine-induced vibrations are particularly problematic as the frequency of the excitation varies according to the running speed of the motor. The vibrations are excited in several harmonics of the main disturbance tone and the vibration takes place in a three-dimensional space.

The studied process is a combination of a marine diesel and a generator mounted on a steel raft supported from each corner. The motor does not have an internal speed regulator, resulting in vibrations with constantly varying frequencies thereof. The motor generates multiple tonal disturbances, originating from the pistons, valves and camshafts, that all have their respective lower and higher harmonics. In essence, a vast number of tonal disturbances are transmitted to the surrounding structures. The control goal is to block three of these disturbance tones, considered the most harmful, from transmitting through the raft mounts into the surrounding structures in any direction. The mounts used to support the raft are a specific combination of passive and active elements forming a patented 'Smart-spring'-concept (Daley *et al.*, 2004). The test process and a mount are shown in Fig. 6.13. The passive component of the mount is used to mitigate the most of the high frequency disturbances, while the active component is used for the mitigation of the remaining tones considered problematic. The actuator is realised as three inertial mass shakers aligned such that they are capable of providing the required control effort in any direction.

Figure 6.13. (a) The test-bed process is a marine diesel engine and a generator mounted on a raft. (b) The raft is supported by a "Smart-spring", which consists of three inertial mass shakers and a passive damping element.

In order to simplify the process and the results thereof, the mitigation is considered only in one corner of the raft. Such simplification can be done without the loss of generality of the results as the problem can be readily extended to cover all four corners. This would just require more computational power which was not available during the time of the tests. The disturbances are generated by the diesel engine running approximately at 800 rpm. The vibration tones to be mitigated are the harmonic multiples of the running frequency, namely 52 Hz, 65 Hz and 78 Hz. Due to the structure of the system, the disturbances in the direction perpendicular to the raft are considered the most harmful. The quantities to be minimised are the perceived accelerations in xyz-directions at the bottom of the mounts, which are obtained by a triaxial accelerometer attached onto the bottom of the mount. The control forces are produced by the mass shakers driven by voltage signals. The resulting control scheme is depicted in Fig. 6.14.

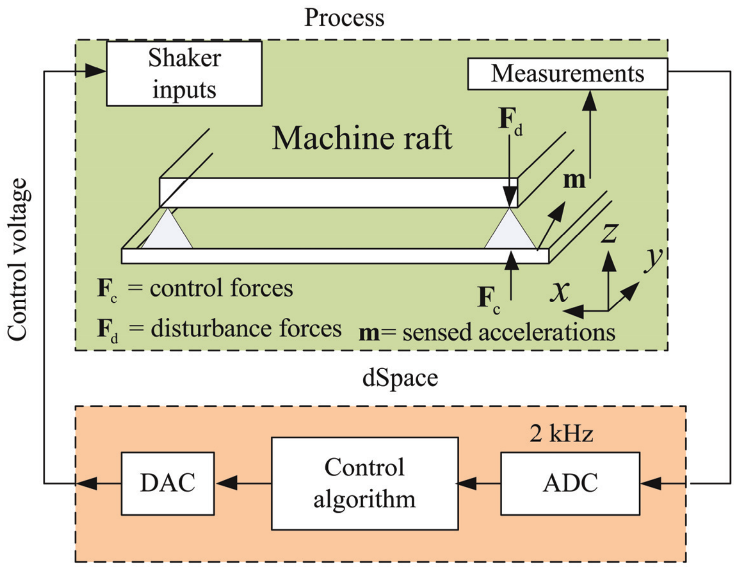

Figure 6.14. Illustration of the control scheme for the suppression of transmitted residual vibrations at the bottom of the mounts.

The control problem is indeed very challenging as the level of the background noise is very high, there are multiple tonal disturbances present in the measurements and the coordinate basis of the measurements and the actuators do not coincide, resulting in a true MIMO-process with significant interconnections thereof. In addition, the disturbance tones are frequency varying although closely related to the running frequency of the motor, which is not measurable. The nonlinear controller with embedded frequency tracking was used to tackle the problem. The process measurements were sampled at the rate of 2 kHz. The time domain performance of the controller is presented in Figs. 6.15-6.17. Due to the high level of the background noise, the performance is assessed from the band-pass filtered signals. According to the results, the control action provided very high relative vibration mitigation in the z-direction, which was also the control goal. In addition, it provided a similar level of absolute mitigation in the x- and y-directions although having smaller relative impact.

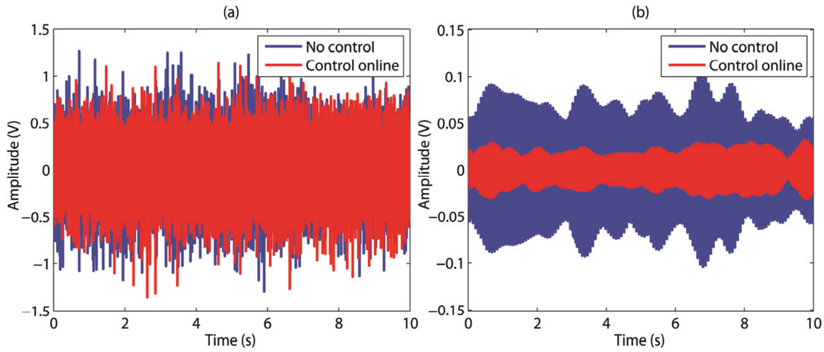

Figure 6.15. Measured accelerations in the x-direction at the bottom of the mount. (a) Actual measurements. (b) Band-pass filtered measurements.

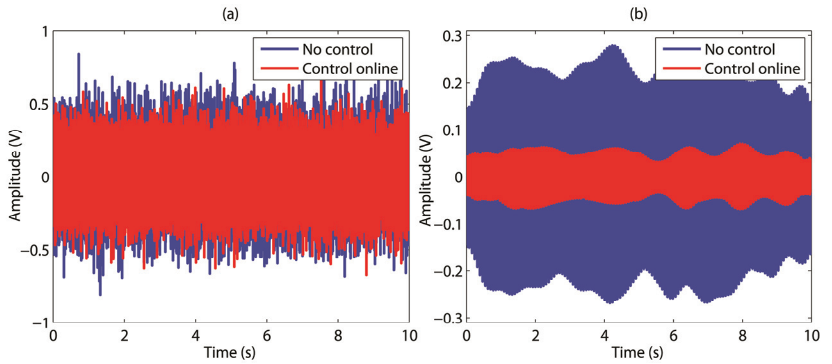

Figure 6.16. Measured accelerations in the y-direction at the bottom of the mount. (a) Actual measurements. (b) Band-pass filtered measurements.

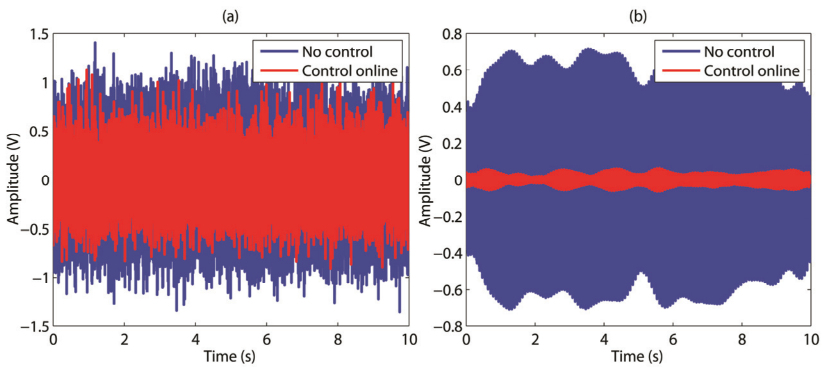

Figure 6.17. Measured accelerations in the z-direction at the bottom of the mount. (a) Actual measurements. (b) Band-pass filtered measurements.

In the systems with very high background noise levels, the true impact of the control effort becomes more distinguishable through the study of the power spectra of the measured outputs. The related spectra are given in Figs. 6.18-6.20. These results agree with the perceived time-domain performance although now the significance of the control effort is more evident. According to the results, the amplitude of all disturbance tones apart from one in y-direction at 78 Hz are driven to the noise floor, which is essentially the best obtainable performance. The estimated frequency of the first tone is given in Fig. 6.21 which confirms the assumption of a constantly varying frequency. Although the variation may seem minimal, it has already been shown in the third case-study that in order to guarantee good robustness, the control effort is effective on a very narrow frequency band. Hence, a static frequency estimate would provide poor control impact.

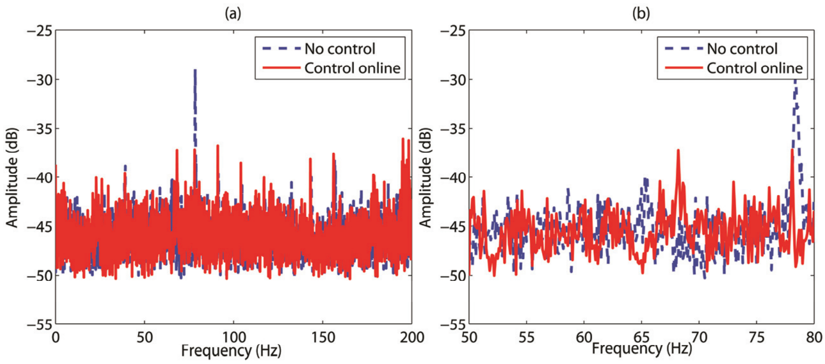

Figure 6.18. The frequency spectra of the measured accelerations in the x-direction. (a) Extended frequency band. (b) Close-up of the frequency band of the most interest.

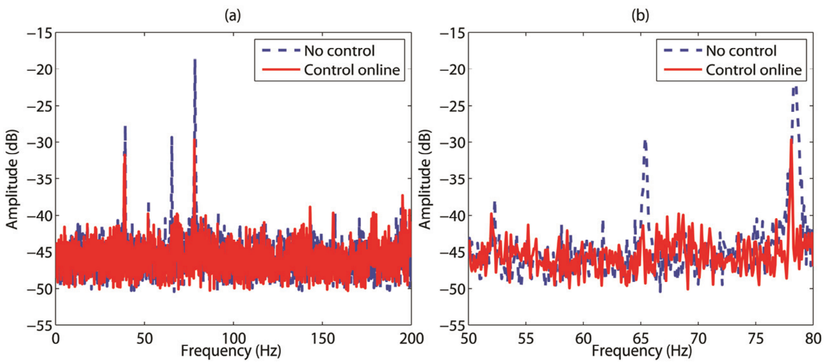

Figure 6.19. The frequency spectra of the measured accelerations in the y-direction. (a) Extended frequency band. (b) Close-up of the frequency band of the most interest.

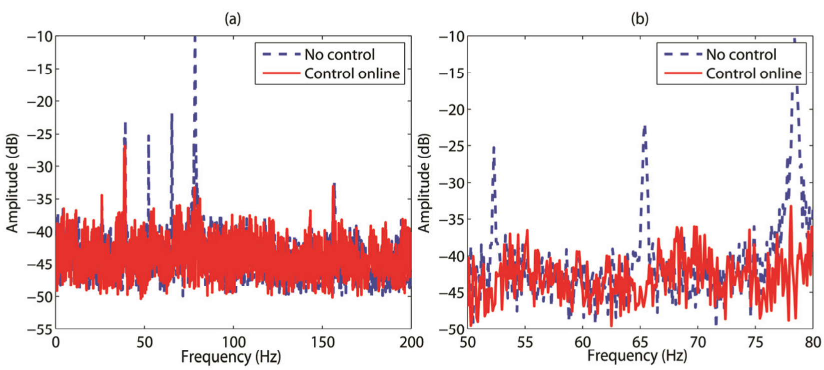

Figure 6.20. The frequency spectra of the measured accelerations in the z-direction. (a) Extended frequency band. (b) Close-up of the frequency band of the most interest.

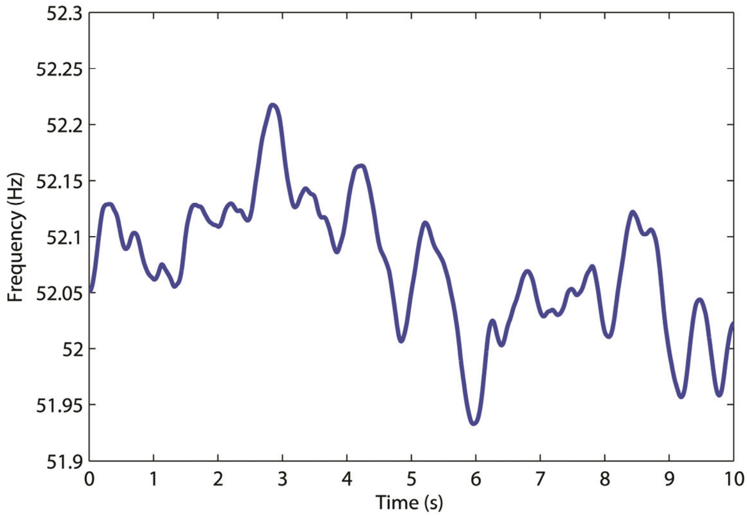

Figure 6.21. Variation of the first disturbance tone over time as given by the frequency estimator.

According to the results, the nonlinear control law is capable of providing very high mitigation of multiple disturbance tones in multiple directions in systems, in which the background noise level is very high, the disturbances are frequency varying and the measurements contain several deterministic frequency tones, which are not to be controlled. In general, the applicability of the control law for general MIMO-processes, especially in those belonging to the family of the processes considered herein, is verified.

7. Conclusions

Vibrations are an unwanted phenomenon present in any physical system. The traditional methods, mainly those based on the passive energy absorption cannot provide such vibration mitigation, which would meet all the standards and requirements of the industry today. Although these methods should still be preferred whenever possible, the field of applications where their performance proves inadequate is increasing by the day. The solution for these high demand vibration suppression issues are the methods based on the active compensation of the tonal disturbances. The field of active vibration control is rather mature and has been under study since the early eighties. However, although the ideas for some of the most effective algorithms still present today were made at that time, their implementation was limited by the availability of sufficient computational power. Since then, several different control approaches have been proposed, varying from linear controllers applicable to the compensation of disturbances with static frequency to nonlinear, adaptive and gain-scheduled approaches applicable to the compensation of disturbances with time varying frequencies. Although these methods are capable of providing a significant suppression of disturbances in certain types of processes, they still lack some generality, either due to the complex choices for the design parameters or due to the controller structure itself.

In this thesis, the necessary steps required to obtain a generic solution for the most of the common vibration problems were presented. The identification routine to obtain a process model for vibration control purposes was presented. The design procedure applying the obtained process model in the synthesis of a novel control law was described in detail. Finally, the essential analysis tools required for the performance, feasibility and robustness analysis were presented in detail. As a whole this thesis allows the process engineer faced with vibration problems to follow the step-by-step design presented herein to obtain a solution for the problem.

A novel control approach to active vibration control was presented. The proposed approach is an optimal nonlinear controller obtained through a gain-scheduling of several linear optimal controllers. The control law is generic; hence being capable of mitigating any number of tonal disturbances in a system with arbitrary input-output dimensions. The controller design is based on normalised process models; hence enabling the use of a very small number of free design parameters, that produce similar performance regardless of the underlying process dynamics. In addition, the design parameters have a natural interpretation, significantly simplifying the design procedure thereof. The controller is designed such that the robustness properties of the closed-loop system can be manipulated through a single design parameter.

An extensive and thorough analysis and evaluation of the proposed control law was carried out. In these analyses the performance, stability and robustness properties of the algorithm were verified. In addition, as a benchmark, the control approach was compared against the most popular existing control approaches. In this evaluation, the proposed control approach was shown to yield the best overall performance although having slightly inferior performance in certain specific scenarios. Finally, the performance of the proposed control approach was assessed in four case studies with real processes used as the test-beds. The control problems chosen as the cases represent many of the problems encountered in the industry today. According to the case studies the control approach was able to provide significant control performance with the capability to very effective vibration mitigation.

Although the proposed control approach gave excellent results in all the cases studied herein, it still has some restrictions in terms of the applicability, as already addressed in the case study III. Namely, the approach can be used for any system for which a model is obtainable. This naturally covers all linear and many of the nonlinear processes. However, the approach is not applicable to processes where either the nonlinearities are unidentifiable or the process dynamics vary according to some unknown and uncertain parameter. The problem with the applicability is now a direct consequence of the absence of a reliable process model, which is a problem for any model-based approach. In a sense, a robust control approach could provide a stable closed-loop system, yet it is still likely, depending on the amount of uncertainty that the performance is unacceptable. These types of problems can be tackled by adaptive control approaches, in which the process model is identified online. Still, there are some remarkable problems as the measurement which the adaptation is based on, is corrupted by the disturbance, resulting in an identification of controlled system with varying dynamics. A potential solution for such problem is already proposed by the author of this thesis; however this problem and its solution are out of the scope of this work.

In conclusion, the approach proposed in this work can be considered as a good candidate for generic control approach to be used for high performance vibration mitigation, when the dynamics of the system under study are identifiable.

References

Ammann OH, Von Karman T, Woodruff GB. (1941). The Failure of the Tacoma Narrow Bridge. *Federal Works Agency*. Washington, D.C.

Anderson BDO, Moore JB. (1989). *Optimal control: linear quadratic methods*. Englewood Cliffs, NJ: Prentice Hall.

Arnold, WF, Laub, AJ. (1984). Generalized eigenproblem algorithms and software for algebraic Riccati equations. *Proceedings of the IEEE*. 72(12), 1746- 1754

Ballesteros P, Bohn C. (2011). Disturbance rejection through LPV gain-scheduling control with application to active noise cancellation. *Proceedings of the 18th IFAC World Congress*. Milano, Italy.

Bar-Shalom Y, Xiao-Rong L. (2001) *Estimation with applications to tracking and navigation*. Chichester, NY: Wiley

Bittanti S, Lorito F, Strada S. (1996). An LQ approach to active control of vibrations in helicopters. *Journal of Dynamic Systems, Measurement, and Control*. 118(3), 482-488

Bittanti S, Cuzzola FA. (2002). Periodic active control of vibrations in helicopters: a gain-scheduled multi-objective approach. *Control Engineering Practice*. 10(10), 1043-1057

Bohn C, Cortabarria A, Härtel V, Kowalczyk K. (2004). Active control of engine-induced vibrations in automotive vehicles using disturbance observer gain scheduling. *Control Engineering Practice*. 12(8), 1029-1039

Chang CC, Yang HTY. (1995). Control of buildings using active tuned mass dampers. *Journal of Engineering Mechanics*. 121(3), 355-366

Chen Y, Zhu C. (2008). Active vibration control based on linear matrix inequality for rotor system under seismic excitation. *Journal of Sound and Vibration*. 314(1-2), 53-69

Chiba A, Power DT, Rahman MA. (1991). Characteristics of a bearingless induction motor. *IEEE transactions on magnetics*. 27(6), 5199-5201

Daley S, Johnson FA, Pearson JB, Dixon R. (2004). Active vibration control for marine applications. *Control Engineering Practice*. 12(4), 465-474

Daley S, Zazas I and Hätönen J. (2008). Harmonic control of a 'smart spring' machinery vibration isolation system. *Journal of Engineering for the Maritime Environment*. 222(2), 109-119

Daley S, Zazas I. (2011). A recursive least squares based control algorithm for the suppression of tonal disturbances. *Journal of Sound and Vibration*. 331(6), 1270-1290

Desoer CA. (1969). Slowly varying system x'=A(t)x . *IEEE transactions on automatic control*. 14(6), 780-781

Dorf RC, Bishop RH. (2011). *Modern control systems*. 21st ed., Upper Saddle River, NJ: Pearson

Du H, Zhang L, Lu Z, Shi X. (2003). LPV technique for the rejection of sinusoidal disturbance with time-varying frequency. *IEE Proceedings – Control Theory and Applications,* 150(2), 132-138

Fan YH, Lee AC. (1997). Design of a permanent/electromagnetic magnetic bearing-controlled rotor system. *Journal of the Franklin Institute*. 334(3), 337-356

Fuller CR, Elliott SJ, Nelson PA. (1996). *Active control of vibration*. San Diego, CA: Academic press

Gasparyan O. (2008). *Linear and nonlinear multivariable feedback control : a classical approach*, Chichester : Wiley

Guo D, Rugh WJ. (1995). A stability result for linear parameter-varying systems. *Systems & Control Letters*. 24(1), 1-5

Gupta NK. (1980). Frequency-shaped cost functionals: Extension of linear–quadratic–Gaussian design methods. *Journal of Guidance and Control*. 3(6), 529–535

Hall SR, Wereley NM. (1989). Linear control issues in the higher harmonic control of helicopter vibrations. *Proceedings of the 47th Annual Forum of the American Helicopter Society,* 955-971. Boston, USA.

Herzog R, Buhler P, Gahler C, Larsonneur R. (1996). Unbalance compensation using generalized notch filters in the multivariable feedback of magnetic bearings. *IEEE Transactions on Control Systems Technology*. 4(5), 580-586

Hätönen JJ, Owens DH, Moore KL. (2004). An algebraic approach to iterative learning control. *International Journal of Control*. 77(1), 45-54

Icerman LJ. (1969). Optimal structural design for given dynamic deflection. *International Journal of Solids and Structures*. 5(5), 473-490

Inman DJ. (2006). *Vibration with control*. West Sussex: Wiley

Jalili N. (2002). A comparative study and analysis of semi-active vibration-control systems. *Journal of Vibration and Acoustics*. 124(4), 593-605

Johansson R. (1993). *System modeling and identification*, NJ: Prentice Hall

Kamen EW. (1990). *Introduction to signals and systems*. 2nd ed., NY: Macmillan

Kareem A, Kijewski T, Tamura Y. (1999). Mitigation of motions of tall buildings with specific examples of recent applications. *Wind and Structures*. 2(3), 201–251

Katayama T. (2005). *Subspace methods for system identification*, London: Springer

Kinney CE, de Callafon RA. (2006). An adaptive internal model-based controller for periodic disturbance rejection. *Proceedings of the 14th IFAC Symposium on System Identification*. Newcastle, Australia

Kinney CE, de Callafon RA. (2007). A comparison of fixed point designs and time-varying observers for scheduling repetitive controllers. *Proceedings of the 46th IEEE Conference on Decision and Control*. New Orleans, USA

Kirk DE. (2004). *Optimal control theory : an introduction*. Mineola, NY:Dover Publications

Knospe CR, Hope RW, Fedigan SJ, Williams RD. (1995). Experiments in the control of unbalance response using magnetic bearings. *Mechatronics*. 5(4), 385-400

Knospe CR, Fedigan SJ, Hope RW, Williams RD. (1997a). A multitasking DSP implementation of adaptive magnetic bearing control. *IEEE Transactions on Control Systems Technology*. 5(2), 230-238

Knospe CR, Tamer SM, Fittro R. (1997b). Rotor Synchronous Response Control: Approaches for Addressing Speed Dependence. *Journal of Vibration and Control*. 3(4), 435-458

Knospe CR. (2007). Active magnetic bearings for machining applications. *Control Engineering Practice*. 15(3), 307-313

Kwakernaak H, Sivan R. (1972). *Linear optimal control systems*. New York: Wiley-Interscience

Köroğlu H, Scherer CW. (2011a). Robust generalized asymptotic regulation against non-stationary sinusoidal disturbances with uncertain frequencies. *International Journal of Robust and Nonlinear Control,* 21(8), 883-903

Köroğlu H, Scherer CW. (2011b). Scheduled control for robust attenuation of non-stationary sinusoidal disturbances with measurable frequencies. *Automatica*, 47(3), 504-514.

Laiho A. (2009). *Electromechanical modelling and active control of flexural rotor vibration in cage rotor electrical machines. Doctoral Dissertation*. VTT Publications (712)

Laub AJ, Heath MT, Paige CC, Ward RC. (1987). Computation of system balancing transformations and other applications of simultaneous diagonalization algorithms. *IEEE transactions on automatic control*. 32(2), 115-122

Lay DC. (2006). *Linear algebra and its applications*. 3rd ed. Boston:Pearson / Addison-Wesley

Lin YY, Cheng CM, Lee CH. (2000). A tuned mass damper for suppressing the coupled flexural and torsional buffeting reponse of long-span bridges. *Engineering Structures*. 22(9), 1195-1204

Liu Y, Waters TP, Brennan MJ. (2005). A comparison of semi-active damping control strategies for vibration isolation of harmonic disturbances. *Journal of Sound and Vibration*. 280(1-2), 21-39

Ljung L. (1999). *System identification: theory for the user*. 2nd ed. Upper Saddle River, NJ: Prentice Hall.

Lovera M, Colanerio P, Celi R. (2003). Periodic analysis of higher harmonic control techniques for helicopter vibration attenuation. *Proceedings of the American Control Conference*. 2, 999-1004

Maciejowski JM. (1989). *Multivariable feedback design*. Wokingham: Addison-Wesley

Merriam-Webster. (1995). *Merriam-Webster's collegiate dictionary*. 10th ed. Springfield, MA:Merriam-Webster

Moore BC. (1981). Principal component analysis in linear systems: controllability, observability, and model reduction. *IEEE transactions on automatic control*. 26(1), 17-32

Moshrefi-Torbati M, Keane AJ, Elliott SJ, Brennan MJ, Anthony DK, Rogers E. (2006). Active vibration control (AVC) of a satellite boom structure using optimally positioned stacked piezoelectric actuators. *Journal of Sound and Vibration*, 292(1-2), 203-220

Nandi S, Toliyat HA, Xiaodong L. (2005). Condition monitoring and fault diagnosis of electrical motors-a review. *IEEE Transactions on Energy Conversion*, 20(4), 719- 729

Olsson C. (2006). Active automotive engine vibration isolation using feedback control. *Journal of Sound and Vibration*. 294(1-2), 162-176

Oppenheim AV, Schafer RW, Buck JR. (1999). *Discrete-time signal processing*, 2nd. ed., Upper Saddle River (NJ): Prentice-Hall

Pai PF. (2009). Three-point frequency tracking method. *Structural Health Monitoring*, 8(6), 425-442

Pai PF. (2010). Online tracking of instantaneous frequency and amplitude of dynamical system response. *Mechanical Systems and Signal Processing*. 24(4), 1007-1024

Preumont A, Kazuto S. (2008). *Active control of structures*. Cornwall: Wiley

Rivin EI. (2003). *Passive vibration isolation*. New York: ASME

Rugh WJ. (1991). Analytical framework for gain scheduling. *IEEE Control Systems Magazine*. 11(1), 79-84

Rugh WJ. (1996). *Linear system theory*. Upper Saddle River, NJ: Prentice Hall

Savaresi SM, Bittanti S, So HC. (2003). Closed-form unbiased frequency estimation of a noisy sinusoid using notch filters. *IEEE Transactions on Automatic Control*. 48(8), 1285-1291

Seidel H. (1993). Selected health risks caused by Long-Term, Whole-Body Vibration. *American Journal of Industrial Medicine*. 23, 589-604

Sharp RS, Crolla DA. (1987). Road Vehicle Suspension System Design - a review. *Vehicle System Dynamics: International Journal of Vehicle Mechanics and Mobility*. 16(3), 167-192

Sievers LA and von Flotow AH. (1988). Linear control design for active vibration isolation of narrow band disturbances. *Proceedings of the 27th IEEE Conference on Decision and Control*. 2, 1032-1037

Sinervo A, Arkkio A. (2112). Including slot harmonics to mechanical model of two-pole induction machine with a force actuator. *Mechanical Systems and Signal Processing*, Available online: (http://www.sciencedirect.com/science/article/pii/S0888327012001379)

Skogestad S, Postlethwaite I. (2005). *Multivariable feedback control: analysis and design*. West Sussex:Wiley

Slotine E, Weiping L. (1991). *Applied nonlinear control*. Englewood Cliffs, NJ: Prentice-Hall

Sommerfeldt SD, Tichy J. (1988). Adaptive control of a two-stage vibration mount. *Proceedings of the 27th IEEE Conference on Decision and Control*. 3, 2039-2044

Song G, Sethi V, Li HN. (2006). Vibration control of civil structures using piezoceramic smart materials: A review. *Engineering Structures*. 28(11), 1513-1524

Spelta C, Savaresi S, Fraternale G, Gaudiano N. (2008). Vibration Reduction in a Washing Machine via Damping Control. *Proceedings of the 17th World Congress The International Federation of Automatic Control*.

Spencer BF, Nagarajaiah S. (2003). State of the art of structural control. *Journal of Structural Engineering*. 129, 845-856

Symans MD, Constantinou MC. (1999). Semi-active control systems for seismic protection of structures: a state-of-the-art review. *Engineering Structures*. 21(6), 469-487

Tammi K. (2007). *Active control of radial rotor vibrations: Identification, feedback, feedforward, and repetitive control methods. Doctoral Dissertation*. VTT Publications (634)

Tammi K, Hätönen J, Daley S. (2007). Novel adaptive repetitive algorithm for active vibration control of a variable-speed rotor. *Journal of Mechanical Science and Technology*. 21(6), 855-859

Teramura A, Yoshida O. (1996). Development of vibration control system using u-shaped water tank. *Proceedings of the 11th world conference on earthquake engineering (11WCEE)*. Acapulco, Mexico.

Van Overschee P, De Moor B. (1996). *Subspace identification for linear systems: Theory –Implementation – Applications*, Dordrecht: Kluwer

Virtanen T. (2006). *Fault diagnostics and vibration control of paper winders. Doctoral Dissertation*. Helsinki University of Technology, Control Engineering (159)

Zazas I, Daley S , Pope SA. (2010). Marine diesel vibration isolation using an RLS based harmonic control algorithm with frequency tracking. *Proceedings of 19th International Congress and Exposition on Noise Control Engineering (INTER-NOISE 2010)*. Lisbon, Portugal.

Zhou K, Doyle JC. (1998). *Essentials of robust control*. Upper Saddle River, NJ:Prentice Hall

Zhou Q, Nielsen SRK, Qu WL. (2006). Semi-active control of three-dimensional vibrations of an inclined sag cable with magnetorheological dampers. *Journal of Sound and Vibration*. 296(1-2), 1-22

Zhou S, Shi J. (2001). Active balancing and vibration control of rotating machinery: a survey. *The Shock and Vibration Digest*. 33(4), 361-371

Åström KJ, Wittenmark B. (1995). *Adaptive control*, 2nd ed., Reading, MA: Addison-Wesley

Appendix: Publications

Aalto-DD 11/2013

ISBN 978-952-60-4977-9
ISBN 978-952-60-4978-6 (pdf)
ISSN-L 1799-4934
ISSN 1799-4934
ISSN 1799-4942 (pdf)

Aalto University
School of Electrical Engineering
Department of Automation and Systems Technology
www.aalto.fi

BUSINESS +
ECONOMY

ART +
DESIGN +
ARCHITECTURE

SCIENCE +
TECHNOLOGY

CROSSOVER

DOCTORAL
DISSERTATIONS